ENGINEERING THERAPEUTIC AVRA NANOPARTICLES WITH ENHANCED UPTAKE AND INTRACELLULAR DELIVERY WITH APPLICATIONS IN INFLAMMATORY BOWEL DISEASE

A Dissertation
Presented to
The Academic Faculty

By

Kevin Ling

In Partial Fulfillment
Of the Requirements for the Degree
Doctor of Philosophy in Chemical & Biomolecular Engineering

Georgia Institute of Technology

May 2018

ENGINEERING THERAPEUTIC AVRA NANOPARTICLES WITH ENHANCED UPTAKE AND INTRACELLULAR DELIVERY WITH APPLICATIONS IN INFLAMMATORY BOWEL DISEASE

Approved by:

Dr. Julie A. Champion, Advisor
School of Chemical & Biomolecular Engineering
Georgia Institute of Technology

Dr. Christine Payne
Department of Mechanical Engineering & Materials Science
Duke University

Dr. Ravi Kane
School of Chemical & Biomolecular Engineering
Georgia Institute of Technology

Dr. Mark Prausnitz
School of Chemical & Biomolecular Engineering
Georgia Institute of Technology

Dr. Andrew Neish
Pathology & Laboratory Medicine
Emory University

Date approved: March 28th, 2018

In Loving Memory of Chow Mui Zee, Ying Li, and Kay Lin

ACKNOWLEDGEMENTS

Graduate school has been a transformative experience. Reflecting upon my time at Georgia Tech invokes every possible emotion and has unexpectedly shaped me into the person I am today. I have grown and matured lifetimes from when I was first moved to Atlanta. I have been extremely fortunate to have met so many wonderful people here that have guided me through this contorted path in my life. I would first life to express my deepest gratitude to my advisor, Dr. Julie Champion. She has been my biggest supporter, motivating and pushing me through the hardest moments. She is a model of who I wish to become. Her insights have shaped how I approach problems in research and life in general. I would also like to thank my committee members Dr. Ravi Kane, Dr. Christine Payne, Dr. Mark Prausnitz, and Dr. Andrew Neish for their advice and support. Their feedback and our conversations have greatly improved the direction of my projects. I thank them for their guidance and taking an interest in my success. I would like to especially acknowledge Dr. Neish for partially adopting me into his lab at Emory University. I have gained a lot from working with him and his generosity is greatly appreciated. Huixia Wu has been instrumental to my work and I value her knowledge and technical expertise. I am extremely grateful for everything she has taught me.

I would also like to thank my many labmates who helped me through the daily grind. The positive lab culture created by my predecessors, Lina, Won Min, Trudy, Anusha, and Xingjie perpetuate a collaborative work environment full of scientific discussion. The enthusiasm brought in from newer labmates, Adam, Alex, Yeongsong, Sung In, Tianxin, Anshul, and Kelly were a great source of energy and a continuation of lively discussion. Dylan, Hannah, Sam, Wei, and Yiri will be welcomed with open arms and continuing the tradition in the lab that I will miss so much. Tim, my fellow comrade and great friend, has always been there when in need. I will

value my discussions with Tim and I am excited for what he and the rest of my labmates will accomplish in the future.

My peers and friends that I have met in graduate school are some of the most interesting people I've had the pleasure of knowing. Though we all had different interests and motivations, our common desire to obtain and build knowledge banded us together. The class that I entered with had such solidarity. Openness and inclusiveness was valued and shared by everyone, which allowed for some animated moments together. I wish the very best for my peers and know we will always be able to share a meal together in future and reminisce on graduate school. Most of all I will miss the most the many nights playing Settlers of Catan with Andrew, Christine, Nils, Weipeng, and Kong. We discussed and contemplated the intricacies of adulthood and life while sharing home cooked meals and an abundance of snacks. I've shared some of my hardest laughs and grown with this group. I will miss them dearly.

None of this would have been possible without the love and support of my family. My dad and mom, both uneducated immigrants, lived the American dream to provide for my sister and I. My sister and I have done our best in return to make them happy and proud. My wife Julia and our energetic dog Zara are my joys every day. I love them so very much and they are truly my hearth and home. Julia's empathetic nature inspires me to work for the benefit of others and her unconditional support drives me to better myself every day. I cannot say enough kind works to express my gratitude for everything my family have given me. This thesis is dedicated to my family members that has passed during my time at Georgia Tech.

Growing up, I've wanted to be the Indiana Jones of medicinal chemistry. I would dream of going to unexplored parts of the world with abundant biodiversity to study and extract new therapies to combat diseases. I marvel at how nature and evolution produce some of the most

amazing tools and how scientists and engineers utilize these instruments for societal benefit. I am motivated by giants such as Tu Youyou, the Nobel Prize recipient in 2015 for her discovery of antimalarial compounds from traditional Chinese herbal medicine. Finding and learning from those who inspire you provides a roadmap to living a good life. Life is full unexpected events that can alter the course we sought to take. Accepting these events as positive outcomes requires immense help from mentors, friends, and family and in this regard, I am most blessed. I have some amazing people in my life that give me the strength to work hard to achieve my goals and to help guide others along the way.

TABLE OF CONTENTS

Page

LIST OF TABLES

Page

LIST OF FIGURES

Page

LIST OF SYMBOLS AND ABBREVIATIONS

5-ASA	5-aminosalicylates
ANS	1-anilinonaphtalene-8-sulfonic acid
AopP	*Aeromonas* outer protein P
AvrA	Avirulence gene A
BSA	Bovine serum albumin
CAM	Cell adhesion molecule
CD	Crohn's disease
CD20	Clusters of differentiation 20
CDC	Centers for Disease Control and Prevention
CoA	Coenzyme A
CPP	Cell penetrating peptide
DAI	Disease activity index
DI	Deionized
DLS	Dynamic light scattering
DMEM	Dulbecco's Modified Eagle Media
DMSO	Dimethyl sulfoxide
DSS	Dextran sulfate sodium
DTSSP	3,3'-Dithiobis(sulfosuccinimidylpropionate)
eGFP	Enhanced green fluorescent protein
ELP	Elastin-like polypeptide
F4/80	EGF-like module-containing mucin-like hormone receptor-like 1
FBS	Fetal bovine serum
FDA	Food and Drug Administration
FITC	Fluorescein isothiocyanate
GALT	Gut-associated lymphoid tissue
GFP	Green fluorescent protein
GP	Glycoprotein receptor
GRAS	Generally regarded as safe
GST	Glutathione S-transferase
H&E	Hematoxylin and Eosin
HCl	Hydrochloric acid
HER2	Human epidermal growth factor receptor 2
HPF	High-power field
HSA	Human serum albumin
IBD	Inflammatory bowel disease
IFN-γ	Interferon gamma
IgG	Immunoglobulin G
IL	Interleukin
IMD	Immune deficiency
IP6	Inositol hexakisphosphate
Iκβα	Nuclear factor of kappa light polypeptide gene enhancer in B-cells inhibitor, alpha
JAK	Janus kinase
JNK	c-Jun N-terminal kinase
LAMP	Lysosome-associated membrane glycoprotein

LDH	Lactate dehydrogenase
MAPK	Mitogen-activated protein kinase
mAvrA	Mutant avirulence gene A
MWCO	Molecular weight cut off
MKK	Mitogen-activated protein kinase kinase
MPs	Microparticles
MPO	Myeloperoxidase
mRFP	Monomeric red fluorescent protein
mRNA	Messenger RNA
MTT	(3-(4,5-Dimethylthiazol-2-yl)-2,5-Diphenyltetrazolium Bromide)
NaOH	Sodium hydroxide
NF-κβ	Nuclear factor kappa-light-chain-enhancer of activated B cells
NiMOS	Nanoparticles-in-microsphere oral system
Ni-NTA	Nickel-nitrilotriacetic acid
NLS	Nuclear localization sequence
NPs	Nanoparticles
OCT	Optimal cutting temperature
OD	Optical density
OVA	Ovalbumin
p-Iκβα	Phosphorylated nuclear factor of kappa light polypeptide gene enhancer in B-cells inhibitor, alpha
PAMPS	Pathogen-associated molecular patterns
PBS	Phosphate buffered saline
PD-L1	Programmed death-ligand 1 (CD274)
PDMS	Polydimethylsiloxane
PEC	Polyelectrolyte complex
PEG	Poly-ethylene glycol
PMN	Polymorphonuclear
PRR	Pattern recognition receptor
PTD	Protein transduction domain
Rab	Ras-related protein
RBC	Red blood cell
RFI	Relative fluorescence intensity
ROS	Reactive oxygen species
S_0	Hydrophobicity index
SAP	Sweet arrow peptide
SCV	*Salmonella*-containing vacuole
SDS-PAGE	Sodium dodecyl (lauryl) sulfate-polyacrylamide gel electrophoresis
SS	Szeto and Schiller
SPI-1	*Salmonella* pathogenicity island 1
SPI-2	*Salmonella* pathogenicity island 2
SGF	Simulated gastric fluid
SIF	Simulated intestinal fluid
siRNA	Small interfering RNA
SMAD7	Mothers against decapentaplegic homolog 7
T3SS	Type three secretion system

TAT	Trans-activator of transcription protein
TGF-β1	Transforming growth factor beta 1
TNBS	2,4,6-Trinitrobenzenesulfonic acid
TNF-α	Tumor necrosis factor alpha
UC	Ulcerative colitis
VAP	Vacuole-associated actin polymerization
VEGF	Vascular endothelial growth factor
VLP	Virus-like particle
VopA	*Vibrio* outer protein A
YopJ	*Yersinia* outer protein J

SUMMARY

Protein therapeutics have emerged as potent and highly specific treatment options offering many advantages over small molecule drugs. Many protein therapeutics currently target extracellular secreted cytokines or receptors on the cell membrane. There is a trove of druggable targets that reside within the cell. Pathogens such as *Salmonella* target these intracellular moieties *via* bacterial effector enzymes to promote its own survival and replication. These enzymes are the product of evolution and have the ability to modulate immune function by modifying key proteins along eukaryotic inflammatory and apoptotic signaling pathways. Utilizing these enzymes in the absence of *Salmonella* can provide a unique opportunity to treat chronic inflammation such as in inflammatory bowel disease. A major challenge to realizing enzymes with intracellular activity as therapies is delivery into cells. *Salmonella* utilizes a needle-like structure that can penetrate the cell membrane to gain access to the cytosol. Without this delivery mechanism, an alternative delivery system must be engineered.

To address this challenge, we engineered a protein nanoparticles (NPs) containing an anti-inflammatory and anti-apoptotic *Salmonella* enzyme with intracellular activity, AvrA. Unlike traditional NP carriers commonly used to deliver drugs, protein NPs have biodegradability into amino acids. These NPs are synthesized by desolvating a solution of soluble protein and stabilizing the nanoclusters with a reducible crosslinker designed to break apart in the reducing environment of the cytosol. Protein NPs exhibit enhanced cellular uptake and internalization compared to soluble protein, and protein NPs maintain AvrA enzymatic function after delivery to cells. Our results show that AvrA NP formulations are internalized by barrier epithelial and immune cells, inhibiting the inflammatory signaling and conferring cytoprotection *in vitro*. Transrectal delivery of AvrA NPs to two murine colitis models reduced

clinical and histological scores of inflammation. Overall, AvrA NPs highlight the potential of protein NPs as delivery vehicles and therapeutics to treat inflammatory bowel disease.

Transrectally delivery is undesirable for patients and also limits delivery to the distal portion of the colon, both of which hinder the clinical potential of AvrA NPs. Therefore, we sought to engineer an oral delivery vehicle to maximize therapeutic potential. The biggest obstacle to oral delivery of proteins is the harsh environment found in the stomach, where low pH, digestive enzymes, and mechanical forces act to break down proteinaceous materials for digestion. We engineered alginate/chitosan hydrogel microparticles (MPs) encapsulating AvrA NPs using a flow focusing microfluidic device for the gastric passage and intestinal release of AvrA NPs. Alginate and chitosan are two naturally derived polysaccharides generally regarded as safe by the FDA. Alginate hydrogels can encapsulate AvrA NPs under mild conditions and exhibit pH responsivity, preventing release in the stomach and allowing NPs to release in the intestine. We show that coating alginate MPs with chitosan increases NP encapsulation efficiency and improves retention of bioactive protein NPs after gastric incubation. Oral gavage of AvrA NPs encapsulated in alginate/chitosan MPs reduced clinical and histological scores of inflammation in a colitis mouse model.

Though we have shown the ability of protein NPs to deliver enzymes to the cytosol of cells, NP delivery vehicles in general suffer from endosomal entrapment that results in low cytosolic delivery efficiency. Achieving endosomal escape is highly desirable and understanding how cells traffic endosomes can provide insight how to avoid lysosomal degradation. NPs, once administrated *in vivo*, encounter a milieu of serum proteins mainly in the blood. The adsorption of serum proteins onto NPs, called the protein corona, can modify the NP's physiochemical properties influencing cellular interactions and how these NPs are processed. In an effort to

understand protein corona formation around protein NPs, we synthesized various protein NPs with different physiochemical properties. We find that properties of the carrier protein govern the properties of the protein NPs after desolvation and observes qualitative differences in the protein corona that forms around protein NPs compared to traditional polymeric NPs.

This thesis focuses on using naturally derived materials as building blocks for drug delivery vehicles and reengineering the tools used by pathogenic bacteria for therapeutic purposes. The protein NP platform and encapsulation with alginate/chitosan MPs is generalizable to other therapeutic proteins. Incorporating multiple therapeutic proteins into a single protein NP delivery vehicle can combat diseases through multiple modes of action leading to a highly effective treatment. The alginate/chitosan MP oral delivery platform can accommodate protein therapeutics, probiotics, and other macromolecules to protect from the harsh conditions of the stomach and released in the intestines. Overall, these results show the clinical potential of implementing protein NPs as intracellular therapeutics and provides an oral delivery platform to do so. Further, we show the ability to control protein NP properties through choice of carrier proteins and observed differences in protein corona that forms around them.

CHAPTER 1 : Introduction

1.1 Inflammatory Bowel Disease

Crohn's disease (CD) and ulcerative colitis (UC), the two major forms of inflammatory bowel disease (IBD), are chronic inflammatory disorders of the gastrointestinal tract resulting from inappropriate and amplified mucosal immune responses to the otherwise normal microbiota existing in the gut[1, 2, 3]. The CDC estimates that approximately 3.1 million people in the US are living with IBD[4] and there is an increasing global prevalence[5, 6]of the disease. The growing incidence of IBD in a relatively short duration of human generations indicates that genetic factors alone are unlikely to explain the pathology. Microbiota coexisting with our gut have substantially shorter generation times making it susceptible to rapid evolutionary changes from the environment such as infection, hygiene, diet, and medication. Whether environmental selection pressures produce a pathogenic microbiome, also called dysbiosis, or if dysbiosis is a consequence of the altered intestinal environment in IBD patients is still unknown[3]. IBD patients have depletion of commensal bacteria resulting in decreased microbial richness[7], increased epithelial permeability allowing increased bacterial translocation[8]. Other mechanisms such as microbial sensing, antigen processing, and oxygen level can also contribute to loss of intestinal function. The unknown pathology of IBD has led to complicated treatment regimens. Patients use a combination of locally acting anti-inflammatory small molecules[9, 10, 11], systemic corticosteroids, monoclonal antibodies[12], and surgery. Although these treatments can be effective for many patients, they have specific windows of efficacy[10], long-term side effects[13, 14, 15], and risk of infection[9, 16] associated with them. Whatever treatment plan is implemented, long-term

monitoring is essential. This includes colon cancer surveillance and continual assessment of remission maintenance drugs every 6-12 months[17].

The primary therapeutic goals for patients with IBD is prevention of ulcerations in the gastrointestinal tract and maintenance of this remission long term. Endoscopic or mucosal healing improves long-term clinical remission and is correlated with reduced relapse rates, need for surgery, and cessation of rectal bleeding[18]. This state of remission also means that a patient is less likely to develop more serious associated symptoms such as colorectal cancer. The first line of defense for patients with mild to moderate symptoms of IBD is small molecule anti-inflammatory, 5-aminosalicylates. If successful, 5-aminosalicylates are also typically given to maintain remission meaning that a patient is likely to continually rely on this medication. If ineffective, the next line of treatment is systemic corticosteroids. Corticosteroids are only used for treatment of the disease and cannot be used for maintenance of remission due to ineffective long-term efficacy and risk of side effects[19]. Patients can become steroid dependent[20] and in some cases steroid withdrawal needs to be closely monitored because prolonged exposure is associated with diabetes, bone loss, hypertension, and infections[21]. More serious cases of gastrointestinal inflammation rely on stronger immunosuppressing chemotherapies such as thiopurines and methotrexate. Though these have more serious side effects such as lymphoma, they are only associated with modest efficacy rates[17, 21].

More recently, monoclonal anti-TNF-α antibodies have been shown to be effective in inducing and maintaining remission. TNF-α inhibitors are a popular approach to combating other autoimmune diseases such as rheumatoid arthritis and immune-related skin diseases such as psoriasis. They have also been shown to be potent agents to induce remission in IBD, however, they are typically reserved for patients who do not respond to 5-aminosalicylates, corticosteroids,

or immunosuppressants. Therefore, anti-TNF-α therapies is used in combination with 5-aminosalicylates, corticosteroids, and immunosuppressants for the maintenance of remission as well. This combinatory usage have also been associated with increased risk of opportunistic infections[22], melanoma skin cancer[23], and lymphoma[14]. Monoclonal antibodies also have the potential to develop immunogenicity meaning they lose their efficacy over time[24] requiring higher dosages and potentially increasing systemic effects.

Another monoclonal antibody that blocks α4β7 integrin is now available as a gut-selective anti-inflammatory[25], which prevents activated T-cells from adhering to the gut endothelium and eventual extravasation into gut mucosal tissue. There have also been other monoclonal antibodies that focus on neutralizing the p40 subunit common on both IL-12 and IL-23[26]. These two cytokines are overexpressed in patients with IBD and are believed to perpetuate a chronic inflammatory state by continually stimulating T-cells. Due to the novelty of these new therapies and lack of long-term safety studies, they are reserved for patients where anti-TNF-α treatment has failed[21]. In the most serious cases, where none of the above treatments are effective in inducing remission, surgery is necessary to relieve abscesses and malignancies. Surgery is not a cure however, as relapses can still occur[17, 21].

Current clinical trials are testing other anti-adhesion targets such as antibodies blocking cell adhesion molecule (CAM) proteins[21] on gut endothelial tissue. Small molecule janus kinase (JAK) inhibitors are also being explored[27]. The JAK family of tyrosine kinases controls many intracellular signaling pathways resulting in inflammatory cytokine production. An oligonucleotide siRNA that silences SMAD7 is also being investigated[28]. SMAD7 is a TGF-β1 antagonist and restoring TGF-β1 activity leads to suppression of pro-inflammatory cytokines such as IFN-γ, TNF-α, and IL-2 thereby reducing overall inflammation. In order for this strategy

to work, the SMAD7 siRNA must achieve intracellular cytosolic delivery where the mRNA substrate is available. Whereas more traditional IBD therapies target secreted cytokines from immune cells or cell surface markers found on T-cells, emerging therapies target intracellular components. Development of JAK inhibitors and SMAD7 siRNA is a shift in IBD strategy to realize the potential of intracellular drug targets. New treatments should also focus on modulating the innate and adaptive immune system to stop the perpetuation of chronic inflammation as well as preventing early stages of IBD from progressing into more serious symptoms.

1.2 Bacterial Effector Protein, AvrA

Areas of chronic gut inflammation are driven by hyper reactive autoimmune cells producing inflammatory cytokines in response to external stimuli. Cells react to these cytokines through receptor-mediated intracellular signaling pathways ultimately leading to a transcriptional response in the nucleus. Inflammatory cytokines can activate two major intracellular signaling highways, the mitogen-activated protein kinase (MAPK) c-Jun N-terminal kinase (JNK)[29, 30, 31] and/or nuclear factor kappa-light-chain-enhancer of activated B cells (NF-κβ)[32, 33, 34] pathways, which control innate immunity, cell growth, proliferation, survival, and death. Enteric pathogenic bacteria have evolved mechanisms that can modulate these intracellular inflammatory and immunoregulatory pathways[35, 36, 37] by injecting bacterial effector proteins via a needle-like type-3 secretion system (T3SS). The most studied gram-negative bacterial pathogenic species *Escherichia, Yersinia,* S*higella,* and *Salmonella* all utilize a conserved T3SS[38] to deliver their virulence factors and are known to cause gastroenteritis. Each of these bacterial species has

evolved unique mechanisms to manipulate host immune response, cytoskeletal dynamics, vesicle transport and signal transduction pathways for survival.

One of these bacterial effector proteins, AvrA derived from *Salmonella*[39, 40, 41], is a member of a family of acetyltransferases that covalently modify and inactivate members of the MAPK superfamily[42]. AvrA is found on *Salmonella* pathogenicity island 1 (SPI-1), a cluster of genes acquired through horizontal transfer[43]. SPI-1 genes are activated and secreted early in infection to promote bacterial internalization and *Salmonella*-containing vacuole (SCV) biogenesis. AvrA is believed to be secreted into the cytoplasm by a T3SS once a SCV is formed to help dampen host immune response and inhibit apoptosis[44]. SCVs are able to recruit nutrient-rich host vesicles to fuse with, allowing *Salmonella* replication within a maturing SCV[45]. After SCV maturation and bacterial replication begins, SPI-2 is activated to inhibit lysosomal maturation and apoptosis. SPI-2 also help direct the SCV to the perinuclear region close to the endoplasmic reticulum and promote the formation vacuole-associated actin polymerization (VAP) to stabilize the SCV. Despite differences in temporal activation of the two SPIs, the two islands are closely linked as several effector proteins are found on both[46].

Identifying and isolating specific effector proteins involved during bacterial infection reveals a unique trove of potential therapeutic drugs. AvrA overexpressed in transfected cells[41] or in a *Drosophila* transgenic model[47] blocked activation of NF-κB, JNK MAPK, and transcriptional activation of a range of inflammatory effector genes. Specifically, AvrA is capable of acetylating key serine and threonine residues on MKK4/7 thus inhibiting phosphorylation of these upstream JNK signaling pathway and blocking apoptosis[47, 48, 49]. Similar results were demonstrated in a yeast model[48] as well. AvrA has also been shown to stabilize intestinal tight junctions via the JNK pathway[50]. In parallel with AvrA's

acetyltransferase activity, it has also been reported that AvrA indirectly deubiquitinates Iκβα by an unknown mechanism, stabilizing phosphorylated-Iκβα (p-Iκβα) and inhibiting further phosphorylation, thereby preventing transcription of NF-κβ[41, 51]. AvrA's ability to inhibit stress signaling pathways without inducing apoptosis is reported in yeast, flies, human, and murine intestinal epithelial[41, 42, 47, 48]. This evolved bacterial protein with combined anti-inflammatory and anti-apoptotic enzymatic functions make it an ideal therapeutic to ameliorate IBD and other forms of inflammation[51, 52].

Other examples of T3SS effectors affecting the MAPK and NF-κβ pathways include OspF and OspG derived from *Shigella*[53, 54]. OspF is a site specific phosphothreonine lyase, which irreversibly removes phosphate groups from p38 in the MAPK pathway[54] inhibiting phosphorylation and signaling. OspF has also been shown to inhibit histone H3 phosphorylation, impairing the access of NF-κβ with its promoter region and thus inhibiting inflammatory genes and cytokines[55]. OspG blocks ubiquitinylation of Iκβα, preventing NF-κβ signaling[56]. VopA from *Vibrio parahaemolyticus* is an acetyltransferase that inhibits the MAPK pathways by acetylating a conserved lysine found on the catalytic loop of all MKKs thereby preventing binding of ATP[57]. This makes VopA potent inhibitor of cytokine production even though VopA has no effect on the NF-κβ pathway[58]. AopA from *Aeromonas salmonicida* is also reported to attenuate host immune response by inhibiting immune deficiency (IMD) and Toll NF-κβ pathways in *Drosophilia*. AopA prevents the nuclear translocation of p50/p65 Rel proteins[59] in the NF-κβ pathway, however, has no effect on the MAPK pathway. Plant pathogens such as *Ralstonia solanacearum*, *Pseudomonas syringae*, and *Xanthomonas campestris* have also been found to contribute to pathogenesis by suppressing host immunity through a similar T3SS[60].

Another acetyltransferase virulence factor, YopJ derived from *Yersinia*, is an ortholog of AvrA[61]. It is involved in bacterial infection by acetylating serine and threonine residues of all MAP kinase kinases (MKKs)[62] and on the activation loop of IKKβ[63], thereby downregulating MAPK and NF-κB signaling, respectively. This leads to inhibition of host immune response and induces apoptosis[61]. Interestingly YopJ activity is shown to be cell type specific. YopJ is able to induce apoptosis in macrophages and dendritic cells[64] but not in neutrophils and endothelial cells[65]. AvrA has also been shown to be differentially expressed depending on the organ location of infection[66]. This seems to suggest that these bacterial effectors rely on cell specific cofactors and triggers from their eukaryotic host for activation. Inositol hexakisphosphate (IP6) and/or coenzyme A (CoA) has been shown to be one of these triggers required for allosteric regulation of all acetyltransferases[67, 68, 69]. AvrA, YopJ, and its other orthologs are stored in a non-active conformation inside the bacterial pathogen until it is secreted by T3SS and binds IP6 and/or CoA to induce an allosteric conformation change to an active state inside the host cell. Furthermore, AvrA is known to be phosphorylated[48] at evolutionarily conserved residues dependent on the host ERK pathway that is regulated by other bacterial effectors[48]. This implies that the activity of AvrA may be controlled by other effectors in its own feedback loop through the regulation of a host signaling pathway[44].

To date, serine/threonine acetyltransferases have not been reported in eukaryotes[67]. Structural analysis of acetyltransferases shows the complex mechanism of enzymatic activity based on allosteric regulation controlled by eukaryotic hosts. This could inspire further research toward understanding of acetylation as a prevalent post-translational modification and allow us to design drugs that can specifically target these bacterial virulence agents without affecting host processes. We could also reengineer these bacterial effectors to combat other inflammatory

diseases through a novel mechanism developed over millennia of co-evolution between pathogen and host. Chronic inflammation in inflammatory bowel is currently treated with nonspecific, systemic small molecules can produce unwanted side effects. The ability to reduce inflammatory signaling without apoptosis is a highly desirable feature that can be achieved with bacterial effectors. However, a major challenge in realizing the therapeutic potential of AvrA, or any exogenous protein effector, is the ability to deliver it locally through the harsh environment of the gastrointestinal tract, and into the cytosol of resident epithelial and immune cells without compromising the biological activity of the protein. *Salmonella* meets this challenge through use of T3SS. However, in *Salmonella* infection AvrA is co-delivered along with other virulence proteins,[48, 70] which can have negative effects, such as promotion of colonic tumorigenesis.[71, 72] Therefore, an alternative delivery approach is necessary to deliver only AvrA in the absence of *Salmonella* and safely access its anti-inflammatory functions. The trigger responsive T3SS in *Salmonella* and other gram-negative bacteria span three cellular membranes, the bacterial inner and outer membranes and the eukaryotic host membrane. This enables pathogenic bacteria to package and protect protein effectors from degradation, gain access to the cytosol and other intracellular compartments, and release these proteins with spatiotemporal control[38]. Without this specialized and evolved delivery system, intracellular protein delivery remains highly elusive despite the great potential of largely untapped targets[73].

1.3 Approaches to Intracellular Protein Delivery

It is estimated that only about ~5-10% of the druggable genome is being targeted by traditional small molecules drugs[74, 75]. This leaves a large number of targets untapped that could

be targeted using protein drugs. Protein drugs are advantageous compared to small molecules drugs[76, 77] because they offer higher specificity, greater activity, and less toxicity conferred by protein's large size and conformation. There is a shift in pharmaceutical strategies favoring more protein-based drugs and this is seen in the growing number of proteins in the top selling pharmaceutical drug list along with an increase in protein biologicals gaining FDA approval[78, 79]. However, most of these proteins bind extracellular cytokines such as TNF-α or bind cell surface receptors for insulin, TNF-α, CD20, VEGF, PD-L1, or HER2[79]. There exists a trove of potential protein targets inside the cell as well. Intracellular proteins play a fundamental role in maintaining all cellular activities. Missing, malfunctioning, or poorly expressed proteins in cells is the cause of most genetic diseases. Delivery of functional proteins can be an unambiguous method of treating these genetic disorders[80] and they can also be used stimulate or inhibit cells by manipulate signaling pathways, such as with effector proteins described in Section 1.2.

Small molecules drugs face lower barriers to intracellular delivery because they are generally capable of diffusing across the membrane and into the cytosol of cells. The structural complexity of proteins presents several challenges to intracellular delivery. Proteins have limited transport to cells because they are susceptible to denaturation from changes in their local environment, enzymatic degradation from proteases, rapid clearance from the body resulting in short circulation half-life, and poor membrane permeability. Cells can engulf proteins in the extracellular environment *via* energy-dependent transport called endocytosis. Once proteins are endocytosed, they are enclosed within vesicles/endosomes destined for lysosomal degradation or to be recycle and exocytosed[73] leading to low delivery efficiency and bioavailability. Great strides have been made to target protein to specific receptors on cells for receptor-mediated

internalization, however, endosomal escape remains a formidable barrier[80] to achieve the therapeutic potential of proteins.

Approaches to improve the intracellular delivery of proteins include mechanical membrane disruption[81, 82], covalent protein fusion modifications[83], and NP-based carrier delivery[77, 80, 84]. These methods to improve intracellular delivery must be appropriately designed and formulated to protect the protein cargo from degradation, denaturation, aggregation, and minimize immunogenic side effects[77] before reaching its therapeutic site. These methods should also facilitate targeting to diseased cells and if endocytosed, methods should enhance the endosomal escape of the protein.

1.3.1 Mechanical membrane disruption

The most straightforward method of delivering proteins intracellularly is by mechanical disruption. Direct insertion, such as with microneedles and nanoneedles, uses solid contact to concentrate pressure to a limited region of the plasma membrane causing a discontinuity in the membrane barrier. Afterwards, a controlled amount of protein can be injected directly into the cytoplasm and even guided to specific organelles such as the nucleus[85]. Despite its efficient method of intracellular delivery, direct insertion suffers from having low throughput capacity and requiring the use of specialized tools to inject into single cells. This method is generally limited to *in vitro* applications as single-cell localization is not achieved in *in vivo* applications[82]. Advances in microfluidics and jet injection, which employs a high-velocity ultrafine stream of proteins in solution instead of a needle, have automated this system of injections and has greatly increased throughput[86]. Another interesting example uses microfluidic constriction or cell squeezing to cause rapid deformation, allowing intracellular delivery of many

biomacromolecules with low cytotoxicity[81, 87]. Current limitations are the inability to accommodate a heterogeneous population of cell sizes as the size of pores formed through squeezing are dependent on the cellular volume.

Electroporation has been the leading technique of membrane disruption capable of delivery to millions of cells[88] and its adoption in research has produced commercially available systems[82]. A typical electroporation setup includes a suspension of cells in between parallel plates where brief electric pulses are used to form a distribution of transient pores in the cell membrane[89]. This conventional setup produces a heterogeneous population of short lasting large pores and longer lasting small pores that allow the diffusion of materials into the cell. Nucleic acid delivery by conventional electroporation is more efficient than for other biomacromolecules. Electroporation partially embeds nucleic acids in the pores due to their dense negative charge resulting in subsequent internalization through receptor mediated pathways instead of direct delivery[89]. For other biomacromolecules, the higher voltages are required to stabilize larger pores results in higher propensity for aggregation and higher cytotoxicity[81]. The inconsistent level of membrane disruption between cells can also result in either insufficient delivery or excessive cell damage[90]. Efforts are being made to improve this system using more directed nanochannel electroporation combined with microfluidics. This combination of techniques concentrates an electric field over a very small area of the cell membrane allowing electrophoretically driven flow into the cell[91]. Similar to the direct injection method, electroporation is limited to mainly *in vitro* and *ex vivo* applications as it is difficult control *in vivo* and increases the possibility of influx from other proteins into the cell creating side effects[92].

Other methods of mechanical membrane disruption include sonoporation or using ultrasound to produce acoustic cavitation that induces transient pores. Sonoporation is preferred

over other physical delivery methods *in vivo* due to the comfort and familiarity in clinical settings[82]. Thermal deviations can promote membrane defects from intense thermal fluctuation causing dissociation of lipids. Live cells have shown to leak at 42^{o}C, and above 55^{o}C small molecules (<1 kDa) rapidly diffuse in and out of cells[93]. At sub-physiological temperatures, ice crystals can form pores that heal when thawed. Cells subjected to rapid thermal phase transition between 0^{o}C and 40^{o}C can also promote intracellular delivery. Thermal methods seem to be confined to small molecule delivery and there are few reports on larger biomacromolecule delivery[88]. Optoporation with lasers produces membrane defects through a combination of mechanical, thermal, and chemical effects from ROS production[94]. Concerns about the destructive power of laser radiation along with need to precisely control the alignment and position of the laser beam to minimize off target ablations makes this low throughput method limited to those who can operate this expensive and sophisticated equipment[82]. A few biochemical methods are also used to cause membrane disruption. Detergents such as digitonin and saponin can disrupt cholesterol rich membranes or pore-forming toxins such as streptolysin O[95] can generate large pores to allow delivery of proteins. The exact mechanism of pore-forming toxins is guided by an unknown mechanism and pore sizes when detergents are used are highly inconsistent[96].

These membrane disruption techniques have strengths as universal intracellular delivery systems, however, they are limited to *in vitro* and *ex vivo* applications since direct physical access to targeted cells is necessary. Transitioning these methods into the clinic requires controlled single cell delivery and currently, electroporation and sonoporation have only been somewhat effective at targeting sections of tissues. It is difficult to control cavitation evenly throughout the tissue, resulting in lower delivery efficiency. In electroporation there is a much

higher risk of inflammation from metal ion deposition originating from the electrodes. Electroporation also requires skilled technicians to properly place the electrodes to prevent injury from off target electric generation[97]. Other general common weaknesses such as high cell-to-cell membrane damage variability, restriction to either adherent or suspended cells, poor throughput and scalability, and not fully understanding cellular membrane recovery has shifted research to using microfluidics as a means of overcoming these challenges[88]. As the ability to scale up these methods improve, further work must be done to transition these techniques *in vivo* with minimal side effects.

1.3.2 Covalent protein fusion modification

Intracellular proteins therapeutic face challenges that elude small molecule drugs. The cell membrane is naturally impermeable to complexes larger than 1 kDa. The negatively charged cell membrane also contributes to repelling the majority of slightly negatively charged proteins as well. Unmodified proteins must enter cells through a mechanical disruption like the methods described above in section 1.3.1, or they must enter through bulk intact processes such as macropinocytosis[98]. Proteins must also maintain proper conformation and avoid proteolysis and clearance while reaching *in vivo* targets. These challenges have motivated research to covalently fuse moieties onto protein therapeutics that can help facilitate entry into the cell across the plasma membrane or extend its half-life *in vivo*. The strategy of covalently fusing moieties to therapeutic proteins is not limited to targeting peptides, but can also include full length proteins and polymers. Covalent modification has been an effective method of overcoming the challenges of *in vivo* intracellular drug delivery.

Viral pathogens have long been the inspiration for many drug delivery methods. Their effectiveness *in vivo* to deliver nucleic information has guided research in the field to study viral mechanisms and components with close scrutiny. One important discovery from research on the HIV virus was the ability of trans-activator of transcription (Tat) protein, to induce fusion with target membranes. Tat is a viral regulatory protein that binds RNA to activate transcription. A domain on Tat is responsible for its nuclear membrane localizing capabilities and when solely expressed, this cell penetrating peptide (CPP) retains its ability to cross the plasma membrane[99]. Since then, other naturally isolated CPPs have been reported, many other variants artificially created and mutated to increase bioavailability. CPPs vary in length, but are generally around 10-30 amino acids depending on their mechanism of action. When a CPP is fused to an intracellular protein therapeutic, it greatly enhances the cytosolic delivery of a molecule many orders of magnitude larger than itself[100]. 1700 unique CPPs have been cataloged[101] that include experimental conditions such as the cell type and cargo. The ability of some regulatory proteins to localize in organelles has also been studied and the motifs responsible for localization have overlap with CPPs. CPPs can be engineered to provide subcellular localization along with enhanced delivery through the plasma membrane[83]. It should be noted that the efficiency of this plasma membrane penetration is debatable as it appears that once CPPs are conjugated to proteins, they are often concentrated within endosomes and unable to access the cytosol[102, 103]. The utility of CPPs is an area of active research and CPP conjugated drugs are being developed in clinical trials[104].

The first discovered and most studied PTDs are the Tat peptide and penetratin, a CPP from homeotic protein antennapedia in drosophila. They are both highly cationic peptides that represent one of the classes of CPPs that are classified by their molecular characteristics. The

other two classes of CPPs are either amphiphilic or hydrophobic in nature[105, 106]. Cationic CPPs rely mainly on positively charged arginines and lysines to form electrostatic interactions with anionic membrane lipids and components to facilitate crossing of the membrane. These cationic tails are typically covalently attached to the ends of protein cargo. Poly-arginine, poly-lysine, and poly-histidine CPPs were engineered to decode the mechanistic differences between the positively charged amino acids. It was found that arginine performed better than lysine and minimum of 8 arginine residues were required for internalization. Increasing the number of arginines led to higher levels of uptake, however, increased cytotoxicity as well[107]. It has also been reported that poly-arginines are quite efficient at lysosomal targeting as well[105]. Poly-histidines have a disputed proton-sponge effect[108] when 4 or 5 residues are present[109]. The supposed endosomolytic ability originates from histidine's amine group that has a pKa of 6.2 and becomes pronotated at lysosomal pH, turning into a more cationic species. Nuclear localization sequences (NLSs) have some sequence overlap with cationic CPPs[106]. Lysine, arginine, and proline based NLSs were all found to localize in the nucleus by transporting across the nuclear pore complex. NLSs are shorter peptides that unable to penetrate other membranes making them poor CPPs alone.

Another example that uses cationic charge to facilitate intracellular delivery is supercharged proteins[110, 111]. A green fluorescent protein (GFP) variant was first engineered to have very high net positive charge (+36 net theoretical charge to molecular weight ratio) and when conjugated to other proteins, this supercharged GFP variant was able to penetrate and deliver directly into mammalian cells. Since, other naturally occurring supercharged proteins have been discovered and have been reported to similarly penetrate cell membrane and deliver cargo.

Amphiphilic CPPs have both hydrophilic and hydrophobic regions that contribute to cell penetration. They are typically longer in length, around 20 amino acids, compared with other CPPs. The hydrophilic region can be cationic in nature to help promote electrostatic interactions with the negatively charged cell membrane, which allows the hydrophobic region of the CPP to embed itself into the membrane, facilitating penetration. Amphiphilic CPPs do not have to be cationic, and positively charged residues that have been mutated to anionic or neutral have been shown to be cell-penetrating as long as these residues remain polar. This suggests that amphiphilicity and mainly hydrophobicity is necessary for membrane translocation[105, 106]. Poly-prolines can also exhibit penetrating capabilities such as the sweet arrow peptide (SAP)[112]. These alternating regions of hydrophilic and hydrophobic regions on amphiphilic CPPs can also assemble into secondary structures such as α-helices and β-sheets that are responsible for cell penetrating capabilities.

Hydrophobic CPPs are emerging peptides. Hydrophobic CPPs have low net charge containing non-polar residues or hydrophobic motifs that confer membrane penetration. For example tryptophan residues improves hydrophobic interactions with the cell membrane because of their propensity to be buried within the cell membrane[109]. For the most part, the penetrating abilities of hydrophobic CPPs are also resistant to sequence scrambling, in contrast to most cationic and amphiphilic peptides. It has been reported that some of these hydrophobic CPPs can directly cross the cell membrane to avoid endosomal entrapment[113].

Combinatory CPPs with intracellular organelle targeting motifs have been gaining traction. Harnessing the penetrating abilities of CPPs coupled with the ability to localize protein therapeutics to organelles makes an extremely site-specific drug. CPPs on their own cannot penetrate organelle phospholipid layers[114] and therefore new peptides are being investigated for

their ability to target and penetrate organelle membranes. The NLS from the tumor antigen of simian virus 40 is one of the most studied, particularly in the field of gene therapy[115]. Commonalities between other known NLSs such as importin-α has shown that a strong positive charge mediated by basic amino acids located at the termini of proteins confers the ability to transport across the nuclear pore complex and achieve nuclear accumulation[105]. Lysosomal sorting peptides are 4-5 amino acids that are tyrosine based containing the patterns YXXØ or NPXY (Y – tyrosine, X – any amino acid, Ø – bulky hydrophobic side chain, N – asparagine, P – proline)[116]. Similarly, when used in conjunction with the tat peptide, they are able to localize cargo into lysosomal or lysosomal-like structures[117]. Szeto and Schiller (SS) have reported peptides capable of targeting mitochondria[118] to reduce intracellular ROS activity. SS peptides are typically 5 amino acids and the common motif relies on alternating aromatic resides with basic/cationic amino acids. Modified tyrosines in the SS peptides with anti-oxidative abilities gives these peptides their intracellular mitochondrial therapeutic abilities. The golgi and endoplasmic reticulum are secretory pathways responsible for packaging and directing intracellular components to subcellular compartments including the plasma membrane. It also is responsible for carrying on posttranslational modifications on proteins making it a highly attractive avenue for targeting. The 4-peptide sequence KDEL added to the C-terminal used in conjunction with a N-terminal tat peptide is able to guide and retain cargo in the ER[119]. Recently, the antimicrobial peptide oncocin has been reported to target bacterial ribosomes[120]. Other proline-rich peptides from this oncocin family have also been shown to inhibit the ability of ribosomes to translate RNA. This expanding field of peptides capable of targeting intracellular organelles offers great potential to maximize the therapeutic potential of intracellular proteins by offering site-specificity. Zinc-finger motifs also have demonstrated intracellular delivery

capabilities based on a similar cationic peptide sequence intrinsic to the zinc-finger structure[121]. When proteins are fused to the zinc-finger domain, it facilitates cytosolic delivery through micropinocytosis.

Albumin conjugation is another method of targeted intracellular delivery[122]. Albumin is a naturally occurring transporter protein that can engage cellular receptors to initiate internalization. Further engineering and biasing interactions toward glycoprotein receptors (Gp18, Gp30, and Gp60) can improve the intracellular delivery capabilities of albumin[123]. Albumin can be recycled by interactions with neonatal Fc receptor leading to longer half-life *in vivo* and allowing more opportunities for accumulation at target locations. Protein drugs smaller than 70 kDa are cleared from systemic circulation by renal filtration. Conjugation of these proteins with hydrophilic polymers such as PEG can reduce clearance by increasing their apparent molecular weight and/or hydrodynamic radius. PEG conjugation can achieve similar results of long lasting *in vivo* half-life by preventing clearance[124]. Albumin and PEG conjugations are nontoxic and have advanced into the market, indicating their widespread use and generally acceptability. Though these techniques are capable to extending half-life *in vivo*, their conjugation leads to alterations in physiochemical properties that can impart conformation changes affecting binding and activity[125].

1.3.3 Nanoparticle carrier delivery

Although CPPs have been widely explored, their unclear exact mechanism of action, concerns about toxicity, and alterations in activity once actually conjugated to a therapeutic hinder their clinical applications[77]. NPs are another approach to intracellular delivery and though they may differ in their mechanism of delivery, covalent modifications can be used in

conjunctions with NPs further enhance their activity. NPs are inspired from viral pathogens. Viruses are highly efficient NP drug delivery vehicles and they are heavily studied both because of their harm to humans and potential to be repurposed for therapeutic delivery. Scientists and engineers have taken a reductionist approach to studying the virus and have refashioned many viral components. Viruses have been depleted of their native genes to prevent replication and pathogenicity and loaded with desired cargo, primarily nucleic acids. Viral vectors have been tested in clinical trials, however, challenges such as immune response, safety and complexity of viral preparations have hindered their ability to gain FDA approval for direct administration[126].

Motivated by these limitations, a vast number of non-viral vectors have been developed[88]. These non-viral vectors generally try and accomplish similar goals as their viral counterparts such as loading and protecting cargo from degradation, target specific areas to maximize therapeutic benefit, and deliver cargo into the cytosol of cells to affect intracellular targets. These non-viral carriers original were engineered for nucleic acid transfection, however, they are being now being designed to deliver other biomacromolecules and proteins as well[76]. The deliver challenges are similar between nucleic acids and intracellular proteins. They are both too large to cross the cell membrane, they must escape endosomes to reach their therapeutic site, they must protect against nucleases and proteases, and they must accumulate in desired locations. Non-viral vectors can be made from inorganic nanomaterials, lipids, polymers, and proteins. Engineering these materials to be nanoscale makes them similarly sized or on the same order of magnitude as native viral pathogens possibly affecting how cells interacts with these materials. These materials have an enormous range in physiochemical properties such as charge, size, hydrophobicity, mechanical properties, composition, and function groups that can affect their ability to load, protect, and deliver protein cargo. Tuning these physiochemical properties can also affect

cellular uptake, endosomal escape, and target specificity[80]. One major problem with implementing these NP carriers is the inability to escape endosomes, leading NPs to lysosomal degradation or endosome recycling and exocytosis. It has been reported that only about 1% of lipid-based NPs actually make it to the cytosol based on studies delivering siRNA[127, 128]. This low efficiency could possibly be unique to siRNA therapeutic, however, it is much more likely to be generally applicable to all intracellular NP delivery vehicles. This means that there is a large potential for improvement.

1.3.3.1 Inorganic

Inorganic NPs made from carbon nanotubes, quantum dots, magnetic materials gold, and silica have been used for the intracellular delivery of proteins and generally have excellent stability over a broad range of temperatures and pH values[129, 130]. Single-wall carbon nanotubes modified for water solubility and biocompatibility have been used to study delivery of proteins intracellularly. Proteins adsorbed onto the surface of the carbon nanotube enter the cell via energy-dependent endocytic processes[131] and capable of intracellular delivery[132]. Some have reported that single wall carbon nanotubes are capable of membrane insertion and diffusion directly into the cytosol, though this mechanism of entry has been associated with thrombus formation as well[80]. Quantum dots have been widely utilized as fluorescent probes due to its narrow and tunable emission spectra. Intracellular protein delivery has been achieved with quantum dots only when used in combination with a CPPs and NLS[133]. Magnetically-mediated delivery approaches can increase the local concentration of target cargo and minimize non-specific interactions. Magnetic NPs also possess an inherent diagnostic tool for magnetic resonance imaging as well. Combining diagnostic and therapeutic tools have been goal of

theranostic nanoplatforms, though there have been few reports of using magnetic NPs to deliver proteins[77]. One report shows that magnetic NPs made from iron oxide hydrophobically and electrostatically bind proteins and enter endothelial cells[134].

Gold NPs have been extensively used in biomedical applications for its biocompatibility, with tunable surfaces via thiol group modifications, and unique spectroscopic properties[135]. Using the high surface area of gold NP, a combinatory lipid-HKRK (histidine – lysine – arginine – lysine) moiety was conjugated to its surface and used to delivery proteins to the cytosol of the cell with high efficiency[136]. These gold NPs formed complexes with protein to make protein-gold NPs and gold NPs can also stabilize nanoemulsions of oil. Using a mixture of protein-gold NPs and gold NPs to coat and stabilize an oil droplet, the oil droplets can then be used for the cytosolic delivery of therapeutic proteins.[137, 138, 139].

Proteins can be loaded through conjugation or adsorption onto the surface of gold, iron, carbon nanotubes, or quantum dot NPs. However, conjugation or adsorption directly exposes the protein therapeutic to serum and cells once they are administered *in vivo*, which could lead to proteolytic activity and cytotoxicity depending on the properties of protein therapeutic itself. Mesoporous silica NPs have been extensively studied because they are inert, non-immunogenic, and possess large internal surface area and pore volume allowing for high encapsulation[140]. These particles are able to protect protein therapeutics from proteases and denaturants because they are able to encapsulate proteins within their protective shell. This NP delivery system still suffers from endosomal entrapment[80].

1.3.3.2 Lipids

Lipids are fatty acids with a hydrophilic head. This amphiphilic molecule can self-assemble into NPs possessing bilayers, called liposomes, or single monolayers, called micelles. This allows various hydrophilic and hydrophobic compounds to be encapsulated[141]. Lipid NP sizes can be controlled based on the lipid formulation and they are able to inhibit access of proteases thereby maintaining protein activity. Cationic lipids have commonly been used to deliver nucleic acids due to strong electrostatic interactions. Modifying proteins to become more negatively charged, such as conjugating cis-aconitic anhydride, can increase the intracellular delivery capabilities when using cationic lipids[80]. These cationic liposomes can adhere to plasma membranes and enter the cell *via* endocytosis or by fusing with the cell membrane allowing for release of cargo directly into the cytosol of the cell[142]. Due to many possible formulations, lipid-based NPs are capable of delivering almost any drug independent of its solubility. This stability however comes at a cost, the release profiles of these encapsulated proteins are not easily controllable and rely on lipid destabilization to release protein cargo[143]. Integration of cleavable disulfide bonds into the lipid can facilitate break up of liposomes once they reach intracellular reducing environments, facilitating release and delivery. Another advantage of lipid-based protein delivery systems is the ability to be lyophilized and administrated upon reconstitution. However, there are issues with immune response once their lipid-based delivery systems are administrated into the body. Serum proteins that mark materials for macrophage clearance, a process known as opsonization, adsorb onto the particles limiting their effect once implemented in humans[144].

Recently, exosomes have been gaining interest as possible drug delivery vehicles because they are similar in composition to cells. Exosome are extracellular vesicles between 40 – 100 nm

derived from intermediate endocytic compartments known as multivesicular bodies that fuse with the plasma membrane leading to their liberation from the cell. Exosomes exist naturally as NPs and function as intercellular communicative tools between cells making them excellent candidates for drug delivery. This also makes them less immunogenic and less cytotoxic compared with cationic lipid-based NPs[145]. A current hurdle is that there is no distinct method of isolating exosomes with high purity, making scaling of this technology difficult.

1.3.3.3 Polymeric

Polymers are macromolecules that can be designed to be biocompatible and encapsulate and control release of therapeutic protein. The properties and morphology of polymeric NPs can be tuned by changing the molecular weight and composition of the repeating units used in the polymer backbone. Furthermore, polymeric NPs can be tuned to be stimulus responsive, meaning that the NPs can change their characteristics dependent on the environment around them. Environmental triggers can be temperature, pH, light, humidity, electric fields, magnetic fields, pressure, certain chemicals, such as glucose, or enzymatic, dependent on specific cell types or microorganisms[146]. Polymers can be engineered with multivalent binding domain to allow strong binding to proteins ensuring high capsulation, however, without specific binding domains, protein encapsulation in polymeric NPs is generally low[77]. Another common issue with using polymeric NPs for the delivery of proteins is the organic solvents essential for preparing protein-containing polymeric NPs[125]. The solvents can denature proteins thereby reducing their biological activity.

Using a network of crosslinked hydrophilic polymers can produce hydrogels capable of retaining large amounts of water yet still possessing 3D architecture useful in protein delivery.

Preparation of hydrogels is mild compared with other polymeric delivery systems as they do not rely on organic solvents. Hydrogels need to be crosslinked physically or chemically to prevent their dissolution. Their high water content makes hydrogels generally biocompatible and soft in nature allowing them to mimic natural extracellular matrices and prevent cell adherence[144]. They are able to load proteins physically with high capacity and protect protein cargo from enzymatic degradation, however, this is limited to proteins that are larger than the pore mesh sizes within the hydrogel[147]. Once encapsulated within the hydrogel network proteins have limited mobility or are immobilized, which is favorable for maintaining their 3D conformation. Nanogels have been engineered to deliver protein intracellularly relying on a pH sensitive or reducible linker to achieve release of encapsulated proteins[147]. These hydrogels can also be designed with stimulus responsivity allowing for hydrogel dissolution and rapid release of encapsulated therapeutics. Without hydrogel dissolution, encapsulated proteins must rely on diffusion and swelling of the hydrogel for release, which could be useful for sustained release applications. The tradeoff of favorable protein encapsulation is that hydrogels tend to have inherent low mechanical strength than hydrophobic polymers. In general, the release profiles of hydrogels are much shorter than that achieved by hydrophobic polymers, however, efforts are being made to increase the polymer concentration or alter crosslinking methods to impart a stronger hydrogel[144].

Another interesting extension of using polymers is using amphiphilic copolymers to form supramolecular assemblies resembling biological membranes[148]. In a similar fashion to amphiphilic lipids, amphiphilic copolymers can self-assemble into vesicles or polymersomes, allowing encapsulation of protein cargo for drug delivery purposes[149]. Similarly, these polymersomes can be designed to be stimulus responsive, providing site specific delivery of encapsulated materials. The synthetic production of polymers allows manipulation and control of

polymersome size, shape, stability, stimulus responsiveness, membrane thickness, fluidity and permeability[148]. Incorporation of several different copolymers can impart multifunctionality to polymersomes allowing construction of theranostic systems or enabling multi-targeting capabilities. However, how these artificial polymersomes interact with cell membranes will still need to be elucidated before they can be clinically implemented.

1.3.3.4 Protein-based

Proteins are natural macromolecules that contain unique functionality making them suitable materials for drug delivery purposes. They are biocompatible as the byproducts of protein degradation are amino acids which are well tolerated *in vivo*. Certain amino acids contain reactive functional groups suitable for crosslinking or conjugation. NPs can be made from proteins either by self-assembly or by covalent chemistry[84]. Virus-like particles (VLPs) are self-assembled protein capsids that contain no viral enzyme protease, reverse transcriptase, and integrase making them safe and unable to replicate inside human cells. VLPs can made, but not limited to, from Gag protein derived from HIV. Fusion construct of Gag with therapeutic proteins allow VLPs to self-assemble and encapsulate the therapeutic protein inside the capsid allowing for intracellular delivery[150]. VLPs encapsulation efficiency is limited to the number of subunits that make up the capsid coat[151]. VLPs are efficiently internalized by cells, however, there is an inherent immunogenicity issue when using these viral proteins. Therefore their applications might be limited toward vaccination where generating a host immune response to crucial for success[152]. Protein ligands can also be attached onto the surface of the VLP allowing for extracellular delivery or binding cell surface receptors and triggering a cellular response[150].

Ferritin and ferritin-like cages are another well-defined hollow protein complex that can be used for drug delivery purposes. Ferritin is an octahedral iron storage protein complex made

from 24 identical subunits. Genetic fusion of therapeutic proteins and peptides to ferritin subunits do not alter cage assembly and have been used to delivery immunogenic materials for vaccine delivery[153]. Ferritin cages are less than 30 nm and their small size allows them to access many parts of the body by passive diffusion and be efficiently internalized by cells. However, they limited by their ability to encapsulate significant payloads and most proteins must be displayed on the outside of the cage. Though this many be advantageous when targeting extracellular components such as cell surface receptors, it may not be suitable for intracellular delivery due to issues with proteases that can access the therapeutic agents. The E2 protein derived from pyruvate dehydrogenase multienzyme complex can self-assemble into a 24-mer hollow structure with a cubic core or a 60-mer icosahedron with twelve 5-nm openings depending the source of the E2 protein[154]. These cages are extremely stable under extreme conditions and proteins can be attached to its interior or exterior for drug delivery with similar properties to ferritin cages[151]. Protein vaults are barrel shaped hollow structures found in most eukaryotic cells assembled from ribonucleoparticles[155]. These structures are approximate 41 x 41 x 72.5 nm^3 constituted mostly of major vault protein which makes up more than 70% of the overall mass. These major vault proteins though strong bound to one another, are non-covalently associated and impart a dynamic structure to the vault characterized by transient opening and closing known as breathing. This breathing process is known to be pH dependent, which can be utilized to load and release protein cargo based on pH stimulus. Protein vaults are not well understood like other protein cages, however, their unique structure and function indicate that there is potential for them to be successfully protein delivery vehicles[151]. Protein cages and vaults present unique monodispersed hollow structures that can be utilized for therapeutic protein loading on its interior or exterior, the low loading capacity greatly hinder their intracellular delivery potential. They may present more

useful applications for delivery to the extracellular targets because genetic fusion of therapeutic proteins to these hollow structures can be achieved with spatiotemporal control.

Fusion proteins made with silk, collagen, or elastin can form various structures dependent on the primary sequence of the self-assembly motif[156]. These fusion constructs differ from protein cages and vaults as they are dense structures that can minimize unused space in the ultimate intracellular delivery vehicle. The most widely used is the elastin-like polypeptide (ELP), a thermal-responsive peptide made from repeating units of VPGXG (V – valine, P – proline, G – glycine, X – any amino acid except proline). These peptides are soluble at low temperatures and aggregate when heated above their transition temperature. When fused to a therapeutic protein, the ELP retains its thermoresponsivity allowing NP formation and delivery[157]. Its thermal-responsive and concentration-dependent coacervation allows for controlling the assembly and disassembly NPs and tuning the release of therapeutic protein[151]. Another interesting example is the genetic fusion of a therapeutic protein to a repebody[158]. Repebodies are engineered scaffold proteins adapted from leucine-rich repeats motifs that are commonly found in variable lymphocyte receptors. Variable lymphocyte receptors are a part of the adaptive immune response in jawless vertebrates and have a characteristic horseshoe-shaped solenoid fold that are researched as alternatives binding scaffolds to immunogloubulin antibodies[158]. Repebodies can be engineered to bind specific proteins, such as EGFR, and when fused to a therapeutic agent such as apoptin, self-assembly into NPs occurs driven by the apoptin[159]. This NPs are monodispersed, have high targeting, and have shown facilitate its intracellular delivery. The insights from these self-assembly driven techniques has led to design of minimal sequences for self-assembly using peptides. When cationic peptides based on poly-lysine and poly-arginine are mixed with therapeutic anionic peptides, they can product spherical

functional nanoparticles[160]. Amphipathic peptides can be mixed with therapeutic proteins to form non-covalent complexes capable of intracellular delivery[136]. These cationic and amphipathic peptides are smaller than other self-assembly motifs and therefore can increase the ratio of therapeutic protein to assembly protein needed for delivery[151]. Cationic peptides still require genetic modifications, however amphipathic peptides do not. There are still issues of cytotoxicity associated with these cationic and amphipathic peptides similar to the CPPs discussed in Chapter 1.3.2 that limit their intracellular applications.

Desolvation is commonly used method to form protein NPs[161]. It is based on the differential solubility of proteins in different solvents. Typically, an organic solvent such as acetone or ethanol is added in a controlled manner to an aqueous solution of soluble protein. The addition of this desolvating agent leads to precipitation of the soluble protein. A schematic of the process can be seen in Figure 1.1. The size of the is dependent on protein concentration, desolvant, the volume ratio of desolvant to protein solution, pH, and temperature[162]. Heat and emulsions can also be used to form protein NPs, however, these techniques are generally produce larger sizes of NPs compared with the desolvant techniques and there is lower preservation of protein structure and function. Protein NP preparation made by heat results in denatured proteins and preparations made with emulsions must also remove all the oil before therapeutic use[84]. Glutaraldehyde is typically used to crosslink the NPs made through desovlation and using cleavable linkers can help make the NP stimulus responsive. An example would be a disulfide bond crosslinker that is capable of being reduced by intracellular GSH to break up the protein NP[163]. Crosslinking requires functional groups that can be found on some reactive amino acids such as primary amines on N-terminus and lysines, carboxyls found on C-terminus, aspartic acid, and glutamic acid, and sulfhydryls found on cysteines. The ease of desolvation along with its

scale up potential makes it an attractive technique for producing NPs, however, use of organic solvents can denature some proteins and desolvated protein NPs are not as monodispersed as self-assembled structures. Desolvated protein NPs do not require fusion to a self-assembly motif and can theoretically achieve a much higher encapsulation efficiency.

Typically, protein NPs have been used to deliver small molecules[164], however, a protein NP could be made entirely of therapeutic protein and would be an effective carrier and therapy combined into one. If desolvated NPs are made entirely of the therapeutic protein, this would maximize therapeutic loading efficiency, however, retention of protein function after exposure to organic solvent and covalent crosslinking is crucial. Making protein NPs completely of therapeutic protein is sometimes not feasible if the therapeutic protein solubility is too low and therefore a carrier protein must be co-desolvated. The addition of a carrier protein can help reduce the size of the final protein NP preparation by increasing the starting protein concentration, a known variable to influence size. The carrier protein can also be another therapeutic protein or multiple therapeutic proteins to create a multi-functional NP. This highlights the modularity of the protein NP delivery system.

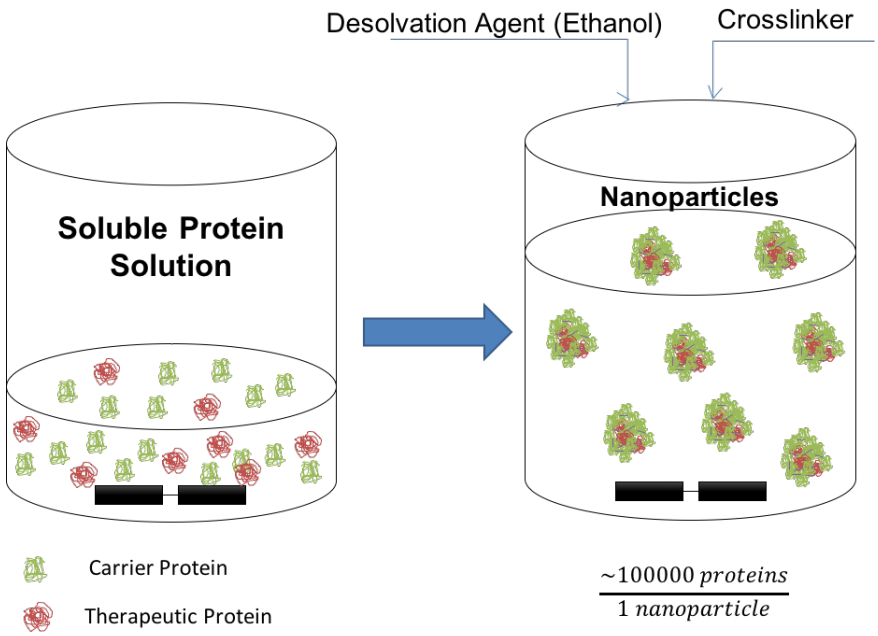

Figure 1.1 Schematic representation of protein NP desolvation. Estimate of number of proteins per NPs are based on the theoretical volume of a protein based on molecular weight and the volume of a 250 nm spherical NP.

1.4 Intracellular Nanoparticle Delivery

Whereas traditional small molecule drugs enter cells mainly through passive diffusion through the cell membrane or active transport *via* binding to a cell surface receptor, NPs are typically internalized by cells *via* endocytosis[165]. Endocytosis is a group of energy dependent processes by which extracellular entities are internalized within a membrane vesicle called an endosome. Depending on the NP size, surface charge, surface hydrophobicity, and the cell type it is interacting with, the endocytic mechanisms by which it enters the cells can be vastly different[166]. NPs internalized *via* endocytic processes are enclosed within endosomes coated with different kinds of cytosolic proteins that polymerize on the cytosolic side of the membrane. These initial protein coatings dictate the intracellular trafficking mechanism and influence the destiny of an NP-containing vesicle in the cell. Most NP delivery challenges occur in this phase

as endosomes containing NPs are usually destined for lysosomal degradation or recycled and exocytosed[127, 128]. Endosomal escape is most desired so NPs can access the cytosol where many druggable targets reside. Though some therapeutics have function in endo/lysosomes and therefore do not require endosomal escape. The lysosome can be the desired location for treating lysosomal storage diseases or for vaccine delivery. Other delivery applications include transcytosis to cross cell barriers and reach a target tissue underneath, such as transcytosis through the lungs or the blood-brain barrier[165]. Therefore, understanding the endocytic mechanisms can provide insight as to how to control cellular internalization and trafficking of NPs.

1.4.1 Endocytosis

Endocytosis is the process by which extracellular materials gain entry inside the cells. It be generally divided into phagocytosis, which is the uptake of large particles, or pinocytosis, which is the uptake of fluids and solutes. Furthermore, pinocytosis can be divided into receptor-mediated process such as clathrin-mediated or caveolae-mediated and nonspecific processes such as macropinocytosis, though now more forms of pinocytosis are being elucidated such as arf6-dependent, flotillin-dependent, cdc42-dependent, and rhoA-dependent processes[167]. Phagocytosis is a special type of endocytic pathway that is predominantly used by phagocytes, such as macrophages, used to clear large objects ranging from 0.5 μm – 10 μm, such as bacteria. If smaller NPs are to target this pathway, they must first be opsonized by immunoglobulins, complement components, and other blood serum proteins. The best-studied receptors that initiate phagocytosis are Fc receptors[168], but mannose/fructose and scavenger receptors are also used for phagocytosis depending on the opsonized proteins and surface chemistry of the NP[169].

Unlike phagocytosis, which is reserved for phagocytes, clathrin-mediated endocytosis is performed by all mammalian cells and is an important pathway for nutrient uptake and intracellular communication[166]. Clathrin-mediated endocytosis is best classified by the clathrin coated pits that form around vesicles that invaginate from the cell membrane. Receptor-mediated clathrin endocytosis is the most studied mechanism however, clathrin coated pits are also known to form stochastically by the clustering of clathrin around a random collision event at the plasma membrane[170].

Caveolae-mediated endocytosis is defined by caveolae proteins that coat vesicles. This type of endocytosis is used abundantly by endothelial cells associated in regions of the lipid membrane with high cholesterol and lipid content[171]. Microdomains on the cell membrane containing high lipid and cholesterol content are called lipid rafts[172]. These unique features are the target for certain pathogens that utilize caveolae-mediated endocytosis such as the SV40 virus[173]. Caveolae-mediated processes are also involved with transcytosis and uptake kinetics are known to occur at much slower rates than clathrin-mediated endocytosis[168]. Caveolae pits are much smaller flask-shaped vesicles, no larger than 50-80 nm, and there is no study that unambiguously shows that caveolae vesicles can accommodate NPs larger than 100 nm[174].

Macropinocytosis is another common endocytic process used by nearly all cells except endothelial cells found in the brain[166]. It is defined by non-specific membrane ruffling creating large vesicles called macropinosomes ranging from 0.5 μm – 10 μm. They are similar to phagosomes, except they form around extracellular fluid instead of solid objects.

There are certain "guidelines" that influence the internalization and uptake of NPs. NP size is known to be a determinant of uptake pathways as well as being crucial to many other *in vivo* functions such as circulating times, targeting and clearance. The size of vesicles involved in

each of the endocytic pathways is used as an approximation of the size of NPs that it can accommodate. Typically the sizes are proposed to be 60 – 80 nm for caveolae processes, ~100 nm for clathrin processes, and particles up to several microns can be internalized through micropinocytosis and phagocytosis. There are instances where NPs larger than the clathrin vesicle size have been shown to utilize that pathway[168]. In general, it appears that many of these endocytic pathways can accommodate smaller particles, meaning more access to the cell and faster internalization.

Surface charge can promote internalization through interactions with the cellular membrane. The negative charge of the plasma membrane means that cationic NP have an electrostatic force driving association and increasing internalization rates. Anionic NPs experience repulsive forces from the cell membrane. However, they can be captured by cells through interactions with positive sites on membrane proteins[175]. Neutral NPs can interact with cells by hydrophobic interactions and hydrogen bonding[176]. Cationic NPs have been reported to enter cells mainly through clathrin mediated endocytosis, anionic NP through caveolae-mediated endocytosis, and neutral NPs via all routes with no preference[166]. However, additional reports showing that cationic and anionic NPs can utilize several or all these pathways highlights the complexity of cellular internalization of NPs.

Hydrophobic NPs have a higher attraction to the cell membrane than hydrophilic NPs, leading to increased uptake kinetics. Poly-ethylene glycol (PEG) has long been used as a surface modification to increase the hydrophilicity of NPs, extending circulation times by preventing uptake and clearance. Hydrophobic NPs have been reported to be internalized by endothelial cells through caveolae-mediated endocytosis[177]. Since caveolae is predominantly localized on lipid rafts, hydrophobic NPs have a higher propensity to associate with these areas.

Of particular interest is the protein corona that opsonizes NPs once they enter biological media. Though some physiochemical properties of NPs are highlighted here as influencing the cellular endocytic processes, it is now known that "bare" NP surfaces are rarely "seen" by the cell. Rather, serum proteins compete and bind to the surface of NPs and this layer, called the protein corona, defines the biological identity of the NP[178]. The total protein concentration in serum is around 60 – 80 mg/mL. When NPs enter the bloodstream, large quantities of serum proteins weakly bind to the surface and over time are replaced by higher affinity proteins following the Vroman effect[179]. The higher affinity proteins that bind to the NP surface do so irreversibly forming the inner "hard corona" where lower affinity proteins protein reversibly bind forming the outer "soft corona". A new report shows that the corona morphology is not a dense shell around the NP, but rather a loose network of proteins[180]. This network of protein is ultimately what interacts with cells, allowing interactions of specific serum proteins with cell surface receptors to dictate internalization.

Different NP physiochemical characteristics were discussed previously as influencing cellular internalization. It is more accurate to portray NP characteristics as influencing the corona that forms around the NP, which will ultimately interact with the cell surface and influence internalization. NP size affects the amount of protein in the corona with larger NPs having more total proteins and smaller NP having increased corona thickness with decreased conformational changes of the adsorbed proteins[179]. NP charge affects the conformation of the adsorbed corona, with cationic NPs denaturing proteins and anionic NPs maintaining protein conformation[181]. NP hydrophobicity can also increase the amount of proteins in the corona, increasing affinities of specific types of serum proteins, and causing more conformational changes[179]. Hydrophilic NPs adsorb "stealth" serum proteins that decrease cellular internalization such as ApoE and

clusterin[182, 183]. The environment in which corona adsorption occurs such as temperature, pH, shear stress, and exposure time can also affect corona composition[166]. Most studies on protein corona are performed on hard NPs such as gold or polystyrene. Protein NPs would theoretically have softer mechanical properties, behaving more like hydrogels. The corona on hydrogels altered based on stimulus responsive hydrophilic polymers allowing tuning of the corona composition on NPs[184]. The protein corona has not been studied on protein NPs and they may behave differently from other NPs since their surface is already comprised of proteins.

1.4.2 Intracellular trafficking mechanisms

Regardless of the pathways NP use to enter the cell, they are all enclosed within vesicles limiting access to the cytosol. This is a major roadblock to utilize NPs for delivery of intracellular protein therapeutics. The initial stage vesicles used to engulf NPs at the cell surface are well known and defined. Materials that enter the cell via phagocytosis are entrapped within phagosomes. Material inside phagosomes are destined for degradation and destruction by acidification and enzymolysis by fusion with early endosomes and eventually lysosomes[185]. Generally, NP delivery aims to avoid this pathway since the usual goal of delivery is to reach the cytosol before lysosomal destruction unless the target of delivery is the lysosomes themselves or if the NPs have a pH or enzymatic trigger.

Clathrin-mediated endocytosis is defined by the cytosolic clathrin proteins that coat the vesicles during membrane bending. Once internalized in the cell, the clathrin lattice will eventually uncoat the vesicle allowing recycling of the clathrin units[170]. These uncoated vesicles will deliver and fuse their cargo to early or sorting endosomes that are slightly acidified (pH ~ 6). Early endosomes eventually mature into late endosomes defined by pH (pH ~ 5). After

maturation, late endosomes will fuse with lysosomal vesicles with the harsh acidic and enzymatic environment that will degrade the contents of the vesicle.

Caveolae-mediated endocytosis is typically associated with lysosomal avoidance and is the preferred route of many pathogens[186]. Once caveolae coated vesicles invaginate into the cell, they fuse with caveosomes or multivesicular bodies, which have neutral pH and lack the enzymes that are typically found in early endosomes[187]. Due to the mild vesicular environment found within caveosomes, targeting caveolae-mediated uptake has been sought as the preferred pathway for nanocarriers. However, it is now debated whether the caveosomes actually exist as their own entity or if they are actually early endosomes[188]. Multivesicular bodies can also become lysosomes facing the same fate as clathrin vesicles[189]. It appears that once these coated pits shed their coat proteins and enter the milieu of other vesicles that reside in the cell, it is hard to determine the ultimate fate of these vesicles.

Macropinosomes are distinct from other endocytic pathways as they do not have any specific coating on them. The intracellular fate of macropinosomes seem to be dependent on the cell type, as macrophage macropinosomes fuse with lysosomes and epithelial macropinosomes are recycled and release their contents back into the extracellular space[190]. Though in most cases, macropinosomes fuses with multivesicular bodies and eventually acidify and shrink[168]. Macropinocytosis also seems to be an important mechanism for nutrient uptake in cancer cells, which tumor cells rely on to meet their unique metabolic needs[191]. This supports the notion that though macropinocytosis is highly conserved in many cells, each cell type utilizes this non-specific endocytic pathway for different needs.

Previously it seemed as though the endocytic uptake mechanism could dictate or determine the intracellular fate of NPs, though more recently this does not appear to be the

case[192]. Crosstalk between the different pathways and new clathrin- and caveolae-independent endocytic pathways have introduced even greater levels of complexity of the trafficking mechanisms in a cell. The low cytosolic delivery efficiency common to many NP delivery vehicles has been a significant challenge. Several techniques have been developed that are reported to promote the endosomal escape of NPs. Methods such as proton-sponge effect, which utilizes the buffering capacity of unprotonated moieties, such as amines, to absorb protons during pH drops leading to an influx of water that eventually bursts the endosome. This mechanism is heavily debated[108] though the effects of release and delivery are still observed. Amphiphilic and hydrophobic CPPs described in Chapter 1.3.2 have also been reported to associate with membrane leading to escape. Many of these techniques still suffer from low efficiency and cytotoxicity[193]. Most vesicles, once internalized, will follow a similar evolution of early endosome to late endosome to lysosome or recycled and exocytosed. Endosomal escape mainly focuses on the pH change as a trigger for moieties that can promote membrane disruption and release though some endosomes may be quickly recycled and never exposed to these triggers. Further studies are needed to elucidate these complex trafficking mechanisms to enable design of NPs with improved delivery efficiency and possibly allow for localization to subcellular targets.

1.5 Oral Delivery

NPs have been used for both localized intestinal delivery and systemic delivery although these appear to be two seemingly different goals[194]. Systemic delivery is most commonly achieve with injections as other routes (buccal, nasal, pulmonary, transdermal, oral) face difficult barriers amounting to extremely low bioavailability[194]. For IBD therapeutics, localized intestinal delivery is desired and therefore methods to achieve systemic delivery will not be discussed further. Oral

delivery is the most pertinent and logical for treating inflammatory bowel disease as therapeutics must reach localize in inflamed regions of the intestine. The oral route is not sensitive to drug size and has a more favorable safety profile due to minimal systemic exposure and reduced immunogenicity, as well as having improved patient compliance[195].

Excluding oral vaccines, there are only six biomacromolecules that are Food and Drug Administration (FDA) approved for oral delivery in the nearly 100 years since the first attempts, speaking to the difficulty of oral administration[195]. The gastrointestinal tract is evolutionally optimized to break down proteinaceous materials. Acidic pH in the stomach denatures and unfolds protein allowing enzymes in the stomach to recognize and access more motifs for cleavage. After leaving the stomach, enzymes present in the small intestine and colon continually work to cleave proteins into small fragments allowing them to be absorbed as nutrients. The presence of mucus creates a physical barrier made up of constantly renewing negatively glycoproteins limiting access to the epithelial cells that reside underneath.

Common methods to increase the oral bioavailability of protein therapeutics involve using protease inhibitors to prevent enzymatic degradation and permeation enhancers to facilitate transport across mucus and through the epithelium[196, 197]. These methods have traditionally been used for systemic delivery of soluble proteins and chronic use of these inhibitors and enhancers can lead to severe side effects[198]. Conjugating proteins with cell penetrating peptides or mucoadhesive polymers can increase targeting and minimize off-target effects. However, these methods still suffer from low penetration and bioavailability from natural mucus turnover[198].

NPs can be used to target inflamed tissue. Inflamed mucosa induced by IBD exhibits different properties than healthy mucosa. A consequence of inflammation is the disruption in the epithelial barrier resulting increased permeability through the mucus. This increase in

permeability is similar to the enhanced permeability and retention effect observed in tumors[199]. NPs preferentially localize in these areas of the intestine as a function of size. 100 nm particles localize better than 1 μm particles, which localize better than 10 μm particles[200]. Anionic NPs are also reported to localize better in inflamed tissue than cationic particles due to the increased presence of positively charged transferrin and proteins from eosinophils[201]. They also face less resistance diffusing through the mucos layer due to electrostatic repulsion. Cationic NPs show no preference toward inflamed tissue as they exhibit mucoadhesive properties due to electrostatic interactions with the negatively charged mucus layer. Regardless of charge, NPs possess passive targeting to inflamed mucosa with smaller NPs able to localize to a greater extent. Gastric passage remains an issue as the stomach as it is the first major obstacle protein therapeutics encounter.

Therapeutic soluble proteins have been co-delivered with protease inhibitors to prevent enzymatic degradation and permeation enhancers to facilitate transport across the epithelium[196, 197]. These methods have traditionally been used for systemic delivery of proteins, though chronic use of these inhibitors and enhancers can lead to severe side effects[198]. Conjugating proteins with cell penetrating peptides or mucoadhesive polymers can increase targeting and minimize off-target effects. However, these methods still suffer from low penetration and bioavailability from natural mucus turnover[198]. To overcome these challenges, localized intestinal delivery of protein therapeutics has typically been accomplished by NPs or MPs made from biodegradable polymers and hydrogels[194]. NPs are able to passively target inflamed tissue[202], enhance mucus penetration, and membrane permeation[203]. MPs can provide a larger depot for protein therapeutics that can be engineered to be stimulus responsive[204]. NPs and MPs can improve protein stability and be engineered to target specific regions of the gastrointestinal tract[199]. Nanoparticles-in-microsphere

oral system (NiMOS)[205], combines these two particulate systems in a unique approach for oral gene delivery[206, 207]. Gelatin NPs encapsulating plasmid DNA were then encapsulated in poly(epsilon-caprolactone) MPs and shown to transfect the small intestine and colon of rats. NiMOS has the advantages of both NP and MP delivery systems as NPs were capable of penetrating the mucosal barrier and MPs protected NPs from enzymatic degradation until they reached the absorbing epithelium.

Alginate and chitosan are two natural polysaccharides generally regarded as safe (GRAS) by the FDA that have been used as NPs or MPs for oral delivery of insulin[208, 209, 210], BSA[211, 212], hemoglobin[213], probiotics[214, 215], and cells[216, 217]. Alginate can form hydrogels under mild gelation conditions ideal for protein encapsulation[218]. A chitosan coat can be used in conjunction with alginate hydrogels to remedy the problems of drug leakage[219]. Alginate hydrogels shrink at gastric pH and the complementary electrostatic properties of anionic alginate and cationic chitosan allow interpolymeric associations strengthened by the protonation of chitosan amine groups at low pH. At intestinal pH, which ranges from pH 6 to pH 7.5 depending on location in healthy individuals but is lower in IBD patients[220], alginate hydrogels swell and the charge of chitosan reverses to negative, allowing release of encapsulated cargo. Alginate/chitosan MPs can also protect against enzymatic degradation by providing steric hindrance and lowered collision opportunities. Mammals lack alginase[221] and chitosanase (though have chitinase[222]) meaning that alginate and chitosan do not get digested *in vivo*, but rather rely on the ionic exchange between the crosslinked calcium ions with extrastitial monovalent sodium or potassium ions to break up the alginate core.

In UC, a form of IBD that mainly localizes in the colon, colon-specific targeting is desirable. Colonic targeting has been accomplished using pH sensitive polymer as coatings. Most

commonly used are methacrylic acid copolymers (Eudragit®)[223]. Varying the composition of the side groups can manipulate the pH at which these polymers dissolve, most commonly in the range of pH 6 – 7 allowing them to bypass the stomach while protecting the active therapeutic. Some issues with this polymer coating include the organic solvents used to dissolve the polymer and the need for careful tuning of different copolymers to achieve desired pH sensitivity[223]. The potential for degradation by bile acids in the duodenum can cause undesirable and premature drug release[202]. Patients with UC generally have lower colon pH than healthy individuals resulting in the polymer coating never dissolving. Redox-responsive targeting systems rely on the abnormally high levels of reactive oxygen species (ROS) produced by activated phagocytes in inflamed intestinal tissue. Polymers have been developed that cleave in response to ROS thereby releasing therapeutic compounds[224]. Colon targeting ligands can also be used to increase therapeutic efficacy and reduce side effects. I-CAM is known to be upregulated in inflamed regions of the colon and antibodies can be used against these adhesion sites. Using antibodies as targeting ligands suffer the same obstacles as protein therapeutics and NPs using these targeting antibodies were shown to deposit in the stomach and upper GI tract[225]. Targeting macrophages *via* mannose receptors, macrophage galactose-type lectin, and F4/80 surface receptors to deliver siRNA have shown positive results as macrophages are the primary perpetuators of inflammation in IBD[202].

1.6 Motivations and Objectives

Inflammatory bowel disease is a debilitating disease and there are significant side effects for current small molecule treatments. Protein drugs are highly specific and possess several advantages over small molecules. While most approved proteins therapies target extracellular

components or cell surface receptors, there exists abundant intracellular components that can modulated as well. AvrA, a bacterial effector enzyme with intracellular activity, is introduced as a potential therapeutic for chronic inflammation with dual anti-inflammatory and anti-apoptotic effects. AvrA is an evolved enzyme possessing a mechanism of action not found in eukaryotes, making AvrA a unique therapeutic to combat disease. The barriers to cytosolic delivery of enzymes with intracellular activity are high and many of the methods used suffer from low encapsulation or reduce the activity of the therapeutic protein during fabrication. Protein NPs offer a means of cytosolic delivery. However, it is not understood how the properties of protein NPs affect their intracellular delivery and cytosolic localization. In particular, the properties are likely to affect the protein corona formed upon contact with physiological fluids, which in turn has a significant effect on cellular uptake and trafficking.

Implementing therapeutic AvrA protein NPs for the treatment of inflammatory bowel disease requires delivery to inflamed regions of the intestine to maximize therapeutic benefit. Transrectally delivery is an effective method for AvrA NPs, however, this route is undesirable for patients and the limited area of therapeutic effect prevent its clinical use. Oral delivery of protein therapeutics is advantageous, but difficult, because the stomach functions to break down proteinaceous materials. Therefore, the gastric passage and intestinal release of protein NPs is crucial for the clinical implementation of AvrA NPs.

The objectives of this thesis are: (1) engineer protein NPs to enhance the intracellular delivery of functional AvrA, (2) maximize cytosolic delivery of AvrA by altering protein NP properties, and (3) develop an oral formulation to improve the clinical potential of AvrA.

1.7 Thesis Overview

The overall goal of this thesis is to develop therapeutic AvrA NPs for the treatment of inflammatory bowel disease. To accomplish the objectives stated in the previous section, Chapter 2 details the synthesis and characterization of protein NPs as delivery vehicle for AvrA and evaluates their performance *in vitro* and *in vivo*. In Chapter 3, an oral delivery vehicle is engineered for the gastric protection and intestinal release of AvrA NPs. In Chapter 4, protein NPs with various physiochemical properties are developed to study the role of adsorbed corona and its contributions to cytosolic delivery. Finally, Chapter 5 summarizes the work in this thesis and provides an outlook with future directions.

CHAPTER 2 : AvrA Nanoparticles for Treatment of Inflammatory Bowel Disease

2.1 Introduction

IBD (CD and UC) are chronic relapsing autoimmune disorders of the intestinal tract that affect 1-2 of every thousand persons in developed countries and incidence is increasing.[5,6] In the intestine they manifest with acute and chronic inflammation, tissue injury, scarring and predisposition to adenocarcinoma, and may also have systemic effects. IBD is generally recognized to represent aberrant immune recognition of the normal commensal microbiota. Current therapy involves inflammatory suppression with local 5-aminosalicylates, systemic corticosteroids, cytotoxic immunosuppressants, or biologicals, such as anti-TNF monoclonal antibodies. While effective, these are fraught with the complications of systemic immunosuppression and other toxicities.[10,11] There is increasing interest in use of beneficial bacteria (probiotics) as a therapy, though to date only modest efficacy has been reported.[226]

It is known that enteric bacterial pathogens have evolved mechanisms to suppress inflammatory and immunoregulatory pathways through active interference with regulators of the inflammatory response.[35,36] Enteric pathogens influence eukaryotic pathways by soluble effector proteins that are translocated into the cytoplasm of target cells *via* a T3SS and have evolved to usurp host cellular functions for the benefit of the invading organism.[227] AvrA, from *Salmonella,* is one such protein. It is a member of a family of acetyltransferases that covalently modify and inactivate members of the MAPK superfamily, and thus have potent and diverse effects on a wide variety of eukaryotic growth, survival and immune pathways.[42] We have shown that AvrA overexpressed in transfected cells,[41] or in a *Drosophila* transgenic model,[47] blocked activation of NF-κB, JNK MAPK, and transcriptional activation of a range of inflammatory effector genes. AvrA acetylates MKK4/7, accounting for the blockade of JNK. Another laboratory demonstrated

similar effects in a yeast model.[48] Remarkably, in yeast, flies, human cells and murine intestinal epithelia, AvrA-mediated signaling blockade occurs without induction of the apoptotic cell death characteristically seen during inhibition of host stress signaling pathways,[41, 42, 47, 48] thus making this activity an ideal therapeutic approach for IBD or other forms of inflammation. However, a major challenge in realizing the therapeutic potential of AvrA, or any exogenous protein effector, is the ability to deliver it locally through the harsh environment of the gastrointestinal tract, and into the resident epithelial and immune cells without compromising the biological activity of the protein. *Salmonella* meets this challenge through use of TTSS. However, in *Salmonella* infection AvrA is a SPI-1 TTSS effector protein that is co-delivered along with other virulence proteins,[48, 70] which can have negative effects, such as promotion of colonic tumorigenesis.[71, 72] Therefore, an alternative delivery approach is necessary to deliver only AvrA in the absence of *Salmonella* and safely access its anti-inflammatory functions.

NPs have been investigated for a variety of intraluminal gut applications including vaccination,[228] diabetes,[229] and IBD[224, 230, 231, 232, 233, 234, 235] that target different cell types for systemic or local delivery. Previous IBD studies have encapsulated small anti-inflammatory drugs or siRNA in biodegradable polymeric micro and NPs.[232] The primary benefits seen were reduced systemic side effects and reduced dosage required for the same therapeutic response. Furthermore, higher particle deposition has been seen in animals with induced colitis as compared to healthy animals, perhaps a consequence of depleted mucus, presence of phagocytic cells, or epithelial barrier disruption observed in inflamed tissue.[200, 232, 233, 236] In the case of protein drugs, however, polymeric delivery particles have limitations. Protein loading is extremely low or the particles are too large to be internalized by cells, and harsh fabrication or degradation conditions can damage the protein.[234, 237, 238, 239, 240] We have adapted a protein desolvation process[241, 242] to create condition-responsive

cross-linked protein NPs made from AvrA that can uncross-link in the reducing environment observed inside cells, while maintaining the bioactivity of the AvrA cargo (Figure 1.1). With these particles, we demonstrate the ability to suppress proinflammatory pathways *in vitro* and tissue inflammation in murine model colitis. This innovative approach has potential as a IBD therapeutic and establishes a drug discovery paradigm that exploits the evolution of bacterial immunoregulatory mechanisms and engineers a NP delivery strategy essential for clinical viability.

2.2 Experimental Methods

2.2.1 Recombinant production of AvrA, mAvrA, and eGFP

eGFP gene was contained in a pPROTet plasmid (Clontech Laboratories) and was expressed constitutively in BL21 *Escherichia coli* with 34 μg/mL of chloramphenicol (VWR) in 2XYT media. eGFP was purified on Ni-NTA agarose (Qiagen) following manufacturer's native imidazole purification protocol.

The AvrA/mAvrA gene was contained in a pGEX-4T-2 (GE Lifesciences) plasmid and expressed in AFIQ *Escherichia coli* with 34 μg/mL of chloramphenicol and 200 μg/mL of ampicillin (VWR) in 2XYT media. AvrA bacterial cultures were grown to o.d. 0.7 at 37^{o}C and induced with 0.4 mM isopropyl β-D-thiogalactoside (IPTG) at 25^{o}C for 4 hr. AvrA was purified first with glutathione sepharose 4B (GE Healthcare) following manufacturer's protocol and then repurified on Ni-NTA agarose following manufacturer's native imidazole purification protocol. Purified proteins were concentrated using 10k MWCO centrifugal ultrafiltration devices (Millipore) using eGFP concentration ~12mg/mL and AvrA concentration ~1mg/mL in elution

buffer (250 mM imidazole, 50 mM sodium phosphate monobasic, 300 mM sodium chloride, pH 8) determined by Nanodrop 2000c (Thermo Fisher Scientific) using MW = 26.95kDa and ε = 61000 cm^{-1} M^{-1} for eGFP and MW = 59.84kDa and ε = 60910 cm^{-1} M^{-1} for AvrA.

2.2.2 Nanoparticle synthesis through desolvation

Protein particles were prepared by the desolvation technique as previously described[162]. In brief, 600 μg of eGFP and ~25 μg of AvrA-GST or mAvrA-GST in 100 μl imidazole solution (250 mM imidazole, 300 mM NaCl, 50 mM NaH_2PO_4; pH 8) were placed in a glass vial. The protein solution was desolvated by continuous, drop-by-drop addition of 400 μl ethanol at a rate of 1 ml/min. After desolvation, particles were crosslinked with 2 mg/ml Dithiobis(sulfosuccinimidyl-propionate) (DTSSP; Pierce) at a ratio of crosslinker to lysines of 1:2.2. After 2 h stirring, the cross-linking reaction was stopped by centrifugation at 1000 g for 1 min and removal of supernatant. Particles were re-suspended in PBS and sonicated on ice for 1 s every 15 s at 30% amplitude, for a total of 5 minutes.

2.2.3 Size, zeta-potential, gels, and western blot characterization of nanoparticles

Particle size distribution was measured by dynamic light scattering using a Zetasizer Nano ZS90 (Malvern Instruments Ltd). All samples were measured at 25°C and a scattering angle of 90°. Average particle size was calculated as the arithmetic mean of the distribution of at least 3 batches of particles and the standard deviation was calculated as the variance between average diameters of the batches using the following settings: proteins setting for NP detection and manufacturer PBS settings as the dispersion medium. The zeta potential was determined by

measuring the electrophoretic mobility of the NPs in PBS and 10 mM HEPES buffer using the same instrument.

2.2.4 Confocal microscopy for qualitative assessment of nanoparticle uptake

J774.A1 cells were purchased from American Type Culture Collection and cultured in Dulbecco's Modified Eagle's Medium (DMEM), supplemented with 10% (v/v) fetal bovine serum (FBS). J774.A1 cells were seeded at a density of 10^4 cells per well in an 8-well chamber slide system (Nunc LabTek II, Thermo Scientific) with growth medium. After 14 hours, cells were incubated for 6 hours with fresh cell media containing 300 μg/ml soluble AvrA-GST and eGFP or AvrA-eGFP NPs. Cells were washed twice with ice cold PBS and fixed with 3.7% paraformaldehyde for 15 minutes at room temperature. Cells were permeabilized with 1% Triton X-100 in PBS for 15 minutes at room temperature and rinsed three times in PBS. Cells were incubated with 2 μM TO-PRO-3 (Molecular Probes) and 0.165 μM rhodamine phalloidin (Biotium) in blocking buffer for 20 min at room temperature. Cells were washed three times with PBS and mounted for imaging in a Zeiss LSM 700 confocal microscope.

T84 model human intestinal epithelial cells were prepared on 0.33-cm^2 permeable filters and cultured in DMEM/F12 supplemented with 5% FBS. T84 cells were used after they had achieved a stable transepithelial resistance of >1,000 $\Omega \cdot cm^2$. T84 cells were cultured in transwell chambers in a 24 well plate. Soluble AvrA-GST and eGFP or AvrA-eGFP NPs were administered to cells and cells were prepared as described for J774.A1 cells. Transwell membranes were cut using a razor blade and mounted onto a glass slide for imaging.

2.2.5 Flow cytometry for quantitative assessment of nanoparticle

J774.A1 cells were purchased from American Type Culture Collection and cultured in Dulbecco's Modified Eagle's Medium (DMEM), supplemented with 10% (v/v) fetal bovine serum (FBS). SK-CO15 epithelial cells were cultured in DMEM with 10% FBS and 1% non-essential amino acids. J774.A1 macrophages or SK-CO15 epithelial cells were plated at a density of $2x10^5$ cells per well in a 24-well dish. After 14-16 hours of incubation, cell media was replaced with fresh media containing 300 μg/ml AvrA-eGFP NPs or soluble AvrA-GST an eGFP and incubated for 6 hours. Control cells were incubated with AvrA-eGFP NPs or soluble AvrA-GST and eGFP at 4^oC. Cells were washed twice with ice cold PBS, scraped or trypsinized, and fixed with 3.7% paraformaldehyde for 15 minutes at room temperature. Fixed cells were washed 3 times by centrifugation with ice cold PBS and permeabilized with 0.25% Triton X-100 in PBS for 15 minutes at room temperature. Cells were rinsed three times in PBS and incubated with purified anti-AvrA antibody in 6% BSA and 10% FBS in PBS for 1h. After this, cells were washed 3 times with PBS and incubated with 20 nM Qdot 655 VIVID secondary antibody conjugate (Invitrogen) in 6% BSA in PBS for 1 hour. Cell were washed 3 times with PBS and analyzed in an LSR II flow cytometer (Becton Dickinson and Company). Positive events were identified as cells with simultaneous increase in green fluorescence and quantum dot fluorescence.

2.2.6 Endocytic route of nanoparticles determined by endocytosis inhibitors

J774.A1 cells were purchased from American Type Culture Collection and cultured in Dulbecco's Modified Eagle's Medium (DMEM), supplemented with 10% (v/v) fetal bovine serum (FBS). SK-CO15 epithelial cells were cultured in DMEM with 10% FBS and 1% non-

essential amino acids. J774.A1 macrophages were plated at a density of $2x10^4$ cells per well in a 24-well dish. After 14-16 hours of incubation, cell media was replaced with fresh media containing endocytosis inhibitors. Macropinocytosis was inhibited using 2 mM amiloride (MP Biomedicals, LLC). Caveolae-mediated endocytosis was inhibited using 300 μM genistein (TCI America). Clathrin-mediated endocytosis was inhibited using 20 μg/ml chlorpromazine (Alfa Aesar). Energy dependent endocytosis was inhibited by incubation at a 4°C (cells were also pretreated at 4°C for one hour prior to NP introduction).

After 1 hour pretreatment with inhibitors, cell media was replaced with fresh inhibitor and AvrA-eGFP NPs or positive controls (Clathrin-mediated: transferrin-CF640R, Caveolae-mediated: BSA-CF640R, Macropinocytosis: 10,000 MW Dextran-CF640R, all purchased from Biotium) suspended in PBS (50% v/v). 25 μg/ml of positive control or 300 μg/ml NPs were used. Cells were incubated for an additional 3 hours, then washed twice with ice cold PBS, scraped and resuspended in PBS. Cells were analyzed in an Accuri C6 flowcytometer and relative endocytosis was quantified as the ratio of mean fluorescence of the sample population to fluorescence of the control population (no particles given).

2.2.7 Endosomal escape determined by hemolysis

Washed red blood cells (RBCs) (Lampire Biological Laboratories) were diluted to a final concentration of 0.5% v/v in PBS solutions at pH 7.4, 6.5, and 5.4. NPs/soluble eGFP/mAvrA/AvrA were prepared at a volume of 100 μL at pH 7.4, 6.5, and 5.4 and incubated with an equal volume of the various RBC solutions at 37^oC for 1 hour (final eGFP concentration = 150 μg/mL, final mAvrA/AvrA concentration = 12.5 μg/mL). After incubation, samples were centrifuged at 500 g to remove intact RBCs and the hemoglobin that was released into the

supernatant was measured in a 96 well plate at an absorbance of 541nm. Relative hemolytic activity was calculated by subtracting the background absorbance of the various RBC solutions from the sample and normalizing to the hemolytic activity of 1% v/v Triton X-100.

2.2.8 Endosomal escape visualized with lysosomal markers

J774.A1 cells were purchased from American Type Culture Collection and cultured in Dulbecco's Modified Eagle's Medium (DMEM), supplemented with 10% (v/v) fetal bovine serum (FBS). SK-CO15 epithelial cells were cultured in DMEM with 10% FBS and 1% non-essential amino acids. 10,000 J774 macrophages were plated in an 8 well glass chamber overnight. eGFP/mAvrA/AvrA NPs/soluble were given to cells for a period of 6 hours (final eGFP concentration = 150 μg/mL, final mAvrA/AvrA concentration = 12.5 μg/mL). Cells were then washed twice with ice cold PBS and fixed with 3.7% paraformaldehyde for 15 minutes at room temperature. Cells were permeabilized with 1% Triton x-100/PBS for 15 minutes at room temperature and blocked with 1% BSA/PBS for 1 hour at room temperature. Lysosomes were labeled with 5ug/mL primary rat anti-LAMP1 antibody (BD Biosciences) overnight at 4^{o}C diluted in blocking buffer. Cells were then incubated with 4ug/mL secondary TRITC goat anti-rat antibody (Rockland) diluted in blocking buffer for 1 hour at room temperature. Nuclei were stained using 0.2 μM Hoechst 33342 (AnaSpec Inc.) for 15 minutes at room temperature. Cells with were washed 3 times with PBS (10 minutes per wash) between each step in the staining procedure. 50/50 PBS/glycerol solution was used a mounting media and samples were sealed with a coverslip and nail polish. Images were taken on Zeiss LSM 700 confocal microscope.

2.2.9 Nanoparticle cytotoxicity determined by MTT and LDH

The cytotoxicity of the capsules was evaluated using lactate dehydrogenase (LDH) assay. 10,000 J774A.1 cells were plated in triplicate in a 96 well plate. 300ug/mL of NPs or sterile water were added to the wells and incubated for 6 hrs and 24 hrs. Controls for maximum LDH activity were also run according to the manufacturer's instructions (Pierce LDH Cytotoxicity Assay, Thermo Scientific). 50 µl of each sample condition was transferred to a 96 well plate. 50 µl of reaction mixture was added to each well and mixed. The reaction was protected from light for 30 minutes and 50 µl of stop solution was added to each well. The absorbance values were measured at 490nm and 680 nm using Biotek Synergy H4 Multimode plate reader (Biotek Instruments Inc) and reported as % cytotoxicity according to the manufacturer's instructions.

25,000 J774 macrophages were plated in a 96 well plate overnight. Media was exchanged for 300 µg/mL NPs for 3hr. After NP incubation, media was replaced with 100 µl of fresh media and 10 µl of MTT solution. Cells were incubated with MTT reagent for an addition 4 hours. 200 µl of DMSO was then added to each well and wells were mixed vigorously to ensure cells were lysed. Absorbance was measured using a Biotek Synergy 2 Microplate reader at 570 nm and 630 nm.

2.2.10 *In vitro* NF-kB luciferase reporter assay for intracellular AvrA activity

HeLa cells were seeded at 6,000,000 cells/well in a 6-well plate and incubated overnight at 37^{o}C. To prepare the transfection agent, 2 µg pGL4 plasmid (Promega) and 15 µL lipofectamine (Life Technologies) were added to 300 µL of serum free media (DMEM, ATCC) and incubated at room temperature for 5 minutes. The cell media was aspirated and the transfection solution was added directly on top of confluent cells for 1 minute. 6 mL of 1% FBS

in DMEM was then added to the well. The transfection agent was incubated with the cells overnight at 37^{o}C. Cells were then trypsinized and plated at 50,000 cells/well in a 96 well plate overnight in 1% FBS in DMEM. Cells were pretreated with NPs (300 μg/mL) for 4 hours and then stimulated with 20 ng/mL of recombinant human TNF-α (R&D Systems) for 1 hour. Afterwards, the media was aspirated and 50 μL BrightGlo reagent (Promega) and 50 μL serum free media were added to each well. Luminescence was measured in a BioTek Synergy 2 Plate Reader.

2.3 Results and Discussion

2.3.1 Synthesis and characterization of AvrA nanoparticles

The therapeutic approach described herein relies on the availability of active, soluble bacterial proteins and the ability to engineer the protein sequences for desired delivery properties. We cloned the genes of AvrA and a mutant form (mAvrA) into pGEX expression plasmids containing n-terminal glutathione S-transferase (GST) and c-terminal 6x-his tags using standard recombinant techniques to produce soluble AvrA-GST and mAvrA-GST fusion proteins. The mutant form contains a single cysteine substitution (C186A) that renders the acetyltransferase inactive and eliminates JNK inhibition and attenuates NF-κB suppressive activity.[41] We expressed AvrA fusion proteins and a carrier protein, enhanced green fluorescent protein (eGFP), in *E. coli* and purified them (Figure 2.1).

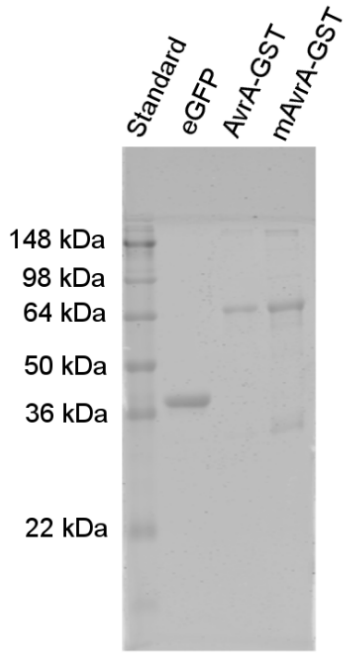

Figure 2.1: Purity of Ni-NTA purified recombinant eGFP and AvrA fusion proteins. Representative SDS-PAGE gel: lane 1 protein standard, lane 2 eGFP, lane 3 AvrA-GST, and lane 4 mAvrA-GST. Note the high purity levels achieved and in all cases a prominent band is observed at the expected molecular weight.

We fabricated protein NPs by desolvating a solution of AvrA and eGFP protein by constant addition of ethanol while stirring (Figure 1.2).[243] The resulting particles were cross-linked with reducible 3,3´-dithiobis[sulfosuccinimidylpropionate] (DTSSP) to stabilize them during delivery (Figure 2.2). DTSSP contains a central disulfide bond that is sensitive to intracellular reducing conditions.[244] By varying imidazole concentration during synthesis, we produced spherical particles with diameters of 125 +/- 25 nm and zeta-potential of -11.3 +/- 0.1 mV in phosphate buffered saline (PBS) and -24.3 +/- 1.1 mV in 10 mM HEPES buffer. We selected this size in order to achieve mucosal barrier penetration and cellular internalization. Previous work has shown that the size, hydrophobicity and charge of particles play an important role in the transport of NPs in mucosa.[228] In order to penetrate mucus, NPs must avoid adhesion to mucin fibers and be small enough to prevent steric hindrance. AvrA-eGFP NPs exhibit

slightly negative zeta-potential in the presence of physiological ion concentrations, which can prevent electrostatic interactions with negatively charged mucin fibers and thus, decrease adhesion to mucus. The size of AvrA-eGFP NPs is within the range of the interfiber spacing of mucin to allow the particles to diffuse through the mucus.[228]

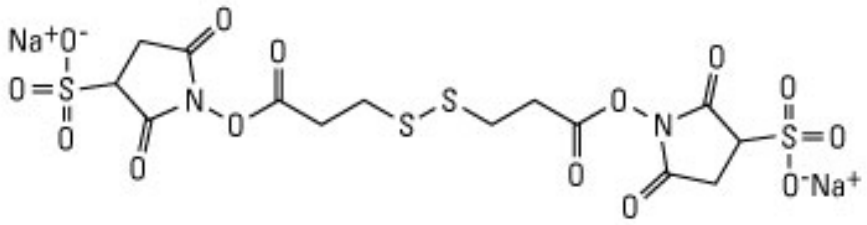

Figure 2.2: Chemical structure of 3,3'-Dithiobis(sulfosuccinimidylpropionate) (DTSSP, Thermo Scientific Pierce). DTSSP is a water-soluble, homo-bifunctional cross-linker that contains a central disulfide bond. DTSSP has two amine-reactive N-hydroxysulfosuccinimide esters at each side of a 12 Å spacer arm.

Though smaller particles may have better delivery properties, they also contain less AvrA than large particles. The NPs contained approximately 316 AvrA molecules per particle. Real time imaging of a *Salmonella* model infection has shown that a different TTSS-secreted effector, SipA, mediates biochemical functions within minutes of infection at a concentration of 1000 molecules/cell.[245] Particles were fabricated from combinations of AvrA-GST or mAvrA-GST and eGFP to create fluorescent particles that could be visualized in specific experiments (Figure 2.3). We substituted bovine serum albumin (BSA) for eGFP in particle formulations that required non-fluorescent particles but similar properties (99.7 +/- 23.1 nm in diameter, zeta potential of -16.9 +/- 0.9 mV in PBS).

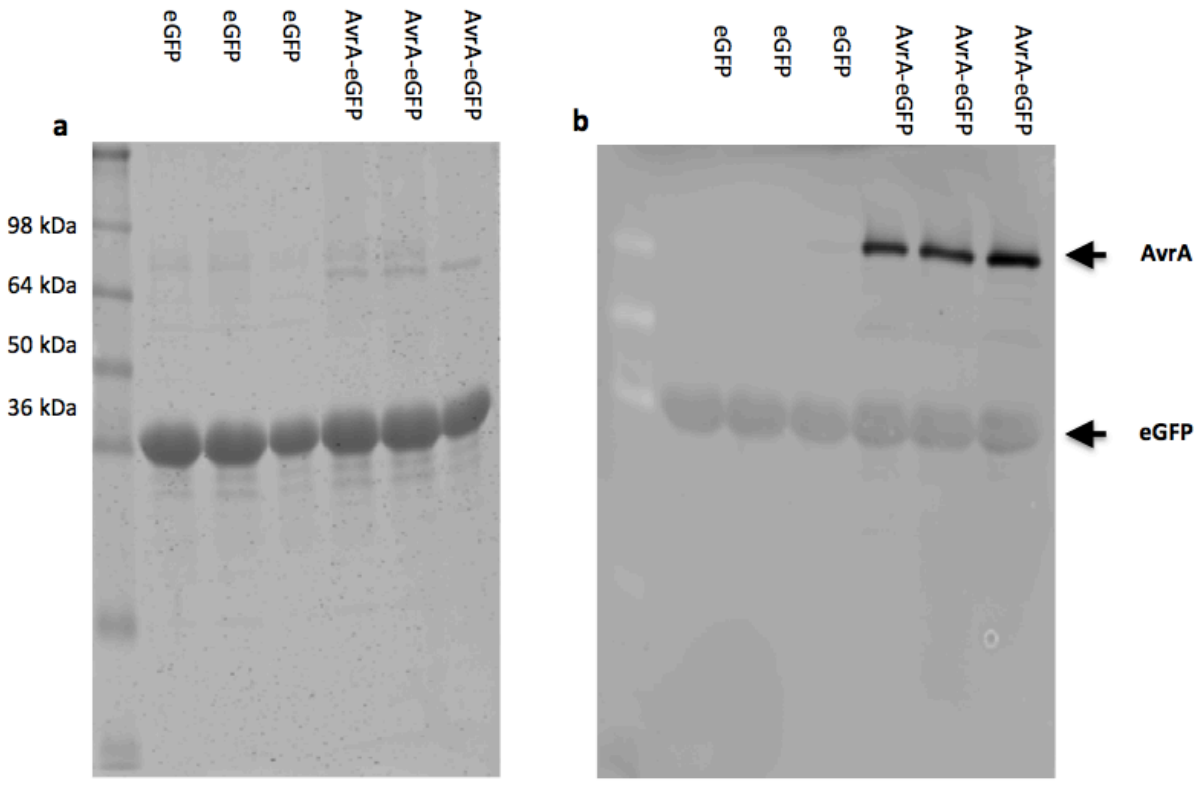

Figure 2.3: Composition of AvrA-eGFP NPs. (a) Representative SDS-PAGE gel for eGFP and AvrA-GST NPs, and (b) representative western blot for eGFP NPs and AvrA-GST NPs, immunostained with anti-AvrA antibodies and showing native fluorescence of eGFP.

2.3.2 Uptake and endocytosis of AvrA nanoparticles

We sought to take advantage of endocytic uptake mechanisms of NPs containing AvrA, since the *Salmonella* TTSS is not feasible for AvrA delivery. We confirmed uptake of AvrA-eGFP NPs by cultured J774A.1 macrophages or T84 polarized epithelial cells using confocal microscopy (Figures 2.4). T84 cells are a highly differentiated epithelial cell line that can recapitulate the barrier and uptake properties of the native epithelial monolayer.[246] J774A.1 macrophages serve as a model phagocytic cell and expectedly showed more eGFP fluorescence.[247, 248] In the NP fabrication process, eGFP and AvrA are co-desolvated and crosslinked together. Internalized eGFP suggests that AvrA is also co-delivered and internalized.

The punctate spots seen in mid-cell optical sections clearly show delivery of NPs, while the lack of green fluorescence in the soluble eGFP images indicates very low uptake of soluble protein.

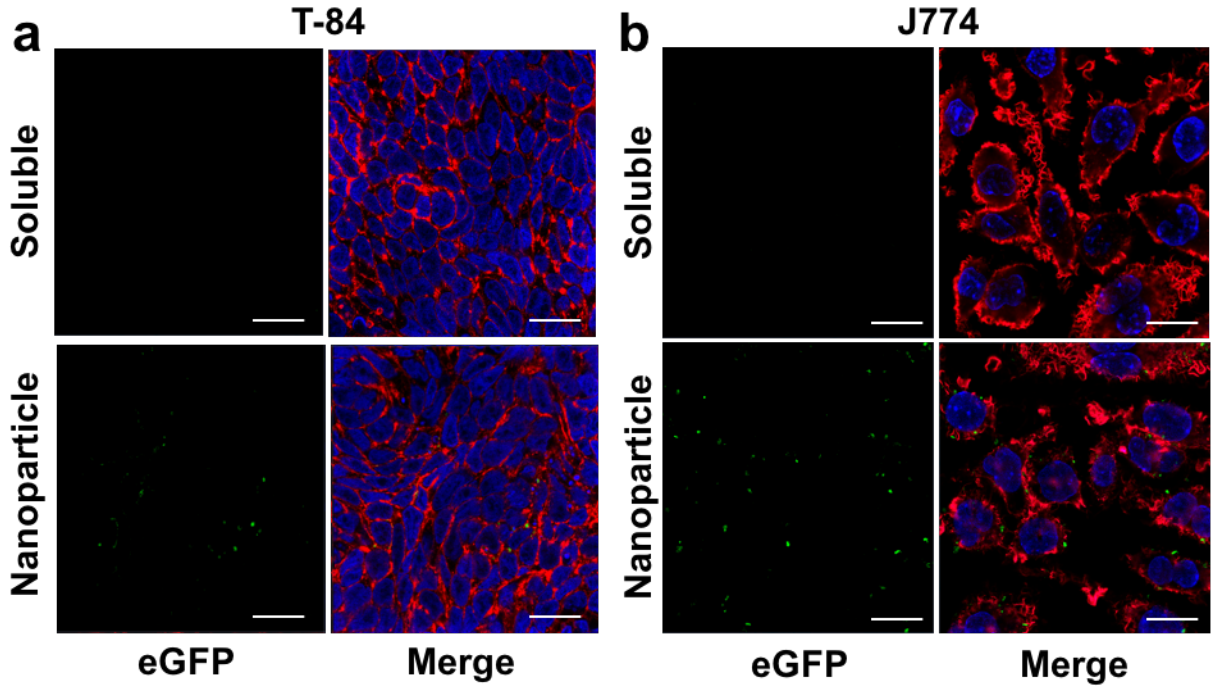

Figure 2.4: Cellular uptake of AvrA particles. Confocal images of (A) T-84 and (B) J774A.1 cells incubated with soluble AvrA and eGFP, or AvrA-eGFP NPs for 6 hours. Images are mid-cell optical section overlays of eGFP fluorescence, nuclear Hoechst dye, and actin filaments labeled with rhodamine-phalloidin (scale bars 20 μm).

Next, we used flow cytometry with anti-AvrA antibodies to quantify uptake of specific AvrA immunoreactivity, as well as eGFP fluorescence. At six hours, 420 times more J774A.1 cells were positive for AvrA and eGFP when treated with NP AvrA-eGFP in comparison to cells treated with soluble AvrA and eGFP (Figure 2.5). SK-CO15 epithelial cells also internalized more NP AvrA-eGFP than soluble AvrA and eGFP in 6 hours. Though only ~10% of J77A.1 or SK-CO15 cells labeled positive for AvrA, significantly more J774A.1 cells labeled positive for eGFP (Figure 2.6). This could indicate that in macrophages the NPs are not completely disassociated and the antibody is not able to access all AvrA still in the NPs, since the eGFP

signal is not dependent on particle dissociation. However, as described in the methods, the dose used for the uptake studies was larger than the dose for *in vitro* activity studies in order to have sufficient signal for imaging. The low signal also necessitated the use of a quantum-dot labeled secondary antibody to detect AvrA. This indicates AvrA is quite potent and we can detect functional activity at lower concentrations than we can detect the "physical presence" of AvrA in cells by fluorescence. Interestingly, eGFP and AvrA-eGFP particles had the same uptake in SK-CO15 epithelial cell line but in J774A.1 macrophages AvrA-eGFP particles were taken up much more than eGFP only particles (Figure 2.6).

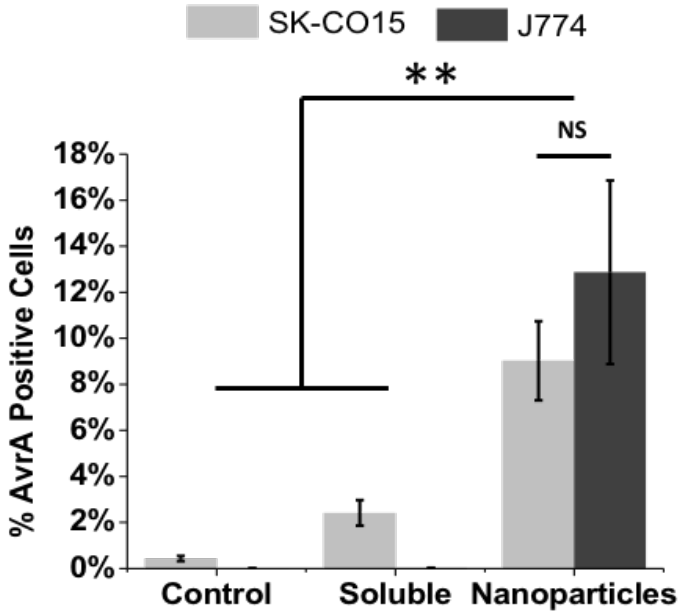

Figure 2.5: Cellular uptake of AvrA particles. Flow cytometry quantification of soluble AvrA and eGFP, or AvrA-eGFP NP uptake in SK-CO15 cells (light gray) and J774A.1 cells (dark gray).

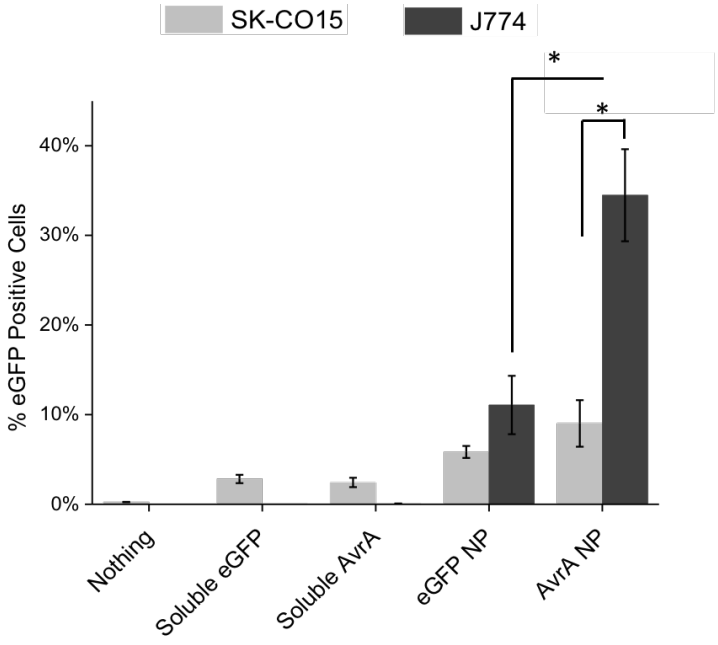

Figure 2.6: Uptake of AvrA-eGFP protein and NPs. Flow cytometry quantification of soluble AvrA and eGFP, eGFP only, and AvrA-eGFP NP uptake in SK-CO15 cells (light gray) and J774A.1 cells (dark gray). (* $p<0.05$)

This is surprising, given that the particles with or without AvrA have the same size and zeta potential and that AvrA is a small fraction of the total protein in a particle (4% by mass). These data indicate that AvrA may play a role in uptake of the particles, though it seems to be cell type specific. YopJ, a close ortholog of AvrA, is another TTSS effector from *Yersinia* that shares sequence similarities with AvrA.[249] YopJ is an anti-inflammatory and pro-apoptotic effector that is known to be cell selective; it induces apoptosis in macrophages and dendritic cells but not in endothelial cells or neutrophils.[65, 250] AvrA could similarly exhibit some manner of specificity. AvrA has been shown to be differentially expressed depending on the organ location of the *Salmonella* infection[66], suggesting potential specificity. Also, as a pathogenic protein, AvrA could contain pathogen associated molecular patterns (PAMPs) able to be recognized by macrophage pathogen recognition receptors (PRRs). Engagement of PRRs by any AvrA present

on the surface of the NP can activate macrophages and increase endocytosis, leading to the difference in uptake seen between AvrA-eGFP and eGFP only NP. SK-CO15 cells are epithelial cells lacking PRRs.

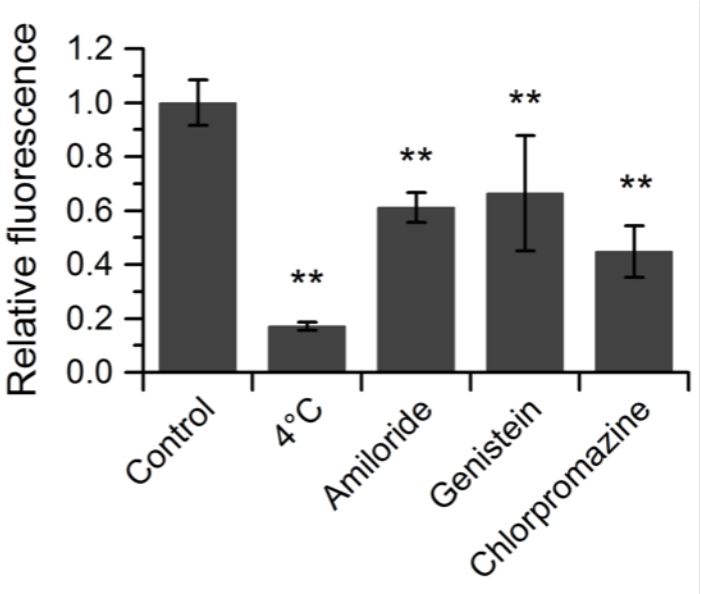

Figure 2.7: Cellular uptake of AvrA particles. Comparison of NP uptake by J774A.1 cells following pretreatment with the indicated drug. Asterisks indicate statistical significance of each cell type treated with inhibitor compared to untreated control.

The route of NP uptake in J774A.1 cells was investigated by flow cytometry using the eGFP signal in the presence of endocytosis inhibitors (Figure 2.7). J774A.1 cells utilize primarily energy-dependent routes, as indicated by low uptake at 4°C. There was no strong preference toward a particular route, as inhibitors for macropinocytosis (amiloride), caveolae-mediated endocytosis (genistein), and clathrin-mediated endocytosis (chlorpromazine) all reduced NP uptake. Co-localization studies in J774A.1 cells of NPs with lysosomal marker anti-Lamp1, confirmed the route of uptake to be endosomal in nature and showed that the majority of NPs are found in lysosomes after 6 hours (Figure 2.8). However, the dose of NPs required for visualization was much higher than that required to detect AvrA activity, as described below.

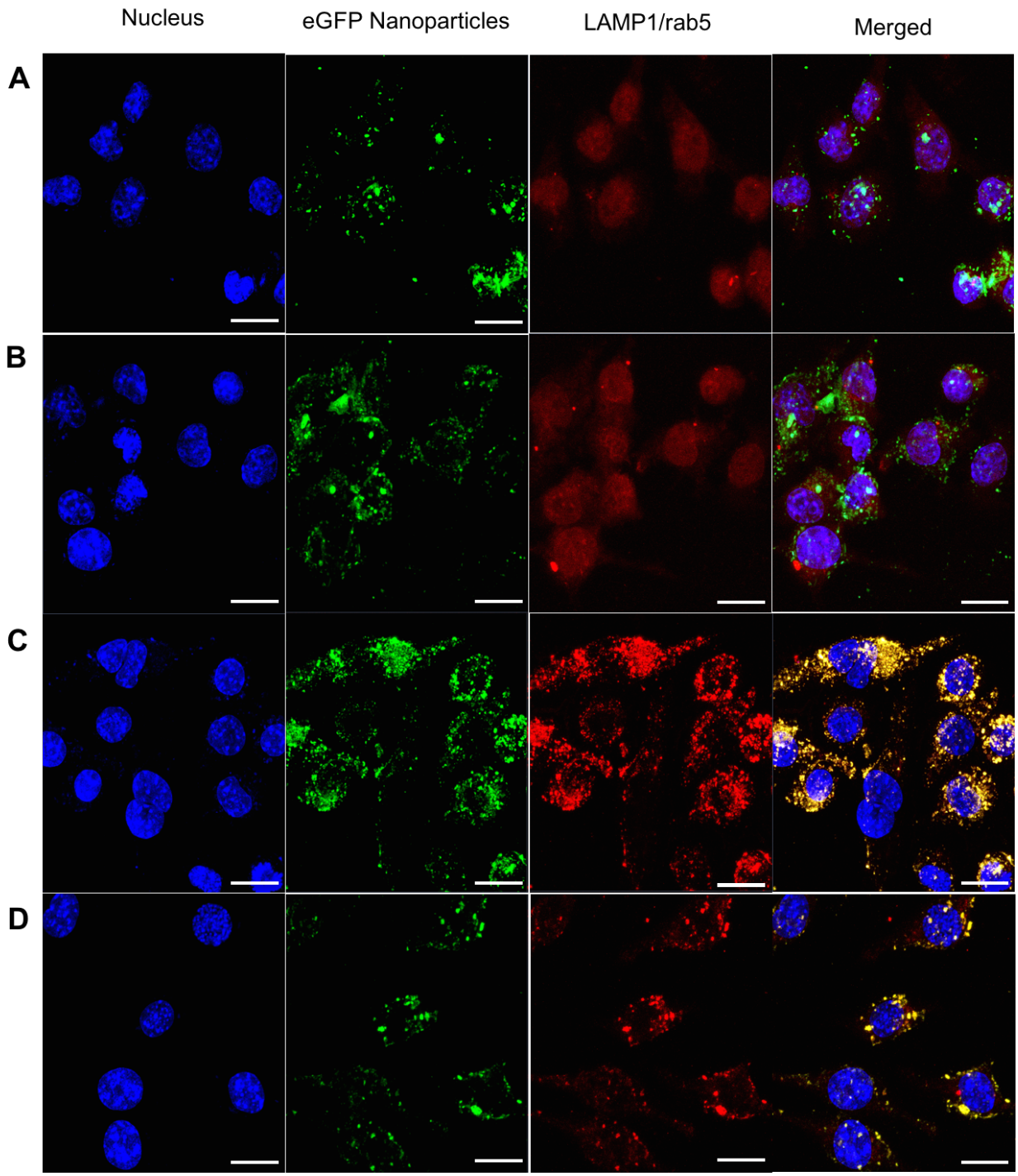

Figure 2.8: Colocalization of eGFP+AvrA NPs with endosomal/lysosomal markers. (A,B) eGFP NPs (green) were incubated with J774 macrophages for 6 hours and labeled with rab5 (red) for early endosomes. (C) eGFP NPs (green) were incubated with J774 and labeled for LAMP1 (red) for lysosomes. (D) Cells were incubated with eGFP+AvrA NPs and labeled with LAMP1. In all cases, cells were labeled for DNA (blue) with Hoechst. The merged column shows that NP colocalization (yellow) is only visible in lysosomal labeling and not visible in endosomal labeling. Scale bar = 20 μm

Though colocalization studies with anti-Lamp1 indicated the majority of AvrA-eGFP NPs are endocytosed and traffic to lysosomes after 6 hours (Fig. 2.8), the detection of single AvrA-GST protein in cell lysates and the functional AvrA activity described below demonstrate that some AvrA protein does reach the cytosol. Though it is difficult to pinpoint endosomal escape mechanisms for most NPs, there are several features of AvrA particles that could contribute to their escape. One contribution could be from osmotic pressure changes that may occur as the crosslinks reduce and particles break up into soluble protein. Reducible polyarginine DNA nanocarriers have been shown to have higher transfection efficiency than those that are not reducible or when disulfide reduction was inhibited.[251] Another possible mechanism is membrane destabilization due to cationic interactions and an osmotic buffering effect by protonation of the 6x-histadine tags on eGFP and AvrA-GST.[252] It is also possible that AvrA itself could have endolytic properties, as there are a variety of bacterial pathogens that produce toxins or effectors that contain domains that assist in endosomal escape by different mechanisms.[193] Hemolysis assays showed that pure, soluble AvrA-GST was significantly lytic with increasing concentration from 10 to 1000 μg/mL and at higher concentrations lysis was increased at neutral pH compared to acidic conditions (Figure 2.9). Considering a single particle in a 200 nm endosome, the AvrA concentration is estimated to be higher than 1000 μg/mL. This suggests AvrA may have endosomal escape properties prior to acidification. However, when the hemolytic activity of mixtures of soluble eGFP and AvrA was assessed, as would be found from a disassembled particle, the lytic activity was completely abolished (Figure 2.10). This suggests that soluble eGFP interferes with any lytic property of AvrA. Interestingly, intact AvrA-eGFP NPs did exhibit some lytic activity, at neutral and slightly acidic pH. NPs made only of eGFP or mAvrA-eGFP showed significantly less, but non-zero, lytic activity at neutral and slightly acidic

pH. This data suggests that intact AvrA-eGFP NPs could contribute to destabilization of endosomal membranes at early stages of acidification. It also suggests more generally that AvrA in AvrA-eGFP NPs has some interaction with cell membranes, in agreement with the observation in Figure 2.6 that AvrA-eGFP NPs are internalized by macrophages more than eGFP NPs.

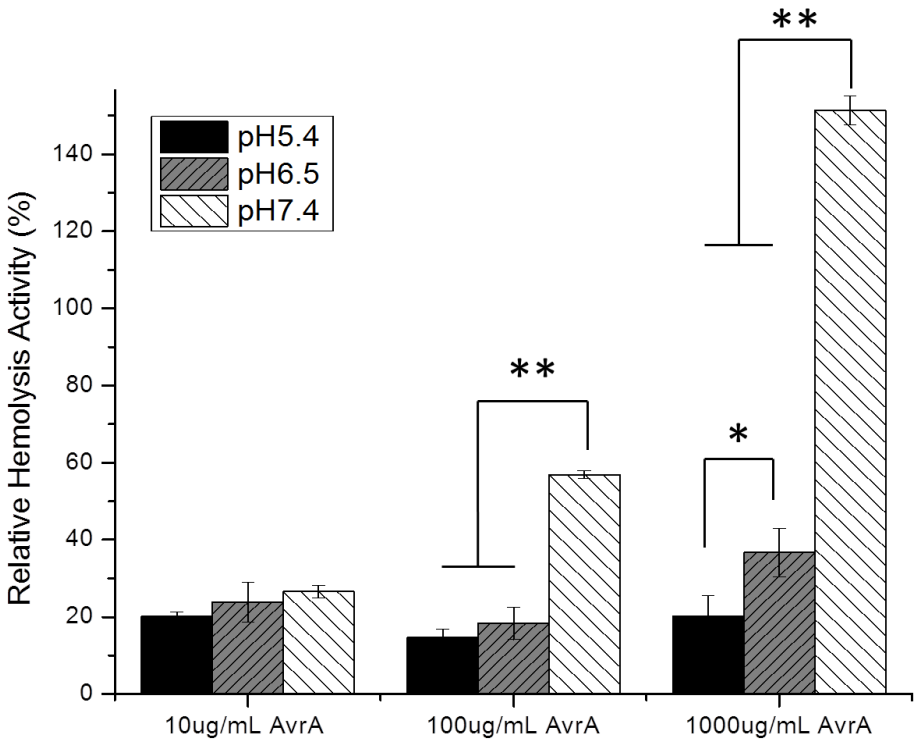

Figure 2.9: Hemolysis of soluble AvrA-GST at different concentrations at pH. Relative hemolytic activity is normalized to a positive control, 1% v/v Triton X-100, after subtracting background absorbance at 561nm. (* $p<0.05$, ** $p<0.005$)

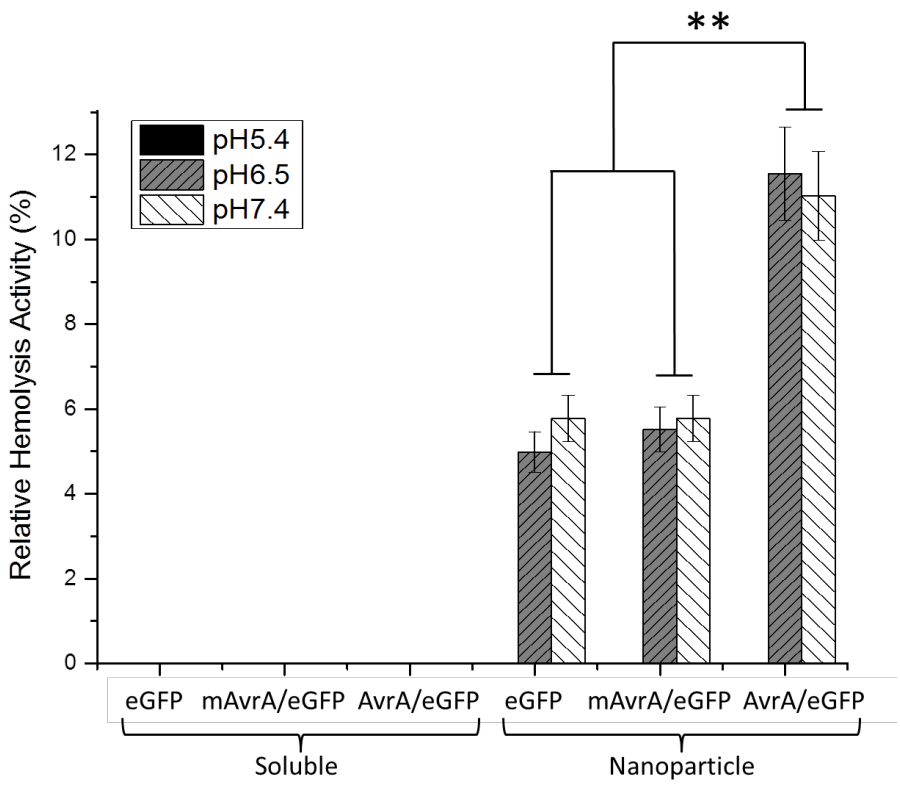

Figure 2.10: Hemolysis of eGFP (150ug/mL) with or without AvrA or mAvrA (12.5ug/mL) as a function of pH. All soluble samples, as well as pH 5.4 NP samples, exhibited hemolysis below background. Relative hemolytic activity is normalized to a positive control, 1% v/v Triton X-100, after subtracting background absorbance at 561nm. (** $p<0.005$)

2.3.3 *In vitro* NF-kB activity and cytotoxicity of AvrA nanoparticles

Importantly, incubation of J774A.1 cells with NPs does not have any cytotoxic effect (Figure 2.11).

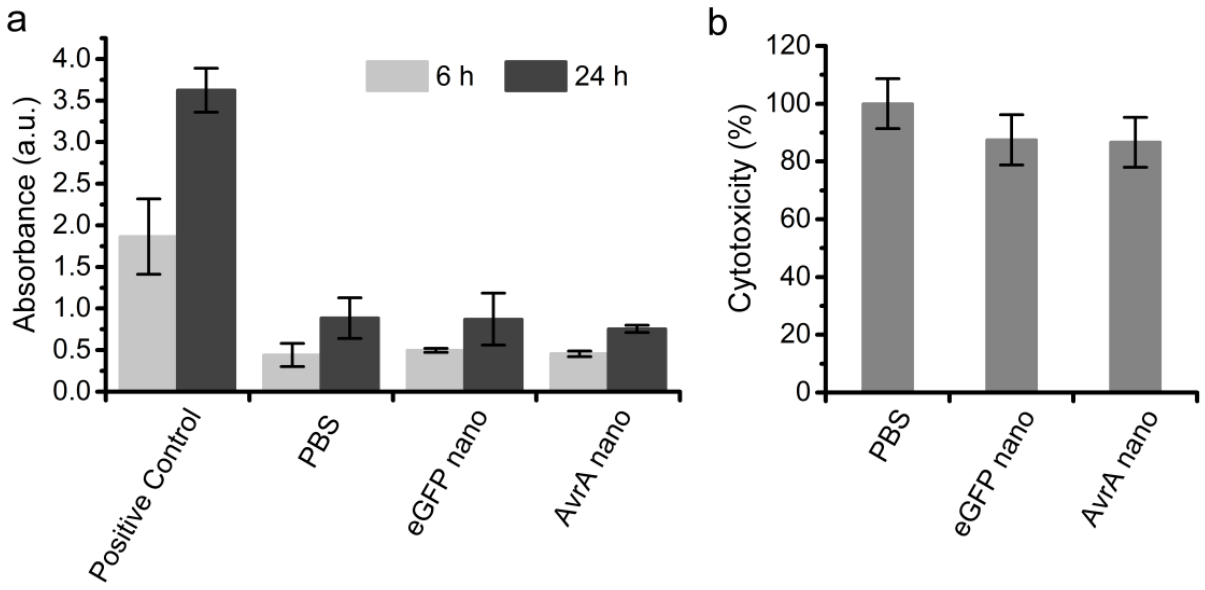

Figure 2.11: Cytotoxicity of AvrA-eGFP NPs. (a) Lactate dehydrogenase (LDH) activity of J774.A1 cells incubated with NP formulations of eGFP or AvrA-eGFP for 6 or 14 hours. (b) Cell viability determined by methyl thiazole tetrazolium (MTT) assay for J774.A1 cells treated with soluble or NP formulations of eGFP or AvrA-eGFP for 3 hours.

AvrA has been shown to inhibit JNK phosphorylation and IκB degradation by transfection and transgenic approaches.[41, 47] Experiments with AvrA-eGFP NP preparations applied to the apical surface of polarized T84 monolayers for 3 hours, to allow particle internalization and dissociation, were successful in partly suppressing both TNF-α induced JNK activation and IκB degradation[41]. AvrA NPs show stabilization of Iκβα after 30 minutes with levels reaching the pre-stimulation levels by 60 minutes. AvrA is hypothesized to act on a distal event in the NF-kB pathway downstream of P-Iκβα.[41] Though Iκβα still is phosphorylated, this does not lead to degradation of Iκβα, thereby preventing NF-kB release and transcription of inflammatory signals. For this reason, levels of P-Iκβα increase over time in the presence of TNF-α and AvrA NPs as Iκβα accumulates due to reduced degradation. JNK inhibition by AvrA NPs was observed to be dose dependent[47] and mAvrA-eGFP NPs, eGFP NPs, and soluble AvrA

did not inhibit JNK[47]. The ability of AvrA NPs to suppress NF-κB activity was confirmed by a luciferase gene reporter assay (Figure 2.12). Partial suppression of NF-κB activity was observed with mAvrA NPs. AvrA, has been shown to also exhibit deubiquitinase activity in the NF-κB pathway that is not entirely eliminated by the C186A mutation.[253]

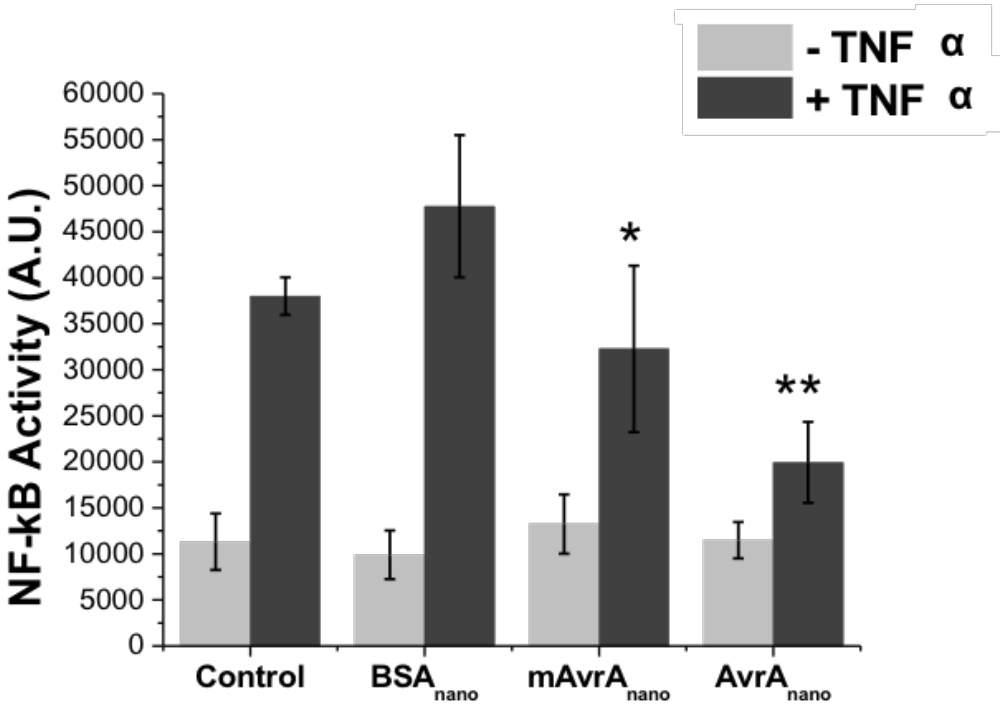

Figure 2.12: AvrA NPs inhibit inflammatory signaling. AvrA NPs were applied for 4 hrs prior to TNF-α stimulation. NF-κβ reporter gene assay (*$p<0.05$ compared with TNF-α control samples, ** $p<0.01$ compared with TNF-α control samples).

Interestingly, mutant AvrA particles also showed significant activity, suggesting the therapeutic enzymatic activity of AvrA in this model is not abolished with a single mutation in the acetyltransferase active site. Mutant AvrA partial activity is reported in literature and seen in the *in vitro* activity data (Figure 2.12), possibly because the deubiquitinase activity in the NF-κB pathway is not entirely eliminated by the C186A mutation.[253] Indeed, many, if not most TTSS effectors are bi-or multimodular proteins with multiple catalytic functions,[254, 255] and other

activities in AvrA may account for partial activity seen *in vivo*. AvrA, specifically, has deubiquitinase activity in the NF-κB pathway that is not completely eliminated by the mutation.[253] A second active site, an SH2-like domain, is also present in AvrA and *Yersinia* ortholog YopJ.[254] Mutation of this D/E-X-E active site reduces YopJ anti-inflammatory function, and is expected to have a similar function in AvrA. This domain should be unaffected by the C186A mutant used in these studies and so its function would remain intact. We have also seen partial function of NPs made from the same mutant of YopJ, in agreement with multiple domains responsible for bioactivity.[256]

The protein NP platform is highly adaptable to a variety of biological molecules and chemistries. NP formation, stabilization, and targeting ligands can be independently modified to suit the biological delivery requirements of different diseased tissues and routes of administration. For example, AvrA NPs could also be used in other models of inflammation that do not require systemic access, such as in the joints, airways, skin, or eyes. In this work both BSA and eGFP were used as carriers for the AvrA and in either case, AvrA was successfully delivered and retained its function. The versatility of the protein NP would allow use of recombinant human serum albumin (HSA) as a carrier in future human clinical applications as it is more physiologically benign and FDA approved. While AvrA was chosen as a model immunosuppressive protein for construction into NPs, this approach could be applied to other proteins. Orthologous acetyltransferases (YopJ, VopA, AopP) have been detected in a variety of bacteria that associate intimately with eukaryotic hosts, and these effectors exhibit extended activity against a wider spectrum of MAPKs. Our lab and others have been studying these related effectors that have variable effects on MAPK and are more potently immune suppressive, but can also be potently pro-apoptotic.[57, 62] The many other classes of bacterial effectors demonstrate

a potentially vast repository of biochemical activities relevant to manipulation of eukaryotic inflammatory signaling, and exploitation of bacterial virulence proteins in yeast and mammalian immune cells has been explored as a synthetic biology approach.[257] However, this method is not limited to bacterial proteins or single types of proteins. Combination therapies of bacterial proteins and human cytokines or small molecule anti-inflammatory agents, for example, may have value in future immunological therapeutics.

2.3.4 *In vivo* activity of AvrA nanoparticles

To detect particle uptake in vivo, we used direct transrectal instillation of AvrA-eGFP particles into both intact and damaged/inflamed murine colons. In tissues evaluated post instillation, eGFP was detected in the extracellular mucus layer of the epithelial cells by anti-eGFP (Figure 2.13). Intracellular eGFP uptake was seen within epithelial cells by 4h in apical cells and in the base of crypts (Figure 2.14). eGFP positive cells were seen in the lamina propria (Figure 2.14) and in F4/80 positive macrophages (Figure 2.14). NP uptake in healthy tissue indicates that NPs are able to penetrate healthy, fully intact mucus and could potentially be used as a protective agent to prevent the spread of inflammation. We were unable to detect AvrA immunoreactivity in vivo, likely due to the small amount of AvrA taken up. Based on the colocalization of eGFP and anti-AvrA signals from in vitro flow cytometry NP uptake experiments, we conclude from the anti-eGFP fluorescence that AvrA-eGFP NPs are taken up and AvrA is present with eGFP. The in vivo images indicate that these particles effectively transverse the mucosal barrier and reach the underlying epithelia, as well as lamina propria monocytes.

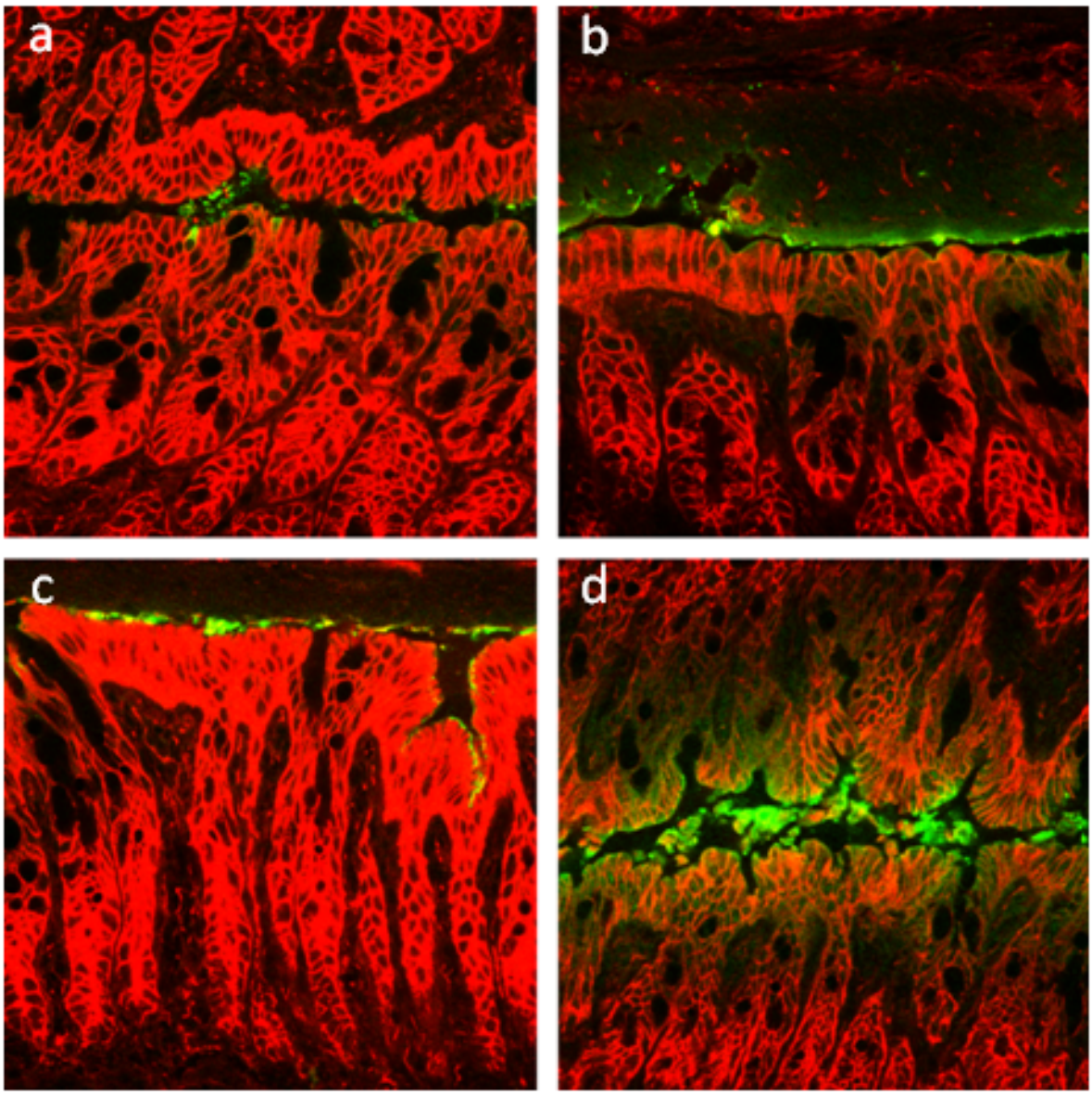

Figure 2.13: Time course of NPs uptake *in vivo*. Particles were instilled transrectally and imaged at (a) 0.5 hour, (b) 1 hour, (c) 2 hours, (d) 3 hours. Particle uptake is marked by eGFP fluorescence (green). Epithelial cells are counterstained with beta-catenin (red) (40x magnification). *Performed in the laboratory of Dr. Andrew Neish at Emory University.

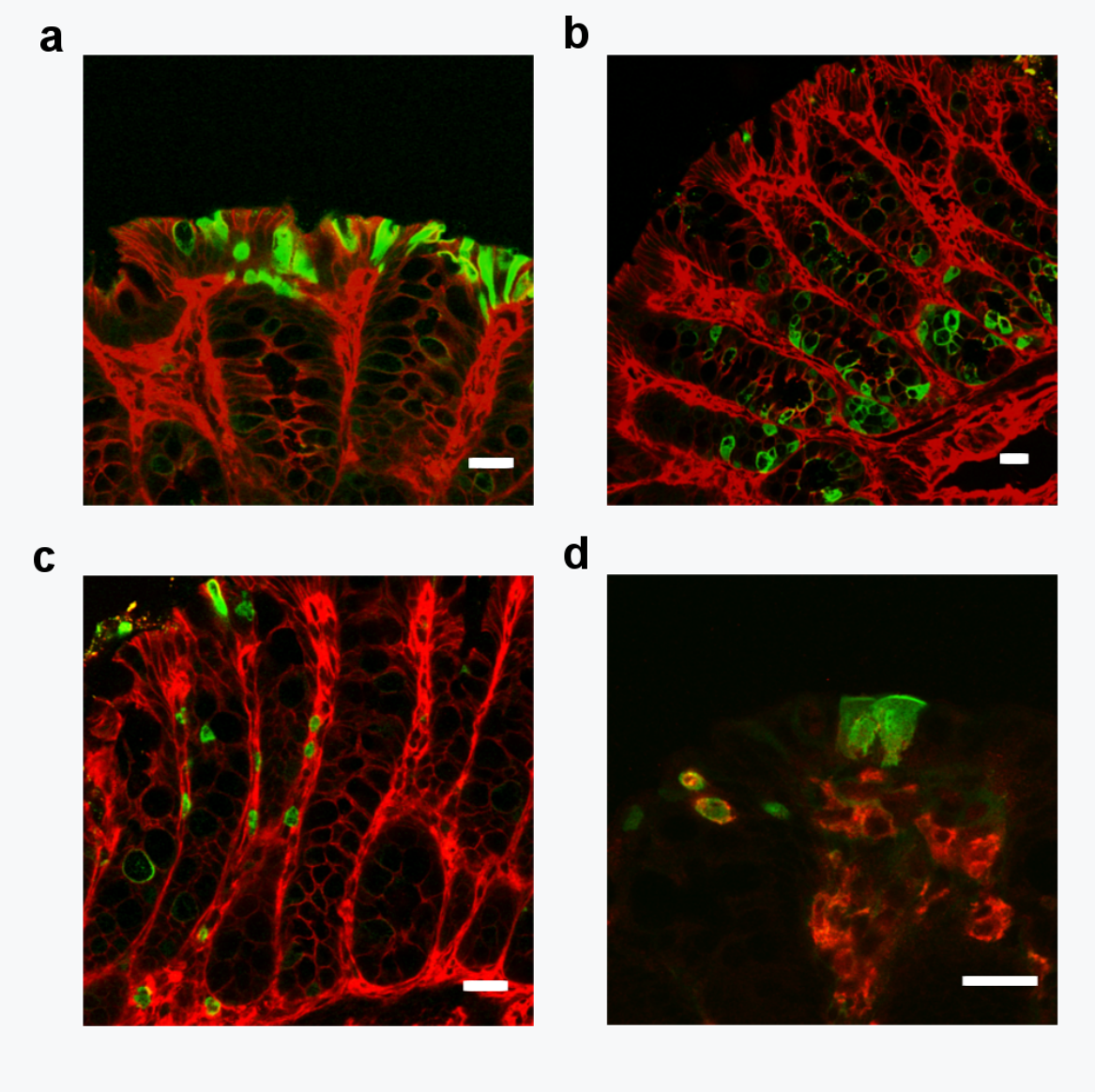

Figure 2.14: Time Mucosal uptake of AvrA-eGFP (12 μg eGFP) particles in healthy murine colonic surface epithelium (a), crypts (b), lamina propria (c), and macrophages (F4/80+) (d) imaged by confocal microscopy (scale bars 20 μm). Particles were instilled transrectally and imaged after 4 h. Particle uptake is marked by anti-eGFP fluorescence (green). Epithelial cells are counterstained with beta-catenin (red in (a–c)) and macrophages stained with F4/80 (red in (d), yellow indicates colocalization of eGFP and F4/80+). *Experiment was performed in the laboratory for Dr. Andrew Neish at Emory University.

Dextran sodium sulfate (DSS) colitis is another in vivo model where the chemical irritant, supplied in drinking water, results in epithelial erosions and subsequent inflammation in the colon within 4–5 days. With this model, we tested NPs both as prophylaxis, administered at 1

day prior and 1 day post initiation of DSS (Figure 2.15), and as a therapeutic design, administered 7 days post initiation of DSS after clinical symptoms have become manifest (Figure 2.15). In both experimental designs, suppression of clinical indices and scores of colonic inflammation were observed. From these experiments we conclude that sufficient quantities of bioactive AvrA are delivered to colonic tissue to suppress acute inflammatory events in distinct colitis models.

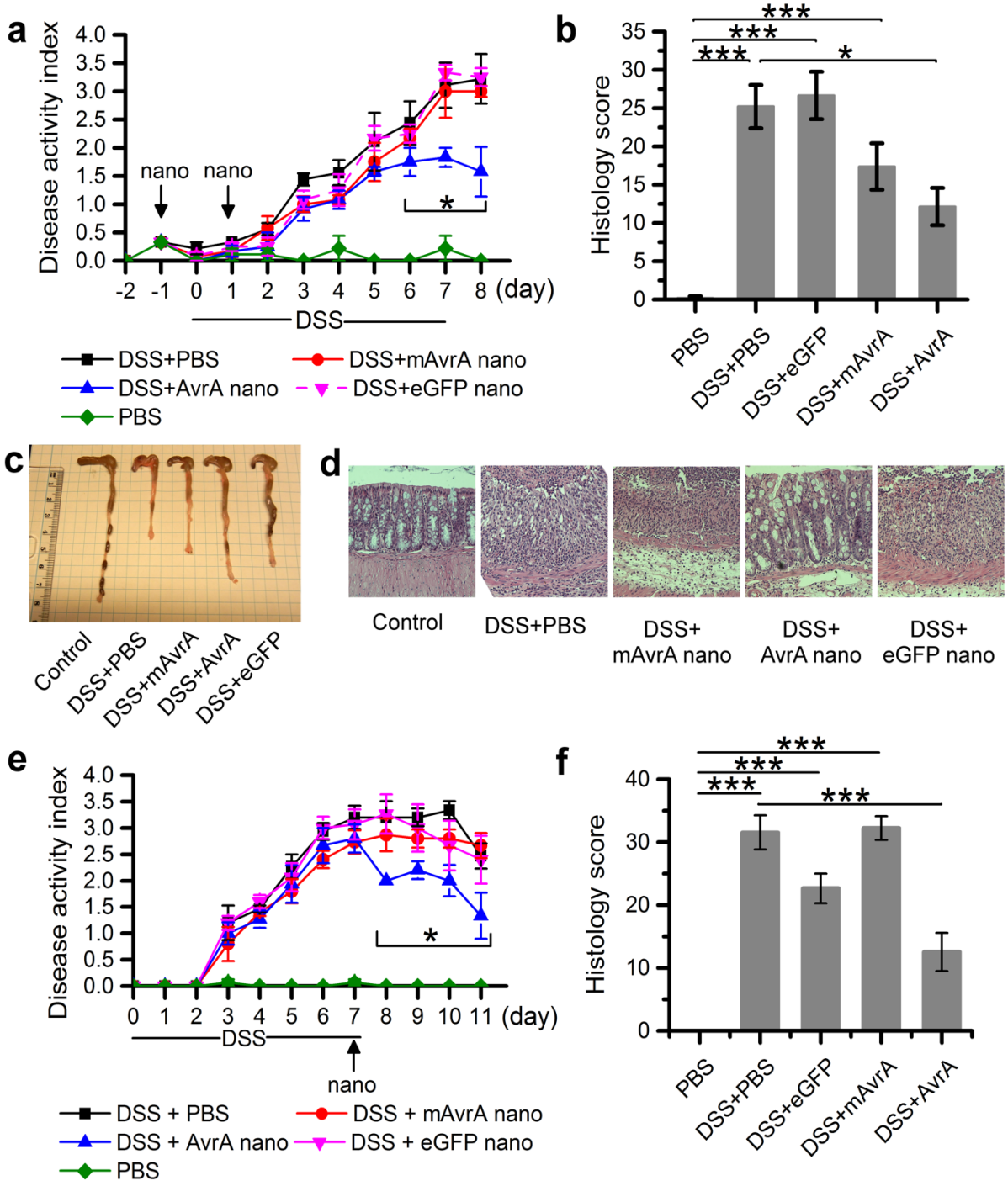

Figure 2.15: Anti-inflammatory effect of AvrA on dextran sodium sulfate (DSS)-induced colitis. (a) Clinical disease activity index and (b) histological scoring of 5 mice per indicated condition receiving two injections (intrarectal) of NPs (900 ng AvrA per injection) while subjected to DSS challenge for 7 days. (c) Representative colon gross pathology from mice treated as indicated in (a). (d) Representative colon histology from mouse treated as indicated in (a). (e) Clinical disease

activity index and (f) histological scoring of 5 mice per indicated condition treated once with NPs (900 ng AvrA) after DSS-induced colitis (*$p < 0.05$). *Experiments were performed in the laboratory of Dr. Andrew Neish at Emory University.

IBD results from aberrant mucosal immune activation, often in the context of genetic susceptibility, resulting in the influx of acute and chronic inflammatory cells into the mucosa. Both the overlying epithelial monolayer and the underlying immune cells of the lamina propria possess the ability to initiate inflammatory reactions during injury.[258] In our murine experiments, restricted to transrectal delivery of NPs into the distal colon, both surface epithelial and monocytic cells in the lamina propria took up NP formulations of AvrA under control and colitic conditions. AvrA particles potently suppressed histologic inflammation and clinical injury in several commonly used *in vivo* models of colitis. It is widely known that there is not a perfect model of IBD. In our studies, we utilized chemical models of acute/self-limited inflammation with DSS and TNBS that occur even in the absence of a functional adaptive immune system. Thus, our data demonstrates an inflammatory suppressive role outside of adaptive regulatory mechanisms. We speculate that use of AvrA NPs in the treatment of a chronic model of IBD, such as IL-10 knockout[259] or T-bet and RAG2 double knockout[260], would lead to similar results of suppression of inflammation markers and disease activity scores because the JNK and NF-κB targets of AvrA are highly conserved inflammatory signaling molecules. Though complications arising from tissue restructuring, such as neoplasia and fibrosis, would likely not be reversed by AvrA NPs, further damage could be prevented and a reversal of symptoms may be observed. To make these NPs clinically relevant, oral delivery is necessary. Future work will entail encapsulation of NPs and oral delivery that will allow AvrA-eGFP NPs access to Peyer's patches and other components of the gut associated lymphoid tissue (GALT) resident in the distal ileum. It will be interesting to determine if such therapeutic strategies affect adaptive immunity.

2.4 Summary

Enteric bacteria have coevolved with humans to develop specific effector proteins capable of immunomodulation. We engineered one such protein, AvrA, to form protein NPs, enabling intracellular delivery of AvrA in the absence of *Salmonella.* AvrA NPs inhibited inflammatory pathways *in vitro* and reduced inflammation in murine colitis models, indicating their potential as a treatment for IBD. Future work could expand the protein NP platform to other bacterial proteins for development of effective therapeutics to combat chronic inflammatory disease.

CHAPTER 3 : Oral Delivery of Protein Nanoparticles using Alginate/Chitosan Microparticles

3.1 Introduction

Crohn's disease (CD) and ulcerative colitis (UC), the two major forms of inflammatory bowel disease (IBD), are chronic inflammatory disorders of the gastrointestinal tract resulting from inappropriate and amplified mucosal immune response to the otherwise normal microbiota existing in the gut[1, 2]. The CDC estimates that approximately 3.1 million people in the US are living with IBD[4] and there is an increasing global prevalence[6] of the disease. Patients are treated with a combination of locally acting anti-inflammatory small molecules[9, 10, 11], systemic corticosteroids, monoclonal antibodies[12], and surgery. Although these treatments can be effective, they have specific windows of efficacy[10], long-term side effects[13, 14, 15], and risk of infection[9, 16] associated with them.

The human mucosal immune system has evolved microenvironments favoring commensal bacteria while inhibiting pathogenic bacteria[261, 262]. Some pathogenic bacteria are able to overcome these evolutionary mechanisms by modulating host response through the injection of bacterial effector proteins via a needle-like type-3 secretion system (T3SS)[38, 263]. One of these bacterial effector proteins is AvrA, from *Salmonella*.[39, 40] AvrA is an enzyme that functions in the cytosol to acetylate key serine and threonine residues on MKK4/7, thus inhibiting phosphorylation and preventing signaling in the JNK pathway and blocking apoptosis[47, 48, 49]. It has also been reported that AvrA indirectly deubiquitinates Iκβα by an unknown mechanism, stabilizing phosphorylated-Iκβα (p-Iκβα) and inhibiting further phosphorylation, thereby preventing transcription of NF-κβ[41, 51]. This evolved bacterial protein

with dual anti-apoptotic and anti-inflammatory enzymatic function can be utilized to ameliorate gut inflammation[52]. Our previous work demonstrated that AvrA delivered by protein nanoparticles (NPs) replaces the need for delivery by *Salmonella* T3SS. Protein NPs are synthesized by desolvation and stabilized with a reducible crosslinker designed to release soluble protein in the reducing environment found in the cytosol. Protein NPs increase cellular internalization of proteins compared to soluble[243]. Protein NPs also have high protein loading, are capable of penetrating the mucus, and can passively target inflamed tissue[199, 200, 236, 264]. AvrA NPs were shown to decrease inflammatory markers *in vitro*, and reduce symptoms of colonic inflammation in two murine colitis models following transrectal delivery[51].

Transrectal delivery is undesirable for patients and also limits delivery to the distal portion of the colon, both of which hinder the clinical potential of AvrA NPs. Therefore, we sought to engineer an oral delivery vehicle to maximize therapeutic potential. The biggest obstacle to oral delivery of proteins is the harsh environment found in the stomach, where low pH, digestive enzymes, and mechanical forces act to break down proteinaceous materials for digestion[195, 199]. Therapeutic soluble proteins have been co-delivered with protease inhibitors to prevent enzymatic degradation and permeation enhancers to facilitate transport across mucus and through the epithelium[196, 197]. These methods have traditionally been used for systemic delivery of proteins, though chronic use of these inhibitors and enhancers can lead to severe side effects[198]. Conjugating proteins with cell penetrating peptides or mucoadhesive polymers can increase targeting and minimize off-target effects. However, these methods still suffer from low penetration and bioavailability from natural mucus turnover[198]. To overcome these challenges, localized intestinal delivery of protein therapeutics has typically been accomplished by NPs or microparticles (MPs) made from biodegradable polymers and hydrogels[194]. NPs are able to

passively target inflamed tissue[202], enhance mucus penetration, and membrane permeation[203]. MPs can provide a larger depot for protein therapeutics that can be engineered to be stimulus responsive[204]. NPs and MPs can improve protein stability and be engineered to target specific regions of the gastrointestinal tract[199]. Nanoparticles-in-microsphere oral system (NiMOS)[205], combines these two particulate system in a unique approach for oral gene delivery[206, 207]. Gelatin NPs encapsulating plasmid DNA were then encapsulated in a poly(epsilon-caprolactone) MPs and shown to transfect the small intestine and colon of rats. NiMOS has the advantages of both NP and MP delivery systems as NPs were capable of penetrating the mucosal barrier and MPs protected NPs from enzymatic degradation until they reached the absorbing epithelium. Adapting NiMOS for protein therapeutics can provide a novel method for localized intestinal delivery. A NiMOS for proteins would need to provide a more stringent pH protective capability as proteins are more sensitive than DNA to pH changes that can cause denaturation.

Alginate and chitosan are two natural polysaccharides generally regarded as safe (GRAS) by the Food and Drug Administration (FDA) that have been used as NPs or MPs for oral delivery of insulin[208, 209, 210], BSA[211, 212], hemoglobin[213], probiotics[214, 215], and cells[216, 217]. Alginate can form hydrogels under mild gelation conditions ideal for protein encapsulation[218]. A chitosan coat can be used in conjunction with alginate hydrogels to remedy the problems of drug leakage[219]. Alginate hydrogels shrink at gastric pH and the complementary electrostatic properties of anionic alginate and cationic chitosan allow interpolymeric associations strengthened by the protonation of chitosan amine groups at low pH. At intestinal pH, which ranges from pH 6 to pH 7.5 depending on location in healthy individuals however lower in IBD patients[220], alginate hydrogels swell and the charge of chitosan reverses to negative, allowing

release of encapsulated cargo. This pH-response trigger should allow alginate/chitosan hydrogels to protect protein NPs at gastric pH and then release them at intestinal pH.

In this chapter, we engineered alginate/chitosan hydrogel MPs encapsulating protein NPs using a flow focusing microfluidic device. The NPs in MPs delivery system was able to protect enhanced green fluorescent protein[265] (eGFP) function in simulated gastric fluid (SGF) and subsequently release functional eGFP NPs in simulated intestinal fluid (SIF). *In vivo*, eGFP delivered orally by NPs in MPs was detected in intestinal epithelial cells of healthy and sick mice. Furthermore, alginate/chitosan MPs were effective in delivering AvrA NPs to reduce clinical and histological indices in a murine dextran sulfate sodium (DSS)-induced colitis model. Altogether these data show the potential of using alginate/chitosan MPs for the gastric passage and intestinal delivery of protein NPs.

3.2 Experimental Methods

3.2.1 Production of recombinant proteins

Recombinant proteins were produced as described previously[51]. Briefly, the eGFP gene in the pPROTet plasmid (Clontech Laboratories) was a generous gift from Dr. Andreas Bommarius and was expressed constitutively for 12 hours in BL21 *Escherichia coli* with 34 μg/mL of chloramphenicol (VWR) in 2XYT media. eGFP was purified with Ni-NTA agarose (Qiagen) following the manufacturer's native imidazole purification protocol. AvrA in the pGEX-4T-2 plasmid (GE Lifesciences) was expressed in AFIQ *Escherichia coli* with 34 μg/mL of chloramphenicol and 200 μg/mL of ampicillin (VWR) in 2XYT media. AvrA bacterial cultures were grown to optical density (O.D.) of 0.7 at 37°C and induced with 0.4 mM isopropyl β-D-thiogalactoside (IPTG) at 25°C for 4 hr. AvrA was purified first with glutathione sepharose

4B (GE Healthcare) following manufacturer's protocol and then purified with Ni-NTA agarose following manufacturer's native imidazole purification protocol. Purified proteins were concentrated using 10 kDa MWCO centrifugal ultrafiltration devices (Millipore) to eGFP concentration ~12mg/mL and AvrA concentration ~1mg/mL in elution buffer (250 mM imidazole, 50 mM sodium phosphate monobasic, 300 mM sodium chloride, pH 8) determined by Nanodrop 2000c (Thermo Fisher Scientific) using MW = 26.95 kDa and $\varepsilon = 61000\ cm^{-1}\ M^{-1}$ for eGFP and MW = 59.84 kDa and $\varepsilon = 60910\ cm^{-1}\ M^{-1}$ for AvrA.

3.2.2 eGFP and AvrA NP synthesis

50 μl of eGFP was added to a glass vial and the volume was completed to 100 μl with AvrA or elution buffer. The mixture was stirred at 700 rpm and desolvated with 400 μl of 200 proof ethanol with a dropwise addition rate of 1 mL/min. 64 μl of 5 mg/ml DTSSP (Pierce) (2.2:1 DTSSP:lysine mole ratio) was added and the mixture was stirred for 90 minutes. The particles were then centrifuged at 500 x g for 5 minutes, supernatant removed, and the particle pellet was resuspended in 0.5 mL of sterile PBS or sterile water. The NPs were sonicated using a sonicate probe (1s on, 3s off, 50% amplitude, 1 minutes) on ice prior to DLS measurement.

3.2.3 NP size and chacterization

Average NP size was characterized using Zetasizer Nano ZS90 (Malvern Instruments Ltd.) with a minimum of three batches of each NP type with three replicates of 10 measurements using the following settings: proteins setting for NP detection and manufacturer PBS settings as the dispersion medium. NP ζ-potential was determined by measuring the electrophoretic mobility of the NPs in PBS using the same instrument. The NP protein concentration was

determined using a BCA assay (Pierce) following the manufacturer's protocol. NP composition was determined using gel electrophoresis by heating 50 μg of NPs in sodium dodecyl (lauryl) sulfate-polyacrylamide gel electrophoresis (SDS-PAGE) loading buffer (50 mM Tris-Cl, pH 6.8, 2% SDS, 100 mM DTT, 0.1% bromophenol blue, 10% glycerol) for 5 minutes at 95°C and loading into a 12% SDS polyacrylamide gel. After SDS-PAGE, proteins were transferred to a nitrocellulose membrane and immunolabelled with Alexa-Fluor 488 conjugated penta-his antibody (Qiagen). Nitrocellulose membranes were then imaged with a Typhoon FLA 9500 (GE Healthcare Life Sciences).

3.2.4 Microfluidic device preparation

A silicon wafer master was designed and fabricated using multi-layer soft lithography techniques and was a generous gift of Emily Jackson and Professor Hang Lu. Polydimethylsiloxane (PDMS) (Sylgard 184, Dow Corning) devices were prepared by thoroughly mixing base polymer to cross-linker at a ratio of 10:1. The mixture was degassed in a vacuum chamber for an hour. PDMS was poured onto the master wafer and cured overnight at 90°C. After curing, the PDMS was cut from the master wafer molds and inlet and outlet access channels were punched with 18 gauge needles. The PDMS devices were plasma treated (PDC-32G plasma cleaner) and bonded onto glass slides and stored at room temperature until further use.

3.2.5 Alginate/chitosan MPs encapsulating protein NPs

4% w/v low viscosity alginate (Protanal LF 200FTS, FMC Biopolymers) was dissolved in deionized (DI) water overnight. Protein NPs were resuspended in DI water and added to stock

alginate solution until the final alginate concentration was 2% w/v (dispersed phase). The dispersed phase was loaded into a syringe equipped with a 20 gauge needle. 1% Span 80 (TCI America) in mineral oil (VWR) was used as the continuous phase and loaded into a syringe with a 20 gauge needle. The syringes placed on a syringe pump (NE-1000, New Era Pump Systems, Inc.) and the needles were connected to the microfluidic device. The flow rate for the aqueous phase was 10 μl/min and the flow rate of the oil phase was 50 μl/min. The collection bath contained 0.5% chitosan (85% deacetylated, Alfa Aesar) and 0.1% $CaCl_2$ (VWR) dissolved in pH 5.5 water under constant stirring. Alginate/chitosan MPs were collected afterwards and centrifuged at 500 x g. The MPs were washed with DI water until no more oil was visually present and stored in DI water until further use.

To view chitosan coating, eGFP NPs were added to the alginate disperse phase and mRFP NPs were added to chitosan collection bath. Crosslinked MPs were collected, washed with DI water and sandwiched between two 24 x 60 mm coverslips. Images were taken on Zeiss LSM 700 confocal.

3.2.6 Optical microscopy

200 μL of chitosan coated alginate MPs were sandwiched between two 24 x 60 mm coverslips (VWR Superslip) and phase contrast and fluorescent images were taken using a Zeiss Axio Observer Z1 inverted microscope. At least 100 microparticles were imaged and diameter was measured using the measurement tool in the Zeiss AxioVision Rel. 4.8 software.

3.2.7 eGFP NP pH recovery

100 ug of eGFP NPs were resuspended in 1 mL of PBS. Hydrochloride acid (HCl) was added to each mixture until the desired pH was reached. Afterwards, the mixtures were incubated at room temperature for 30 minutes. The fluorescence was measured using a Bio-Tek Synergy 2 plate reader. To recover fluorescence, sodium hydroxide (NaOH) was added to each solution until the pH = 7.4. Afterwards, the mixtures were incubated at room temperature for 30 minutes and the fluorescence was re-measured using a Bio-Tek Synergy 2 plate reader.

3.2.8 *In vitro* simulated fluid assay

Simulated gastric fluid and intestinal were made according to updated recipes[266]. 50 mL of either gastric fluid or intestinal fluid was incubated with 4 mg of MPs containing 200 ug of eGFP NPs at 37°C under constant rotation. At defined time points, the solution was centrifuged at 500 x g and 500 μL of supernatant was collected and replaced with 500 μL of fresh simulated fluid. For experiments requiring intestinal incubation after gastric incubation, the gastric pellet was washed two times with PBS in order to neutral remaining gastric buffer. The collected supernatants were then analyzed for fluorescence in a plate reader or BCA assay was used to determine protein concentration.

3.2.9 Detection of protein NP uptake in cells

HeLa cells were cultured in Dulbecco's modified Eagle's medium (DMEM), supplemented with 10% (v/v) fetal bovine serum (FBS). Media was also supplemented with 1% penicillin/streptomycin, and cells were incubated in a 5% CO_2 humidified air atmosphere. HeLa

cells were plated at a density of 100,000 cells per well in a 24-well dish. After 14−16 h of incubation, cell medium was replaced with media containing 200 μL MP released eGFP NPs or a fluorescent equivalent of eGFP NPs that have not undergone encapsulation and 200 μL of media incubated for 6 hr. Cells were washed twice with ice cold PBS and trypsinized. Cells were resuspended in 0.4% Trypan Blue (Corning) to quench non-internalized green fluorescence[267] and analyzed in an LSR II flow cytometer (Becton Dickinson and Company).

3.2.10 *Ex vivo* small intestine NP uptake

Care of experimental animals was performed in accordance with Emory University IACUC institutional guidelines. C57BL/6J mice were sacrificed and small intestine was removed (n = 3). 10 cm of small intestine was cut and filled with 500 μL of MP released eGFP NPs in a modified everted gut sac model[268] or "intestinal sausage casing" tied with dental floss. The intestine was then submerged in DMEM with 10% FBS overnight at 37°C. Intestines were then cut longitudinally and washed with PBS twice before being fixed in 3.7% paraformaldehyde for 30 minutes at room temperature. Fixed colonic e*x vivo* small intestine sections were stained for cytoskeletal and nuclear markers. Actin was labeled with 0.165 μM phalloidin-rhodamine (Biotium) and the nucleus was stained using 0.2 μM Hoechst 33342 (AnaSpec Inc.) for 30 minutes at room temperature. Cells with were washed 3 times with PBS (10 minutes per wash). 50% glycerol in PBS was used a mounting solution and samples were sealed with a coverslip and nail polish. Images were taken on Zeiss LSM 700 confocal.

3.2.11 *In vivo* small intestine NP uptake

C57BL/6J mice were fasted overnight and empty MPs (4 mg), unprotected eGFP NPs (200 μg), and eGFP NPs in MPs (4 mg MPs, 200 μg NPs) were administrated to mice via oral gavage needles (Cadence Science), in a total volume of 200 μL (n = 5). After 4 hours, mice were sacrificed. Small intestines and colon were removed and embedded in O.C.T. compound (Tissue-Tek) and snap frozen in isopentane on dry ice. 20 μm frozen section were cut using CryoStar NX70 Cryostat (Thermo) and mounted on glass slides. Swiss roll colonic frozen sections in optimal cutting temperature (OCT) solution were cut using the CryoStar NX70 Cryostat (Thermo) into 20 μm sections. A PAP pen (Thermo) was used to draw circles around the sections. The sections were fixed with 3.7% paraformaldehyde for 15 minutes and washed in a slide holder dunking into PBS 10 times and left to soak for 10 minutes. The cell surface was immunostained with 100 ng/mL rabbit anti-β-catenin (Proteintech) and eGFP was labeled with 50 ng/mL rat anti-GFP (Biolegend) antibodies. 100 ng/mL of sheep rhodamine conjugated anti-rabbit IgG (Rockland) was used as β-catenin secondary antibody. 50 ng/mL of goat ATTO 647N conjugated anti-rat IgG (Rockland) was used as eGFP secondary antibody. Nuclei were stained with Hoechst 33342 (AnaSpec Inc.). Intestinal uptake of protein NPs was imaged using a Zeiss LSM 710 confocal laser scanning system. Image analysis was performed using Matlab to quantify the number of red and green pixels. A 2D maximum projection confocal image of various sections of the colon was converted into an array of 512 x 512 pixels with each pixel containing red, blue, and green values that range numerically from 0 to 255. A 20% threshold (of the maximum pixel value) chosen as a cutoff point. Red, blue, and green pixel intensities about the threshold returned a true value and pixel intensities below the threshold returned a false value. The number of true green pixels was counted and normalized by the number of true red

pixels. Normalized green pixels count from empty MPs were taken as the baseline compared with unprotected eGFP NPs and eGFP NPs in MPs.

3.2.12 *In vivo* DSS colitis mouse model

Dextran sulfate sodium (36000-50000 MW; MP Biomedicals) colitis was induced by giving 3% w/v DSS in autoclaved MilliQ water as drinking water and allowing mice to drink *ad libidum* for 10 days. Treatment groups (n = 5) of PBS, 200 μg of AvrA NPs (16 μg of AvrA), 4 mg empty MP, 4 mg eGFP NPs in MPs (200 μg of NPs), and 4 mg AvrA NPs in MPs (200 μg of NPs, 16 μg of AvrA) were administrated via an oral gavage needle. Total volume of gavage was 200 μL. Mice were gavaged once a day for 5 days prior to introduction of DSS. Afterwards, mice were gavaged daily for the 10 day duration of the DSS in the water supply. Disease activity was monitored daily. Disease activity index was calculated as the sum of the scores of stool consistency (0: hard, 2: soft, 4: diarrhea), fecal occult blood using Hemoccult Sensa (Beckman Coulter) (0: negative, 2: positive, 4: macroscopic) and weight loss (0: <1%, 1: 1-5%, 2: 5-10%, 3: 10-20%, 4: >20%). Disease score was calculated as the average of these three parameters. After the 10^{th} day on DSS, mice were sacrificed and colons were removed and fixed in 3.7% formalin for 1 day in a "swiss roll" orientation then transferred to 70% ethanol for 3 days before being embedded in paraffin. Caecum was removed, washed with PBS, and stored as whole tissue in -80°C.

Paraffin embedded sections were deparaffinized using the Autostainer XL (Leica), circled with a PAP pen (Thermo) and immunostained with 100 ng/mL rabbit anti-β-catenin (Proteintech) and 50 ng/mL rat anti-GFP (Biolegend) antibodies. 100 ng/mL of sheep rhodamine conjugated anti-rabbit IgG (Rockland) was used as β-catenin secondary antibody. 50 ng/mL of

goat ATTO 647N conjugated anti-rat IgG (Rockland) was used as eGFP secondary antibody. Nuclei were stained with Hoechst 33342 (AnaSpec Inc.). Inflamed colonic uptake of protein NPs was imaged using Zeiss LSM 710 confocal laser scanning system.

3.2.13 MPO assay

Caecum was homogenized with a Polytron PT 1200E handheld homogenizer in ice-cold potassium phosphate buffer (50 mmol/l K_2HPO_4 and 50 mmol/l KH_2PO_4, pH 6.0) containing 0.5% hexadecyltrimethylammonium bromide (Sigma-Aldrich) and then centrifuged at 17500 x g for 15 minutes. Supernatants were collected and added to 1 mg/mL o-dianisidine hydrochloride (Sigma-Aldrich) and 0.0005% H_2O_2, and the change in absorbance at 450 nm was measured on a Bio-Tek Synergy 2 plate reader. One unit of MPO activity was defined as the amount that degraded 1 μmol peroxidase per minute. The results were expressed as absorbance per milligram of tissue.

3.2.14 Histology

Colonic swiss rolls embedded in paraffin were cut using Microm HM 325 Rotary Microtome (Rankin Biomedical) into 10 μm slices, deparaffinized, and stained with hematoxylin and eosin using Autostainer XL (Leica). Photographs were taken using a Nikon Eclipse E600 w/ Q-Imaging with 2x, 10x, 20x, and 40x objectives. Histological examination was performed by two independent observers on hematoxylin–eosin slides of paraffin colon sections. Histology score was assessed for severity of inflammation (0: none, 1: slight, 2: moderate, 3: severe), PMN infiltration/HPF (0: <5, 1: 5–20, 2: 21–60, 3: 61–100, 4: >100), depth of injury (0: none, 1: mucosa, 2: mucosa and submucosa, 3: transmural), crypt damage (0: none, 1: basal 1/3, 2: basal

2/3, 3: only surface epithelium intact, 4: entire crypt lost), and adjusted to tissue involvement by multiplication of percentage factor (x1: 0–25%, x2: 26–50%, x3: 51–75%, x4: 76-100%)[269].

3.2.15 Statistics

Significance was assessed by a one-way ANOVA or Student's unpaired t-test at a significance level of $p < 0.05$. All data shown is representative of at least three independent measurements unless indicated otherwise.

3.3 Results and Discussion

3.3.1 Synthesis, characterization, and stability of protein NPs

AvrA was expressed as a fusion protein containing a N-terminal glutathione S-transferase (GST) tag to improve AvrA solubility[270] and a C-terminal 6x-His tag for purification. Protein NPs were synthesized by desolvating either a solution of eGFP or eGFP and AvrA with ethanol under constant stirring[162, 243] (Figure 3.1) to make eGFP NPs or eGFP+AvrA NPs, shortened to AvrA NPs for the rest of this report. The nanoclusters formed were crosslinked with reducible 3,3'-dithiobis-[sulfosuccinimidylpropionate] (DTSSP) to stabilize them. DTSSP was chosen because it contains a disulfide bond sensitive to the reducing conditions found in the cytosol[271]. Dynamic light scattering (DLS) showed eGFP NPs had a diameter of 270 ± 55 nm, polydispersity index (PDI) of 0.352 ± 0.153, and ζ-potential of -11.6 ± 0.9 mV in phosphate buffered saline (PBS). When AvrA was co-desolvated with eGFP to make AvrA NPs, the properties were similar with NP diameter of 281 ± 52 nm, PDI of 0.327 ± 0.074, and ζ-potential of -11.6 ± 0.6 mV in PBS. Composition of NPs was verified by western blot following reduction

(Figure 2.3). We estimate that each AvrA NP contains on the order of 5,000 molecules of AvrA and 100,000 molecules of eGFP based on the volume of a spherical NP and the theoretical volumes of the proteins based on their molecular weight and average protein partial specific volume[272]. Using eGFP as a carrier for AvrA in the NP allows for fluorescent tracking of the NPs and eGFP fluorescence serves as a proxy for protein activity.

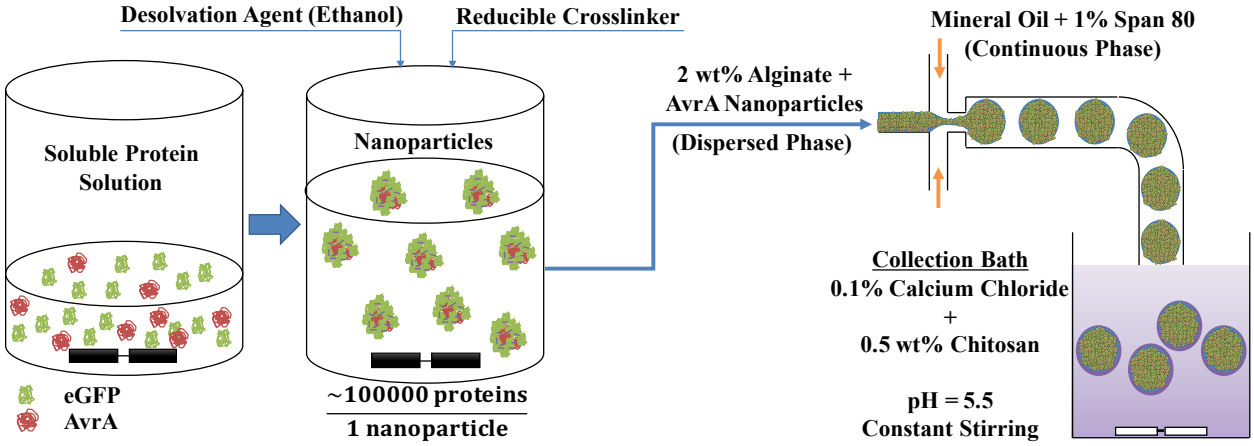

Figure 3.1: Synthesis and Characterization of Protein NPs in MPs. Schematic representation of AvrA NP desolvation, NP loading into alginate droplets via flow focusing microfluidic device, and NPs in MPs simultaneous crosslinking and coating with calcium and chitosan.

Simulated gastric fluid (SGF) and simulated intestinal fluid (SIF) containing digestive enzymes were incubated with eGFP NPs to test the ability of NPs alone to retain protein stability[266]. SGF and SIF are based on a fasted state of the stomach. Fed state versions of SGF and SIF are also made available, however, the pH of the gastric fed state is 5 compared to 1.6 in the fasted state. We chose to do all *in vitro* simulated fluid studies in the harsher fasted state conditions to test the durability of our NPs and oral delivery vehicle. Figure 3.2 shows that eGFP NPs lose 30% of its fluorescence in SIF and 100% of its fluorescence in SGF. pH appears to be the main driving force behind loss of eGFP fluorescence since was no time dependence as would be expected with enzymatic degradation of eGFP. Loss of fluorescence is dependent on the pH as seen in Figure 3.2. Up to pH 3, eGFP fluorescence can be recovered by adjusting the pH back

to 7.4. Below pH 3, the fluorescence cannot be recovered and there seems to be an irreversible loss of more than 50% of eGFP fluorescence. Soluble eGFP has been reported to completely lose fluorescence at pH 2, however, it is able to undergo complete fluorescence recovery when buffered back to pH 8[273]. As the limit for eGFP NPs to fully recover is pH 3, it appears that NPs lose some ability to recover pH-induced fluorescence loss compared with soluble protein. The pH-induced loss of eGFP fluorescence is due to pronation of tyrosine-66 affecting the interaction with the chromophore within its β-can[274]. The inability of eGFP NPs to completely recover fluorescence suggests that the crosslinking may affect the ability of tyrosine-66 to reengage the chromophore. This is informative because it demonstrates the need for buffering capacity in an oral delivery vehicle. We have previously shown that AvrA NPs are active in the murine colon physiological environment[51], so the harsh conditions found in the stomach would be the major limiting step in implementing an oral formulation. It is therefore necessary to design and encapsulate therapeutic NPs within an oral delivery vehicle that is capable of buffering against the gastric pH.

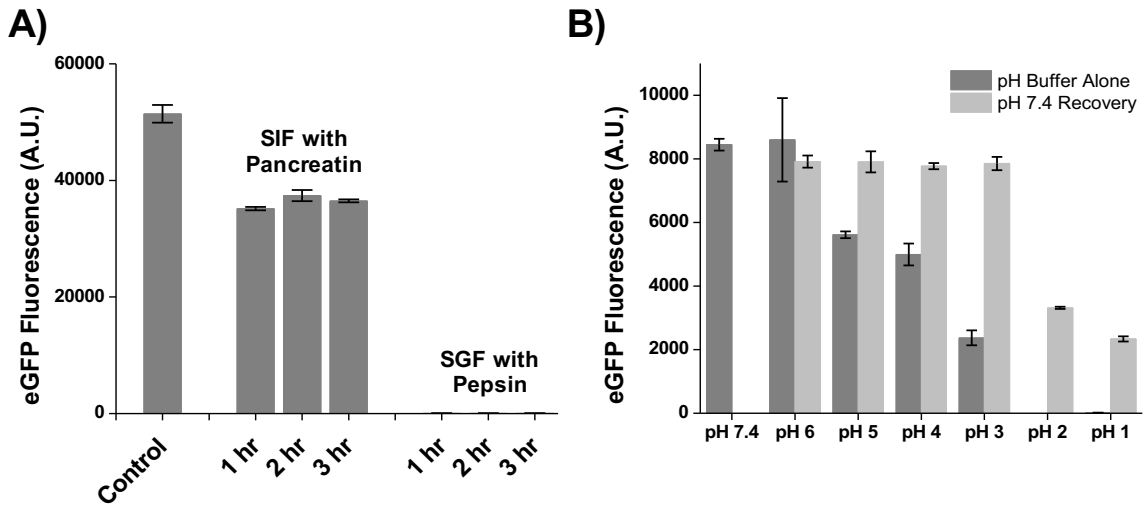

Figure 3.2: *In Vitro* eGFP NP Stability. A) eGFP NP stability in simulated intestinal and gastric fluids. B) eGFP NP fluorescence pH dependence and fluorescence pH recovery

AvrA NPs were mixed with alginate and droplets were formed using a flow focusing microfluidic device (Figure 3.1). The droplet size was controlled by tuning the flow rates of the dispersed and continuous phase. Droplets were then crosslinked with calcium. A representative phase contrast and fluorescent image is seen in Figure 3.2 Alginate MPs crosslinked with calcium have an average size of 311 ± 41 μm and have a ζ-potential of -12.6 ± 1.9 mV in water (Figure 3.3). Alginate MPs have a tadpole morphology resulting from the uneven calcium gelation at the oil/water interface in the collection bath. This morphology has been reported before with alginate microparticles[275]. Alginate MPs had an eGFP NP encapsulation efficiency of 24.0 ± 4.4% with most of the NPs lost occurring during crosslinking. The collection bath contained 81.6 ± 9.5% of the initial eGFP NPs.

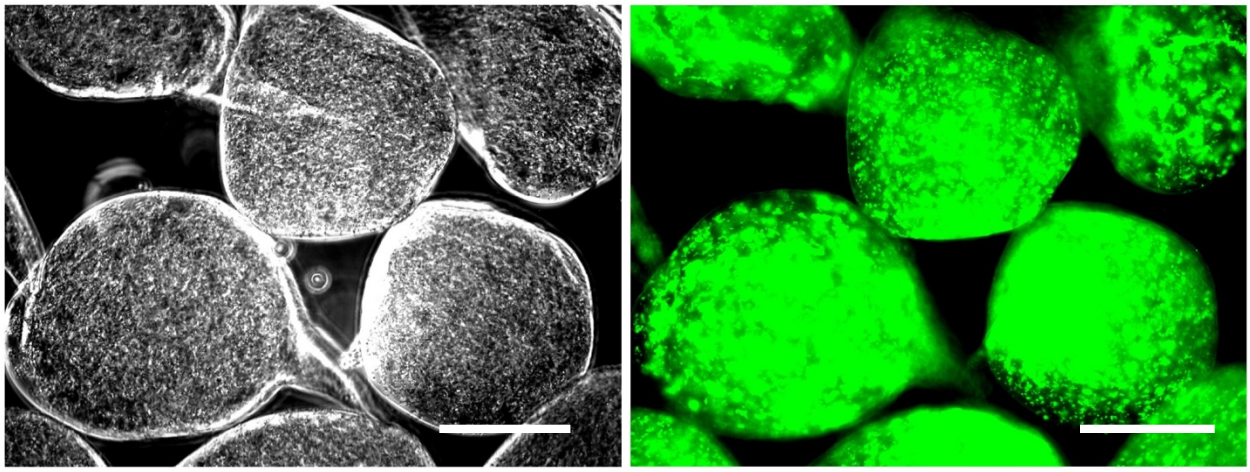

Figure 3.3: Phase contrast images of alginate only microparticles (left). Corresponding green fluorescence image (right). Scale bar = 200 μm

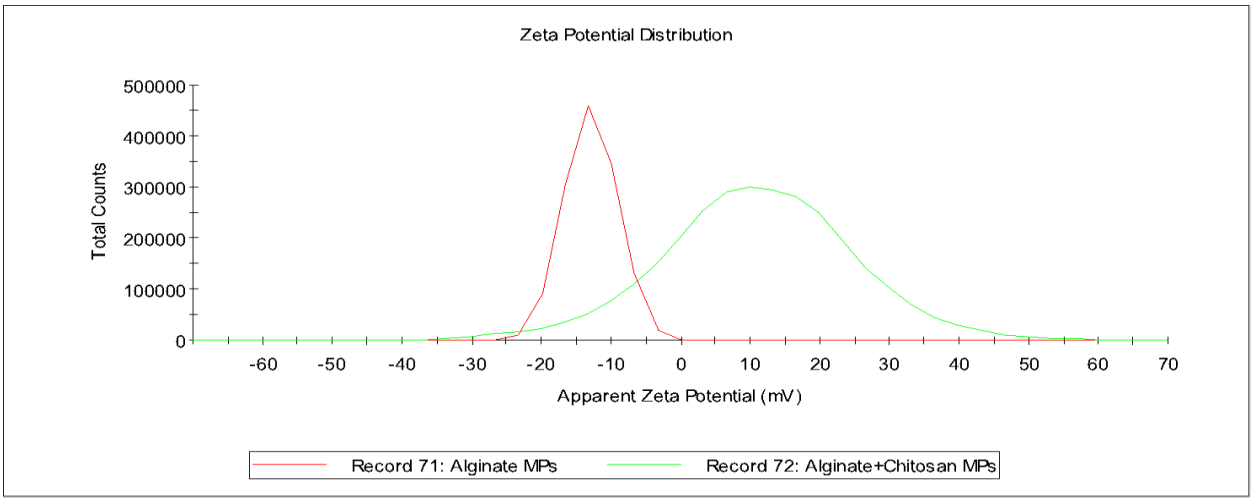

Figure 3.4: Zeta potential of alginate microparticles compared with alginate/chitosan microparticles.

3.3.2 Alginate/chitosan MPs protect and release eGFP NPs in simulated fluids

In an effort to improve the encapsulation efficiency, chitosan was added into the collection bath with calcium. eGFP NPs were encapsulated within alginate MPs, coated with different chitosan coatings, incubated in SGF, and then washed in PBS to buffer them back to

physiological pH to measure MP fluorescence retention. We found that without the chitosan, alginate MPs did not retain any eGFP NP fluorescence, as seen in Figure 3A. This could be due to a combination of drug leakage and irreversible pH denaturation of the proteins in the NPs. Alginate MPs have a reported pore size distribution between 5 - 200 nm throughout the entire core with smaller pore size distribution near the surface of the MP[218]. As a pH-responsive polymer, alginate MPs also shrink at low pH and swell at physiological pH. The NPs are ~275 nm, suggesting that it is unlikely that they would diffuse out of the alginate MP during the SGF incubation. Therefore, the majority of the fluorescence loss seen in Figure 3.5 is likely due to the pH denaturation rather than eGFP NP leakage. In either case, the inability of the alginate MPs to retain eGFP fluorescence following SGF incubation demonstrates the necessity of a coating.

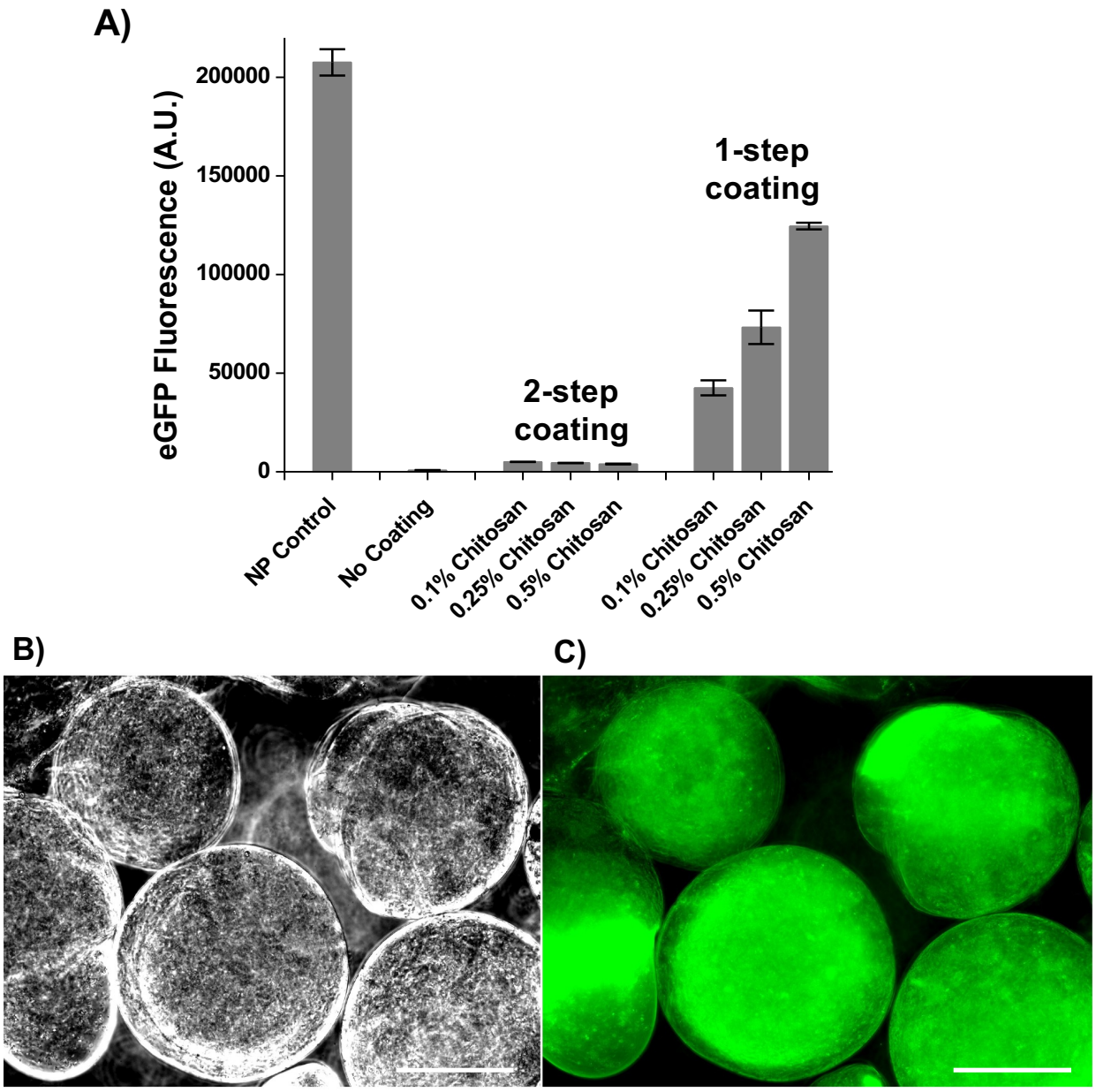

Figure 3.5: *In Vitro* Gastric Protection of eGFP NPs in MPs. A) Effect of chitosan coating on eGFP NPs in MPs following gastric incubation. B) Representative phase contrast image of eGFP NPs in MPs and C) fluorescence image of eGFP NPs in MPs. Scale bar = 200 μm

Chitosan coatings on alginate hydrogels have been studied for their ability to make a polyelectrolyte complex (PEC) capable of reducing drug leakage[219, 276, 277]. Chitosan can also provide buffering capacity in the gastric environment through pronating of its amine groups[278, 279] which have a pKa of ~6.2. The alginate core could also provide some buffering capacity by

pronation of carboxyl groups, which have a pKa of ~3.4, though to a lesser extent than chitosan due to the differences in pKa between the amine and carboxyl groups. Coating chitosan onto alginate MPs after calcium crosslinking ("two-step" process) did not improve protection of eGFP fluorescence in SGF better than alginate only MPs, as seen in Figure 3.5. The two-step coating was ineffective in producing a sufficient chitosan layer and provided no additional SGF protection. We speculate that the failure of the two-step process to make sufficient protective chitosan coating is due to the loss of the electrostatic driving force. The G residues on the alginate chain were already saturated with calcium, which is an ionic crosslinker that allows the alginate to gel. After calcium crosslinking, the alginate beads are submerged in a pH 5.5 chitosan solution. The pH of the solution is near the pKa of the chitosan to prevent unwanted protein hydrolysis and denaturation, whichmeans that a lower percentage of the chitosan amine groups are protonated. This coupled with the calcium saturated carboxylate groups on alginate leads to little to no chitosan coating on the MPs.

A 1-step simultaneous chitosan coating and calcium crosslinking process leads to competition of calcium and chitosan for alginate binding sites, and increases the amount of chitosan on alginate MPs. Increasing amounts of chitosan in the collection bath, with constant calcium concentration, leads to higher retention of eGFP fluorescence in SGF as seen in Figure 3.5. Figure 3.5 shows that higher concentrations of chitosan in the collection bath confers increasing gastric protection of eGFP fluorescence. Increasing the chitosan concentration lead to overall higher levels of gastric protection consistent with other reports[208, 210, 211] but can also hinder NP release[211]. 1-step 0.5% chitosan coating was chosen and used for all future experiments as it was the most effective in retaining eGFP NP fluorescence.

Alginate/chitosan MPs have an average size of 335 ± 50 μm determined by phase contrast microscopy. A representative phase contrast and fluorescent image is seen in Figure 3.5. Particles are more spherical compared with alginate only MPs and have an acorn morphology more than tadpole morphology. This "acorn" morphology is owed to the uneven coating and crosslinking that occurs when alginate droplets enter the collection bath interface. Alginate/chitosan MPs had an eGFP NP encapsulation efficiency of 59.9 ± 1.1% and only 37.1 ± 10.0% of the initial eGFP NPs were found in the collection bath. The addition of chitosan in the collection bath increased the eGFP NP encapsulation efficiency by approximately 35%. When chitosan is introduced in the collection bath, it acts as a crosslinker in addition to the calcium and increases the overall rate of crosslinking and, therefore, retention of the NPs.

The alginate/chitosan MPs ζ-potential was measured to ensure that a chitosan coating was achieved. Alginate/chitosan MPs have a ζ-potential of -12.6 ± 1.9 mV in water (Figure 3.4). The switch in sign from negative to positive when chitosan was introduced was predicted given the complementary electrostatic properties of the two polysaccharides. The chitosan coated alginate MPs encapsulating eGFP NPs or AvrA NPs were analyzed with confocal microscopy to support that the chitosan coating procedure was successful. eGFP NPs were mixed with alginate and monomeric red fluorescent protein (mRFP) NPs were mixed with chitosan prior to NPs in MPs fabrication. A confocal cross section (Figure 3.6) indicates that green alginate MPs have a red chitosan coating around them. We estimate the chitosan coating is approximately 30 μm from the images. A summary of all NPs and microparticles used in this report is in Table 1.

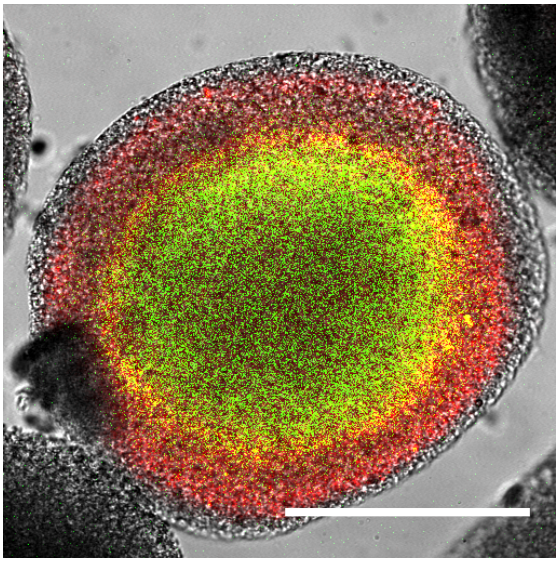

Figure 3.6: Confocal slice of alginate/chitosan microparticle. eGFP NPs were loaded into the alginate and formed the alginate core. mRFP NPs were loaded in the chitosan and make up the chitosan coating. Scale bar = 200 μm.

Table 3.1 Size and ζ–potential of NPs and Microparticles

Particle Name	Diameter	ζ–potential (mV)	Cartoon
eGFP NP	270 ± 55 nm	-11.6 ± 0.9 mV	
eGFP+AvrA NP (AvrA NP)	281 ± 52 nm	-11.6 ± 0.6 mV	
Empty Alginate MP	311 ± 41 μm	-12.6 ± 1.9 mV	
Empty Alginate/Chitosan MP (Empty MP)	339 ± 52 μm	+10.0 ± 3.5 mV	
eGFP NP in Alginate/Chitosan MP (eGFP NP in MP)	334 ± 47 μm	+14.3 ± 9.1 mV	
eGFP+AvrA NP in Alginate/Chitosan MP (AvrA NP in MP)	335 ± 50 μm	+12.8 ± 7.9 mV	

One-step 0.5% chitosan coated alginate MPs were tested for release of functional eGFP NP cargo after simulated gastric incubation. Figure 3.7 shows fluorescence of eGFP NPs released from MPs that have been incubated in either SIF only or SGF followed by SIF. eGFP

NPs in MP exhibited fast burst release in both cases. This shows that MPs are able to both protect eGFP NPs in SGF and subsequently release them in SIF. Approximately 70% of encapsulated NPs were released.

To ensure that MP released NPs were still able to be taken up by cells, they were incubated with HeLa cells. In Figure 3.7, MP released eGFP NPs achieve an uptake efficiency of ~65% normalized to cells that internalized eGFP NPs that were never encapsulated in MPs. This indicates most of the released NPs are able to be taken up by cells *in vitro*.

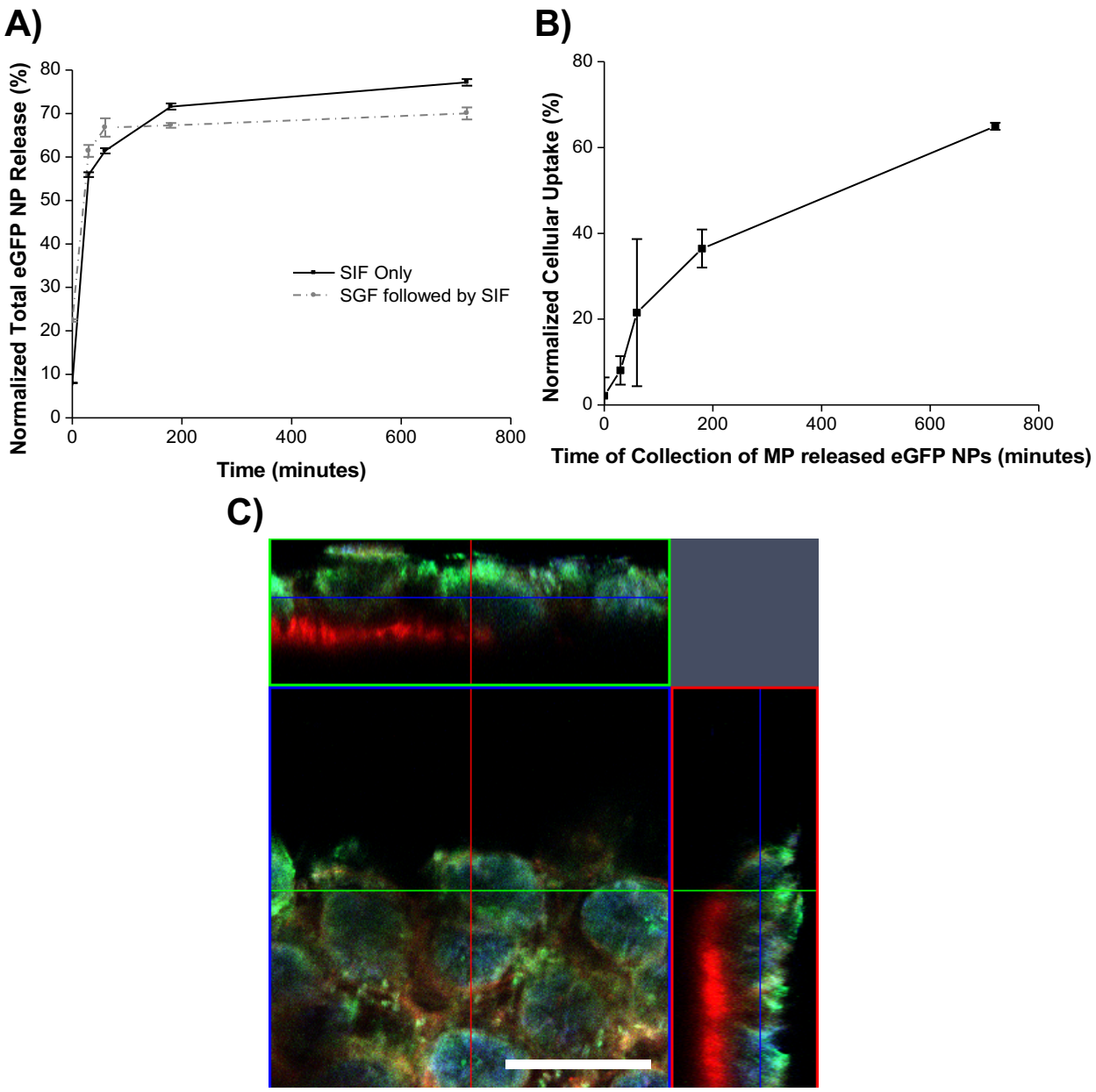

Figure 3.7: *In Vitro* release of eGFP NPs from MPs. A) eGFP NPs release kinetics from 1-step 0.5% chitosan MPs in SIF with and without prior incubation in SGF, normalized to eGFP NPs in MPs that have not undergone simulated fluid incubated. B) MP released eGFP NPs uptake in HeLa cells normalized to an fluorescent equivalent amount of eGFP NPs that have not been encapsulated. C) MP released eGFP NPs associate with *ex vivo* section of mouse small intestine (scale bar = 100 μm). Actin is stained in red, nuclei in blue, and green signal is native eGFP fluorescence.

To evaluate if NPs released from MPs can penetrate mucus and associate with the underlying cells, they were incubated with *ex vivo* sections of small intestine from mice.

Confocal images in Figure 3.7 show active (fluorescent) protein associated with cells found in the villi and crypt regions. We cannot conclude there was active uptake as the cells in *ex vivo* sections may not have been viable during the entire incubation period. However, the SIG-SIF MP released eGFP NPs were able to penetrate the adherent mucus layer to reach the cells underneath and motivates *in vivo* assessment. Altogether, these results show that alginate/chitosan MPs protect eGFP NPs in the simulated gastric environment and subsequently release them in simulated intestinal fluid in a form that can be internalized by cells and cross mucus.

3.3.3 Oral delivery of NPs in MPs protect and release eGFP NPs in healthy mice

After establishing the protection and release of eGFP NPs from alginate/chitosan MPs *in vitro*, we assessed performance in an *in vivo* oral delivery model. Healthy mice were gavaged with empty MPs, unprotected eGFP NPs, and eGFP NPs in MPs after overnight fasting. After 4 hours, mice were sacrificed and the duodenum, jejunum, and colon were harvested, immunostained for eGFP, and imaged by confocal microscopy. Figure 3.8 shows a table of representative images of crypt cells and villi in the duodenum and jejunum of mice. No eGFP was detected in mice gavaged with empty MPs. eGFP was detected in the duodenum and jejunum of mice that were gavaged with both unprotected eGFP NPs and eGFP NPs in MP. The first third of the intestine, the duodenum, immediately follows the stomach and receives bile, stomach acid, and digestive enzymes still working to break up the contents of the stomach. The jejunum constitutes the largest portion of small intestine and has primary uptake function. Expectedly, we observed more eGFP in the jejunum than the duodenum, especially in the crypt region and within the villi.

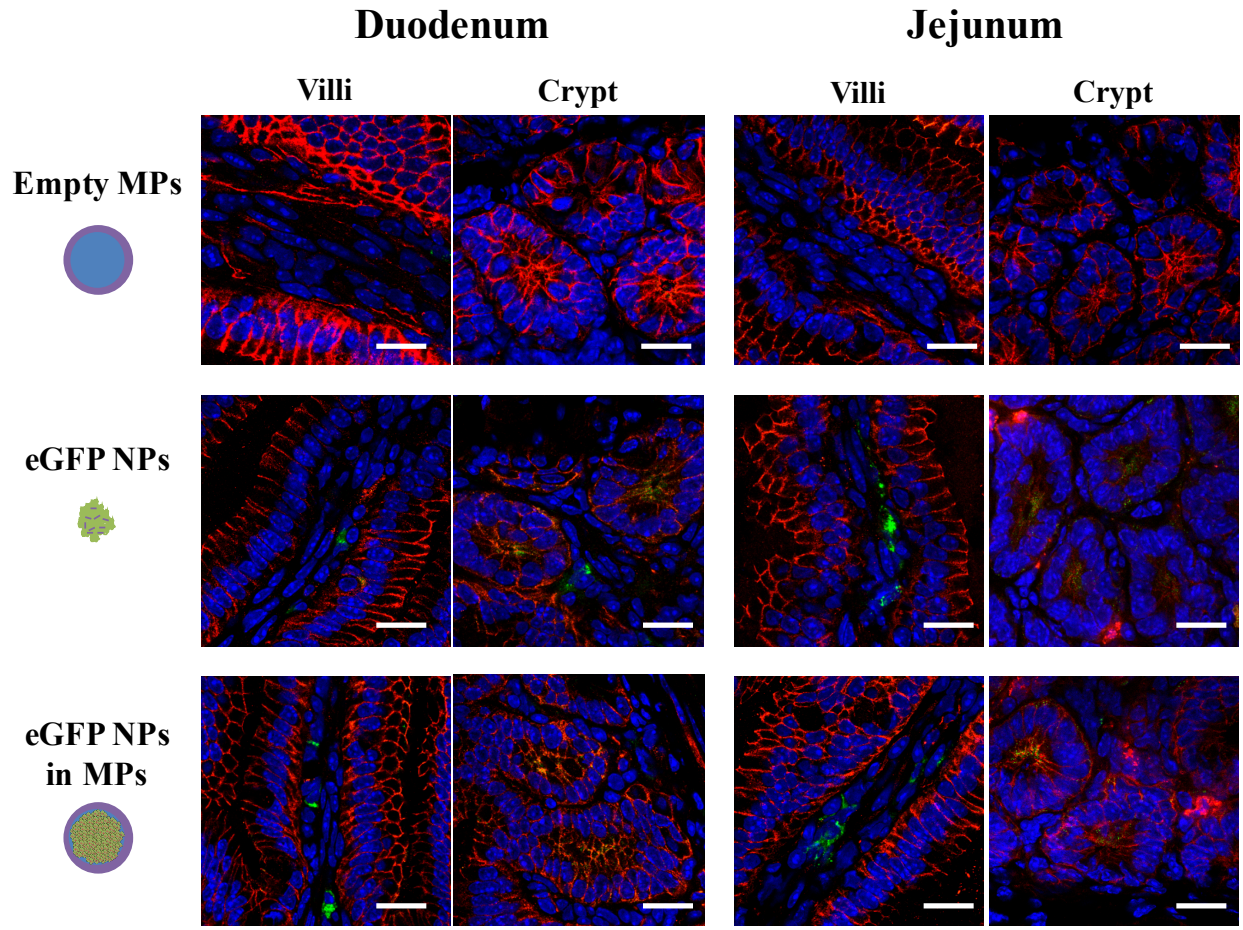

Figure 3.8: Oral delivery of eGFP NPs in MPs gavaged to healthy fasted mice. Representative confocal slices of from 20 μm sections of different sections of the intestine. Villi are long fingerlike projections that sample the contents of the lumen. The lamina propria, which is located within the villi, is where immune cells residue. Crypts are regions farthest from the lumen inhabited by stem cells that differentiate into enterocytes, goblet cells, Paneth cells, and endocrine cells. Nuclei are stained with Hoechst in blue, β-catenin is stained with anti-β-catenin in red, and eGFP is stained with anti-eGFP in green. Scale bar = 20 μm.

Detecting eGFP NPs in the crypts implies that eGFP NPs are released from MP and are able to penetrate the mucus to reach cells furthest away from the lumen of the intestine. Our NPs were designed to penetrate the mucus and enhance cellular internalization. The slight negative ζ-potential of the NPs coupled with their size allows NPs to repel the mucin fibers and diffuse through their dynamic, dense polymeric network[199, 200, 202]. The eGFP signal that was associated

with cells within the lamina propria was promising because it suggests that eGFP NPs are penetrating the epithelial layer of the villi. Immune cells are known to residue within the lamina propria[280] however, from these images the specific cell types cannot be identified without staining of specific immune cell surface markers. Of particular interest was the difference in positive detection of eGFP in the colon of mice between unprotected eGFP NPs and eGFP NPs in MPs as seen in Figure 6A, B. We observed more eGFP in the colons of mice gavaged with eGFP NPs in MPs compared with unprotected eGFP NPs. Unprotected eGFP NPs were unable to fully transverse the small intestine to reach the colon and the majority of the uptake was limited to the jejunum. eGFP NPs in MPs were able to access the entire length of the gastrointestinal tract including the colon.

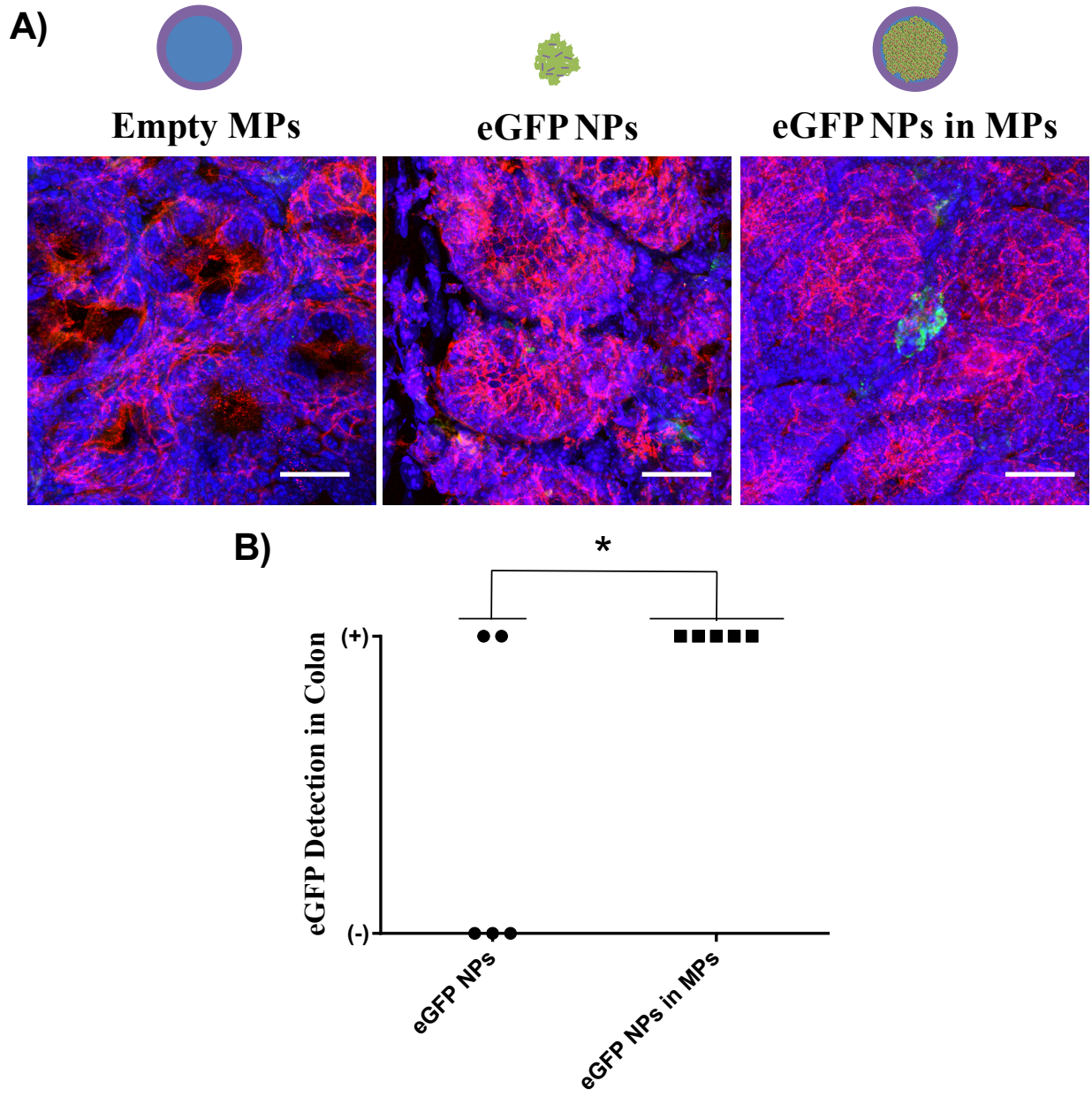

Figure 3.9: Oral delivery of eGFP NPs in MPs (4 mg of MPs, 200 ug of NPs) gavaged to healthy fasted mice (n=5). A) Representative 2D maximum projections taken from the colon. B) Matlab analysis of eGFP signal in 2D maximum projections. Baseline green fluorescence was determined from control mice gavaged with empty MPs. A positive score indicates that the green fluorescence was significantly different from the control. A negative score indicates not significant different from the control. $P < 0.05$

It should be noted that a polyclonal anti-eGFP primary antibody and fluorescently conjugated secondary antibody were used to detect eGFP in the intestine and colon. Oral

gavaged eGFP NPs spread over the entire length of the gastrointestinal tract and therefore concentrations in specific sections were too low to detect eGFP by its native fluorescence, which necessitated immunohistochemistry to amplify the eGFP signal. Another caveat is the gastric pH difference between mice[281] and humans[282]. Mice gastric pH reaches a low of 3 while in humans gastric pH can be as low as 1. This difference means that additional optimization could be required to achieve similar delivery in humans. Also in IBD patients, the pH in the small intestine and colon is slightly lower than in normal healthy individuals[202]. This could lead to reduced or slower release of NPs from the MPs.

3.3.4 AvrA NPs in MPs reduce inflammation in murine DSS-induced colitis

Inducing inflammation in the small intestine of mice generally requires transgenic knockout mice models or adoptive T-cell transfer and even in those cases, inflammation is limited to the ileum[259]. More common models are chemically induced colitis that offer a straightforward method to study gut inflammation[283]. Detection of eGFP in the colon of healthy mice was a motivator to pursue preclinical applications of a therapeutic for IBD. AvrA NPs were loaded into alginate/chitosan MPs and gavaged daily into mice for 5 days. After pretreatment, 3% DSS (36000 – 50000 MW) was added to the drinking water and the mice were allowed to drink *ad libitum* for an additional 10 days while continuing to receive daily AvrA gavages. DSS is a sulfated polysaccharide that is toxic to intestinal epithelial cells of the basal crypt[283, 284]. It induces severe inflammation restricted to the colon perpetuated by an innate immune response. After DSS treatment, mice were sacrificed and the colons were harvested and preserved as swiss rolls. Representative images are shown in Figure 3.10. Evidence of eGFP was observed in the colonic surface epithelium and crypt cells in DSS treated mice that received AvrA NPs in MPs

and eGFP NPs in MPs but not the other treatment groups. This suggests that AvrA NPs are still able to be released from MPs and penetrate the mucus in an inflammatory environment to reach the underlying cells, similar to the results in healthy mice in Figure 3.8.

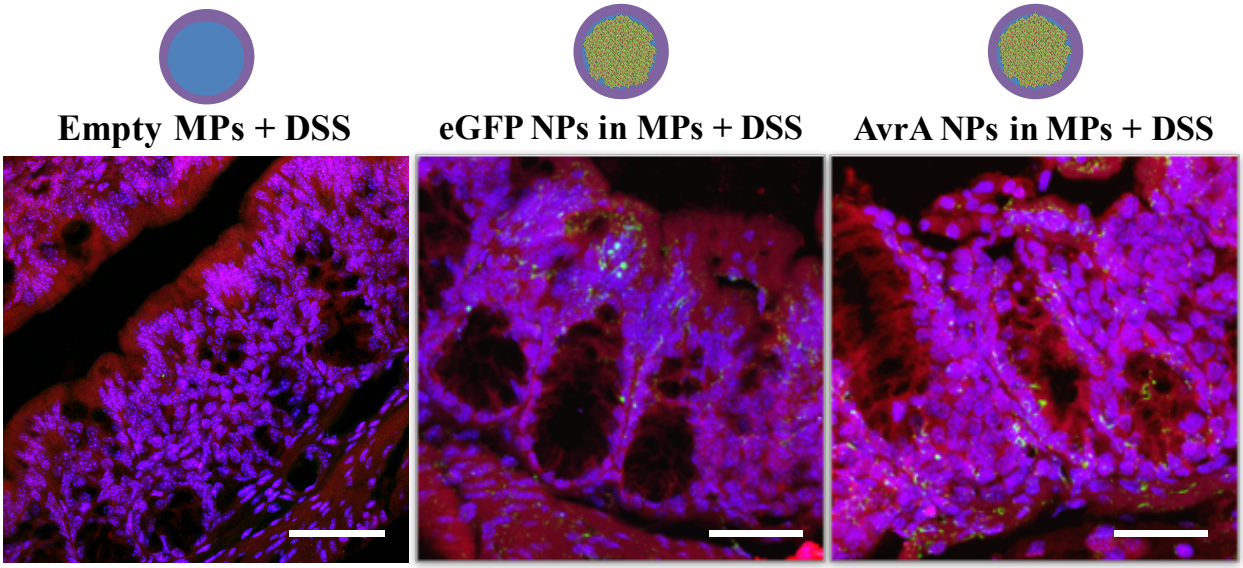

Figure 3.10: Oral Delivery of AvrA NPs in MPs uptake in inflamed mucosa. Representative confocal images of a 10 μm paraffin embedded colonic swiss roll from a mouse treated with empty MPs, eGFP NPs in MPs, and AvrA NPs in MPs (4 mg of MPs, 200 ug of NPs). Nucleus is stained in blue, b-catenin is stained in red, and eGFP stained in green. Scale bar = 50 μm.

Weight change was recorded as a macroscopic clinical indicator of colitis symptoms[285]. The daily weight change percentage as compared to pretreatment for the course of this experiment is seen in Figure 3.11. There was no significant difference between any of the experimental groups (n = 5) during the pretreatment phase, suggesting no major negative effect of any treatment group. After DSS was introduced, all experimental groups exhibited a minor increase in weight gain and then a steady decrease until the mice were sacrificed. Mice receiving 4 mg of AvrA NPs in MPs (containing 200 μg of AvrA NP with 16 μg of AvrA) had significantly less weight loss than mice receiving no treatment. All other DSS treatment groups (AvrA NPs, Empty MPs, and eGFP NPs in MPs) exhibited the same amount of weight loss as untreated DSS mice. Figure 8B shows disease activity index (DAI) that was assessed after DSS

was introduced to evaluate the clinical progression of colitis. DAI is a combined score of weight loss compared to pretreatment weight, stool consistency, and fecal occult blood. DSS mice receiving AvrA NPs in MPs showed a significant reduction in DAI during the last 4 days of treatment compared with the DSS untreated group. All other treatment groups show no significant reduction compared with the untreated group.

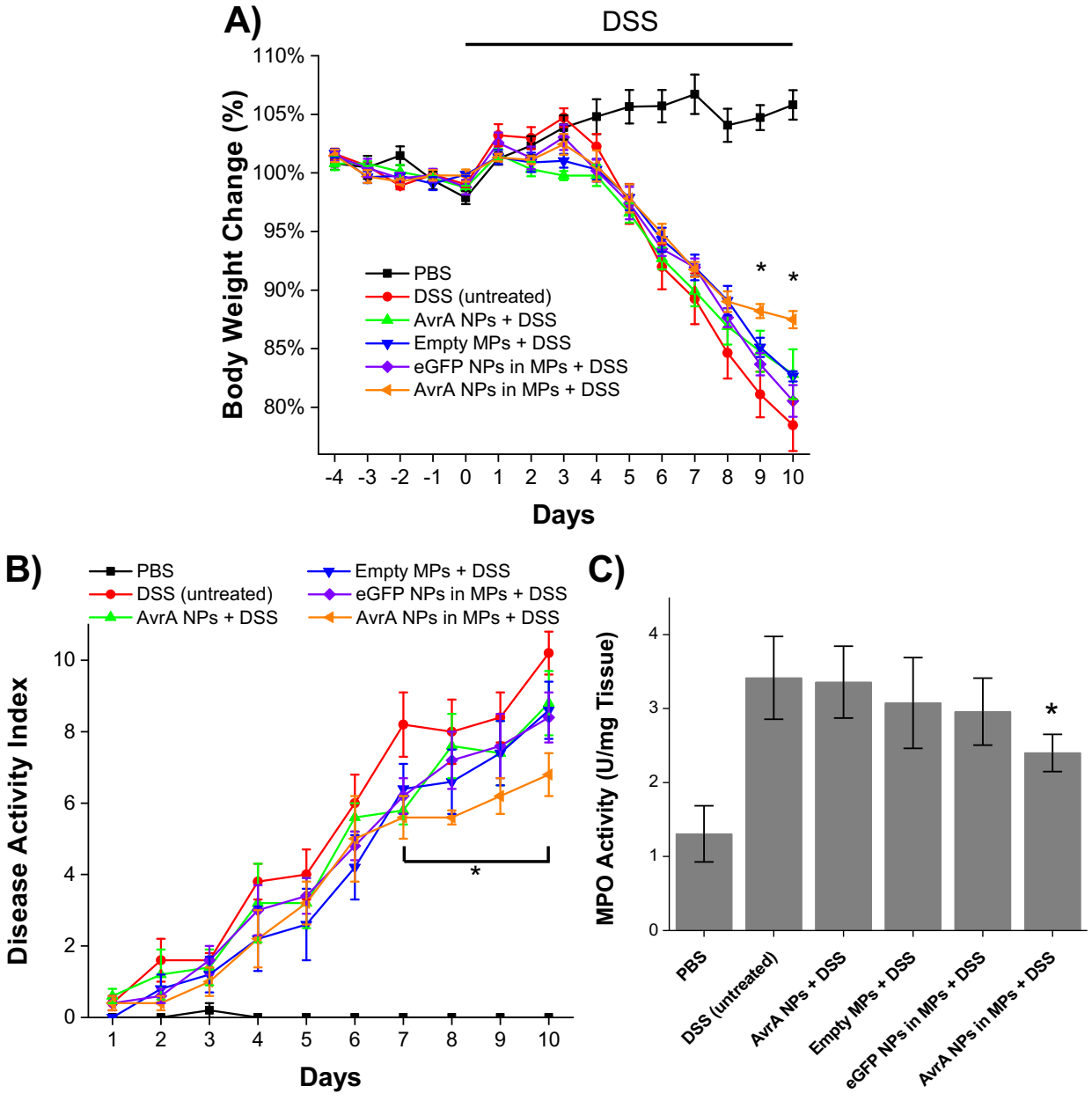

Figure 3.11: Oral Delivery of AvrA NPs in MPs in murine DSS-induced colitis improve clinical scores A) Body weight change of mice (n = 5) receiving daily oral gavages (4 mg of AvrA NPs

in MPs (200 μg of AvrA NP, 16 μg of AvrA)). 5 days of pretreatment followed by 10 days of co-treatment with DSS. * $p < 0.05$ compared to DSS group. B) Clinical disease activity index scoring of 5 mice per indicated condition after DSS was introduced. * $p < 0.05$ compared with DSS group. C) Intracellular myeloperoxidase activity of caecum harvested from mice. * $p < 0.05$ compared with DSS group.

We measured intracellular caecal myeloperoxidase (MPO) activity as a proxy for neutrophil infiltration[286], a downstream effect of inflammation. The results are seen in Figure 3.11. AvrA NPs in MPs was the only treatment group that significantly reduced caecal MPO activity in DSS-induced colitis mice. This reduction in MPO activity supports the reduction in weight loss and the reduction in disease activity index seen in Figure 3.11.

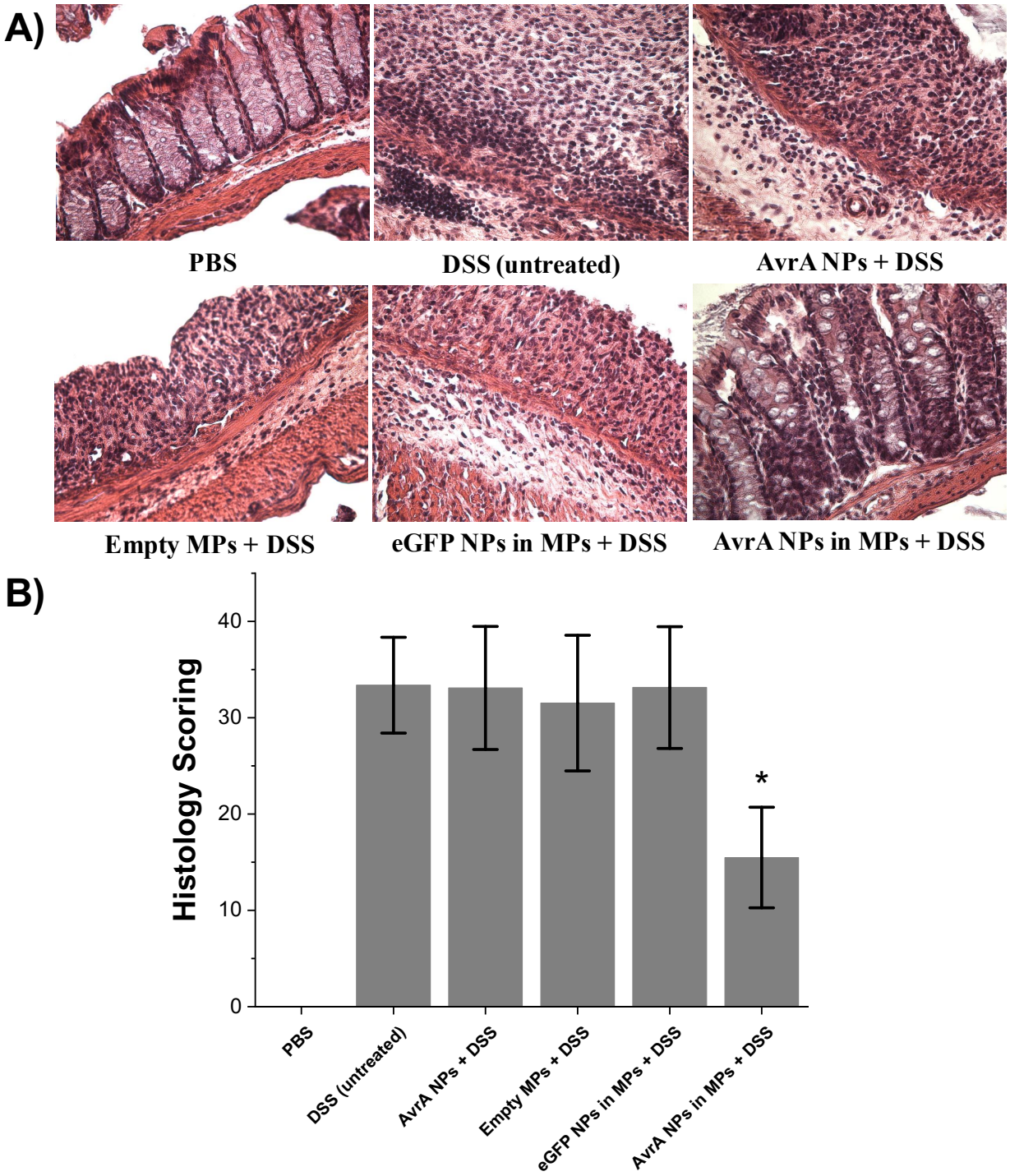

Figure 3.12: Oral Delivery of AvrA NPs in MPs in murine DSS-induced colitis improve histological scores. A) Representative histological sections of 10 μm paraffin embedded swiss rolls under 40x magnification. B) Histological scoring of 5 mice per condition. * $p < 0.05$ compared to DSS group.

Histology was performed on 10 μm paraffin slices taken from the colonic swiss rolls subjected to hematoxylin and eosin staining (H&E). Representative images are seen in Figure 3.12. We observe loss of crypt architecture, inflammatory cell infiltration, and muscle thickening in experimental groups receiving DSS. However, in mice gavaged with AvrA NPs in MPs, we see a reduction in severity of these histological markers, which is quantified as crypt damage, polymorphonuclear (PMN) infiltration under high-power field (HPF), depth of injury, and severity of inflammation, in Figure 3.12. Low magnification whole swiss roll colonic sections stained with H&E are in Figure 3.13. These images give a sense of the overall severity of the colitis between the different experimental groups. Combined, these results suggest that AvrA NPs are able to reduce the downstream macroscopic effects of DSS-induced colitis when delivered in alginate/chitosan MPs.

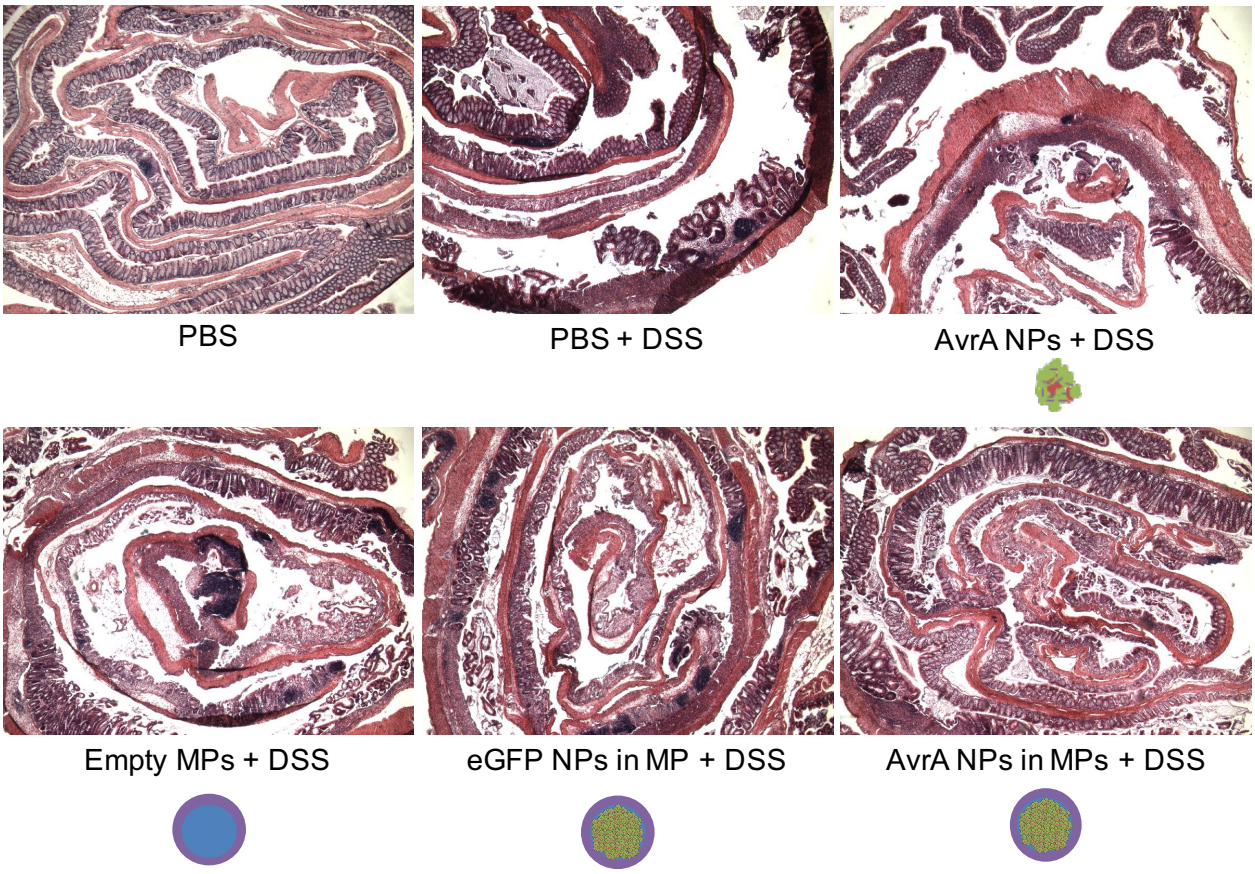

Figure 3.13: Representative histological sections of 10 μm paraffin embedded swiss rolls under 4x magnification.

We have previously shown[51] that two doses of 10 μg of AvrA NPs (900 ng of AvrA) administered transrectally significantly reduced DSS-induced colitis and symptoms. The current treatment plan requires daily doses of 4 mg of MPs, which contains 200 μg AvrA NPs (16 μg of AvrA in each dose), for 2 weeks. Based on the comparison of these dosing schemes, we estimate that alginate/chitosan MPs have colonic delivery efficiency of ~1%. This suggests that most of the NPs are being taken up much earlier in the gastrointestinal tract or they are irreversibly entrapped within the alginate and chitosan MPs. There is significant room to improve the colonic delivery efficiency of AvrA NPs. Others have reported the colon-homing abilities of therapeutic NPs within alginate/chitosan hydrogels[285]. This system does not use microparticles, but rather two separate gavages of first the alginate/chitosan mixture followed up the gelation solution containing their NPs. A straightforward method would be to provide an additional coating on our MPs with a biocompatible pH-sensitive polymer such as Eudragit ®[223] that can tune the release of NPs from MPs in a desired pH environment. Although the AvrA NPs have low colonic delivery efficiency, they could prove to be effective in treating CD, which can manifest much farther upstream in the gastrointestinal tract[21].

3.4 Summary

AvrA is a bacterially derived enzyme capable of immunomodulation via intracellular activity. Previous work demonstrated that transrectal delivery of AvrA NPs was successful in reducing inflammation in murine colitis models. To implement AvrA NPs as a clinically viable treatment, we engineered gastro-protective alginate/chitosan MPs as an oral delivery vehicle

capable of releasing AvrA NPs in the small intestine and colon. Alginate/chitosan MPs protected protein activity in SGF *in vitro* and reduced macroscopic symptoms in a murine DSS-induced colitis pre/co-treatment model. This platform could be expanded to use alginate/chitosan MPs to encapsulate and orally deliver other bacterial protein therapeutics, vaccines, or antibodies to the small intestine and/or colon.

CHAPTER 4 : Carrier Proteins to Control Protein Nanoparticles Properties for Assessing Protein Corona and Cellular Interactions

4.1 Summary

NPs have been widely used to improve intracellular drug delivery[287]. In most cases, NPs are internalized by energy dependent endocytic processes. However NPs or their encapsulated drugs must escape endosomes to gain access to the cytosol prior to lysosomal degradation or endosome recycling[288]. This is a significant challenge for many NP systems and reduces the efficiency of cytosolic drug delivery, especially for macromolecules such as proteins.

Soluble proteins typically cannot cross the cell membrane to reach the cytosol directly. Protein NPs offer a means to turn soluble protein into a colloidal drug carrier, capable of enhancing cellular uptake through active endocytic uptake mechanisms[289] and altering biodistribution[290]. Protein properties and characteristics (size, charge, and hydrophobicity) affect the final protein NP structure and properties, which, in turn, affect cellular interactions and uptake. It is known that size, shape, surface charge, surface chemistry or functionality, hydrophobicity, and the absorbed protein corona all affect the ability of nanomaterials to be internalized and trafficked[291]. For example, size and charge of NPs can regulate receptor-mediated internalization. Size affects the binding capacity of NPs to receptors by modifying membrane wrapping kinetics[292]. Charge affects the adsorption of serum proteins and alters conformational charges affecting their accessibility to receptors (e.g. scavenger receptors)[293]. Cationic NPs have increased cell binding over anionic NPs due to the electrostatic interactions with the negatively charged cell surface. While these cationic particles may promote cell binding, they also promote formation of a protein corona that marks them for cell clearance[293]. The protein corona that forms around anionic NPs reduce cellular internalization[294]. However,

the protein mediate anionic NP binding to native receptors on the cell[293]. NP surface properties can also promote affinity toward specific receptor-mediated endocytosis pathways[177, 295, 296] and allows for targeting preferred endocytic routes. Cationic NPs have been reported to increase internalization by clathrin-mediated endocytosis[296], but are guided toward degradation[168]. Anionic NPs have decreased internalization rates and are guided toward caveolae-mediated endocytosis, however, are not marked for degradation[168]. The importance of serum protein corona formation on NPs has been revealed as NPs become closer to clinical implementation. However, most of the NP used to study corona are limited to solid inorganic materials such as gold or dense polymeric NPs such as polystyrene.

Protein NPs are made of proteins and present an inherent pseudo-corona on their surface. Properly folded proteins minimize their free energy and orient their hydrophobic domains in their cores. Unfolding and denaturing proteins allows these hydrophobic regions to interact and increase the propensity to aggregate. It is unknown how what the conformation of proteins on the protein NP surfaces are, however, due to the method of synthesize, it is likely that some unfolding occurs. How then do the folded serum proteins interact with protein NP surfaces and how this differs from traditional NP carriers is one of the main question we sought to explore in this chapter. Therefore, studying protein NPs with different surface properties can elucidate these differences. Little is known about how the properties of the carrier protein translate to protein NP characteristics, which ultimately affect the cellular uptake mechanism of the NP. Furthermore, the increasing realization that proteins in various physiological fluids, such as blood, interact with NPs and can modify their size, surface charge, surface composition, and functionality. This chapter aims to understand how protein NP properties can alter protein corona formation which will ultimately dictate cellular interaction. We elucidate the role of carrier proteins in desolvation

to produce protein NPs with different properties and how these different protein NP properties affect the composition of the protein corona. The future goal is to influence cellular interactions to increase cytosolic delivery.

4.2 Experimental Methods

4.2.1 Protein nanoparticle synthesis through desolvation

Protein NPs were prepared by desolvation technique as previously described[51] with minor modifications. Bovine serum albumin (BSA) (Sigma-Aldrich) was dissolved in MilliQ water to a concentration of 200 mg/mL. 3,3'-dithiobis(sulfosuccinimidyl propionate) (DTSSP; Pierce) was dissolved in MilliQ water to 15 mg/mL immediately prior to use. The bottoms of 1.5 mL LoBind microcentrifuge tubes (Eppendorf) were cut and 100 µL of BSA solution was transferred in with a flea stir bar (VWR). Tubes were placed upside down and stirred at 600 rpm in the cold room (4ºC) for 10 minutes. 200 µL of pre-chilled 4°C ethanol (Decon Labs) was added at 1 mL/min to desolvate the BSA. 128 µL of DTSSP solution was added immediately after ethanol desolvation. The solution was stirred for an additional 90 minutes in the cold room. Afterwards, the solution was transferred to another centrifuge tube and centrifuged at 7,000 x g for 5 minutes. The supernatant was discarded and the pellet was resuspended in 500 µL of sterile PBS and sonicated on ice for 1 s every 3 s at 65% amplitude for 1 minute. The solution was then centrifuged at 5 minutes at 500 x g. The supernatant was collected, pellet discarded, and subjected to additional centrifugation for 5 minutes at 500 x g. The supernatant was then collected, pellet discarded, and subjected to a final centrifugation step of 10 minutes at 21000 x g. The supernatant was

discarded, and the pellet was resuspended in 500 µL of sterile PBS and sonicated on ice for 1 s every 3 s at 65% amplitude for 1 minute to make the final BSA NP product.

OVA (Sigma-Aldrich) was dissolved in PBS to a concentration of 6.2 mg/mL. DTSSP was dissolved in PBS to 10 mg/mL immediately prior to use. 100 µL of the OVA solution was transfered to a 0.5 dram glass vial with a flea stir bar and stirred at 650 rpm on a stir plate. 400 µL of 100% ethanol was added at 1 mL/min. Afterward, the solution was transferred to a 1.5 mL LoBind microcentrifuge tube at centrifuged for 5 minutes at 7,000 x g. The supernatant was discarded and the pellet was resuspended in 475 µL of sterile PBS and sonicated on ice for 1 s every 3 s at 65% amplitude for 1 minute. 25 µL of the DTSSP solution and a flea stir bar were added, the microcentrifuge tube inverted and stirred at 650 rpm on a stir plate at room temperature. After 60 minutes, stir bar was removed and the solution was centrifuged for 30 minutes at 18,000 x g. The supernatant was discarded and the pellet was resuspended in sterile PBS and sonicated on ice for 1 s every 3 s at 65% amplitude for 1 minute to obtain the final OVA NP product.

Avidin (e-Proteins) was dissolved in imidazole elution buffer (250 mM imidazole, 300 mM NaCl, 50 mM NaH_2PO_4; pH 8) to a concentration of 10 mg/mL. DTSSP was dissolved in MilliQ water to a concentration of 4 mg/mL immediately prior to use. 100 µL of the avidin solution was transferred to a 0.5 dram glass vial with a flea stir bar and stirred at 650 rpm. 400 µL of acetone (VWR) was added at 1 mL/min. 64 µL of the DTSSP solution was added and the solution spun for an additional 90 minutes at room temperature. Afterwards, the solution was transferred to a 1.5 mL LoBind centrifuge tube and centrifuged for 5 minutes at 7,000 x g. The supernatant was discarded and the pellet was resuspended in 500 µL of sterile PBS and sonicated on ice for 1 s every 3 s at 65% amplitude for 1 minute to obtain the final avidin NP product.

4.2.2 Size, zeta-potential, and concentration measurements of nanoparticles

Average NP size was characterized using Zetasizer Nano ZS90 (Malvern Instruments Ltd.) with a minimum of three batches of each NP type with three replicates of 10 measurements using the following settings: proteins setting for NP detection and manufacturer PBS settings as the dispersion medium. NP ζ-potential was determined by measuring the electrophoretic mobility of the NPs in PBS using the same instrument. The NP protein concentration was determined using a BCA assay (Pierce) following the manufacturer's protocol.

4.2.3 Protein nanoparticle hydrophobicity measurements determined by ANS

8 mM of 1-anilinonaphthalene-8-sulfonic acid (ANS; TCI America) was prepared in 0.1 M phosphate buffer (81 mL of 0.2 M dibasic sodium phosphate, 19 mL of 0.2 M monobasic sodium phosphate, and 100 mL of distilled water) as a stock solution immediately prior to use. 2 mL aliquots of BSA, OVA, and avidin as NPs and soluble protein were prepared at 100 μg/mL, 50 μg/mL, 25 μg/mL, 10 μg/mL, and 5 μg/mL in 0.1 M phosphate buffer. 10 μL of the stock ANS solution was added to each protein aliquot along with a 0.1 M phosphate blank solution. These aliquots were vortexed for 10 seconds and the fluorescence intensity was measured in a Bio-Tek Synergy 2 plate reader using 390 nm as the excitation and 470 nm for the emission. The relative fluorescence intensity (RFI) was calculated as the difference between the fluorescence values of the protein solutions compared to the blank. The RFI values of each sample was plotted against the protein concentration and the slope of the line was determined by linear regression and reported as the hydrophobic index (S_0)[297].

4.2.4 FITC conjugation

FITC conjugation of serum allows fluorescent detection of serum proteins separate from protein NPs during SDS-PAGE analysis. Fluorescein isothiocyanate (FITC; Sigma-Aldrich) was dissolved in dimethyl sulfoxide (DMSO; BDH) to 0.2 M. 2.5 mL FITC was mixed with an equal volume of 0.1 M sodium carbonate-bicarbonate buffer at pH 9 (10 mL 0.1 M sodium carbonate and 90 mL of 0.1 M sodium bicarbonate). The buffered FITC solution was mixed with an equal volume of fetal bovine serum (Seradigm Premium Grade; VWR) and rotated for 2 hrs at room temperature. Afterwards, the mixture was transferred into a 3.5 kDa MWCO membrane (Spectrum Laboratories Inc.) and dialyzed into PBS.

FITC conjugation of nanoparticles allows fluorescent detection of NPs uptake in cells. The buffered FITC solution was mixed with equal volumes of BSA, OVA, or avidin NPs with a concentration of 2 mg/mL and rotated at room temperature for 2 hrs at room temperature. Afterwards, the mixtures were transferred into a 10 kDa MWCO Slide-A-Lyzer MINI dialysis device (ThermoFisher Scientific) and dialyzed into PBS.

4.2.5 Protein corona preparation using FITC-conjugated serum

1 mg of BSA, OVA, and avidin NPs, and polystyrene beads (polybead carboxylate 0.20 μm microspheres; Polysciences) were incubated with 1 mL of FITC-conjugated serum at 37°C for 1 hr under end over end rotation. Afterwards, the NP-serum mixtures were washed by centrifugation at 7,500 x g for 10 minutes at 4°C. The supernatant was collected and stored for future analysis. The pellet was resuspended *via* pipetting with 1 mL of sterile PBS. A total of 5 washes were performed to remove the soft corona. After the wash steps, the pellet was resuspended with 20 μL of sterile PBS representing the final product of NPs with hard corona.

4.2.6 Gel analysis of protein corona

10 μL of NPs with hard corona obtained in the previous section were heated with 30 μL of sodium dodecyl (lauryl) sulfate-polyacrylamide gel electrophoresis (SDS-PAGE) loading buffer (50 mM Tris-Cl, pH 6.8, 2% SDS, 100 mM DTT, 0.1% bromophenol blue, 10% glycerol) for 15 minutes at 95°C and 20 μL were loaded into a 12% SDS polyacrylamide gel. After SDS-PAGE, the gels were analyzed for FITC fluorescence using a Gel Dox XR+ Gel Documentation System (Bio-Rad). After FITC imaging, the gels were stained with Coomassie.

4.2.7 Confocal microscopy for qualitative assessment of nanoparticle uptake

HeLa cells were cultured in (DMEM), supplemented with 10% (v/v) (FBS). Media was also supplemented with 1% penicillin/streptomycin, and cells were incubated in a 5% CO_2 humidified air atmosphere. HeLa cells were plated at a density of 10,000 cells per well in an 8-well chamber slide system overnight. After attachment, cells were then incubated with 500 μg/mL of FITC-conjugated BSA, OVA, and avidin NPs that were preincubated in media for 1 hr at 37°C. NPs were incubated with cells for 12 hrs. Afterwards, cells were washed twice with ice cold PBS and fixed with 3.7% paraformaldehyde for 15 minutes at room temperature. Cells were then permeabilized with 1% Triton X-100 in PBS for 15 minutes at room temperature. Actin was stained with 0.33 μM phalloidin-tetramethylrhodamine B isothiocyanate (phalloidin-TRITC; Sigma-Aldrich) for 15 minutes at room temperature and the nucleus was stained with 0.2 μM Hoechst 33342 for 15 minutes at room temperature. Cells were washed three times with PBS in between each step in the staining procedure. 50/50 PBS/glycerol solution was used a mounting

media and samples were sealed with a coverslip and nail polish. Images were taken on Zeiss LSM 700 confocal microscope and analyzed with Zen Black software (Zeiss).

4.2.8 Nanoparticle cytotoxicity determined by MTT

10,000 HeLa were plated in a 96 well plate overnight. After attachment, media was replaced with BSA, OVA, and avidin NPs that were preincubated with media for 1 hr at 37°C. Different concentrations of NPs incubated with cells. After 6 hrs of NP incubation, media was replaced with 100 μl of fresh media and 10 μl of MTT solution. Cells were incubated with MTT reagent for an addition 4 hrs. 200 μl of DMSO was then added to each well and wells were mixed vigorously to ensure cells were lysed. Absorbance was measured using a Biotek Synergy 2 Microplate reader at 570 nm and background absorbance 630 nm was subtracted. Cell viability was normalized to control cells that received an equal volume of PBS without NPs diluted in fresh media.

4.3 Results and Discussion

4.3.1 Synthesis and characterization of BSA, OVA, and avidin nanoparticles

To elucidate the role of carrier protein in influencing protein NP properties after desolvation, model cationic, anionic, hydrophobic, and hydrophilic carrier proteins were used. Avidin is a highly basic 66 kDa tetrameric protein with a pI = 10.1 that is normally studied for its strong binding interaction with biotin. Avidin is rich in arginine (eight/subunit) and lysine (nine/subunit) that allows it to be positively charged under physiological conditions. Bovine

serum albumin (BSA) is an acidic 66.5 kDa protein with a pI = 4.7 that is used in many biological applications for its relative bio-inertness and low cost. BSA was selected for its anionic and hydrophobic properties. Ovalbumin (OVA) is a 45 kDa protein with a pI = 5.2 that is commonly used in immunological studies. It possesses hydrophilic properties[298] in contrast with hydrophobic BSA, though their pI values are similar. These model proteins were chosen for their varying range in surface charge and hydrophobicity and because they are well characterized and easily obtainable.

Solutions of soluble BSA, OVA, and avidin were desolvated to form nanoclusters and stabilized with a cleavable disulfide bond crosslinker, DTSSP, to make BSA, OVA, and avidin NPs. The desolvation method of producing protein NPs is described earlier in this thesis. Size was the main criteria used when optimizing protocols to synthesize NPs. It was necessary to create protein NPs of similar size to control for size-dependent effects of protein corona formation. Studies have shown that the larger the NP, the more surface area is available for corona adsorption and size influences the conformation of these serum proteins[179]. NPs with a size between 250 – 290 nm were obtained. A summary of the model proteins, their studied properties used in this chapter, and their DLS plots are seen in Figure 4.1.

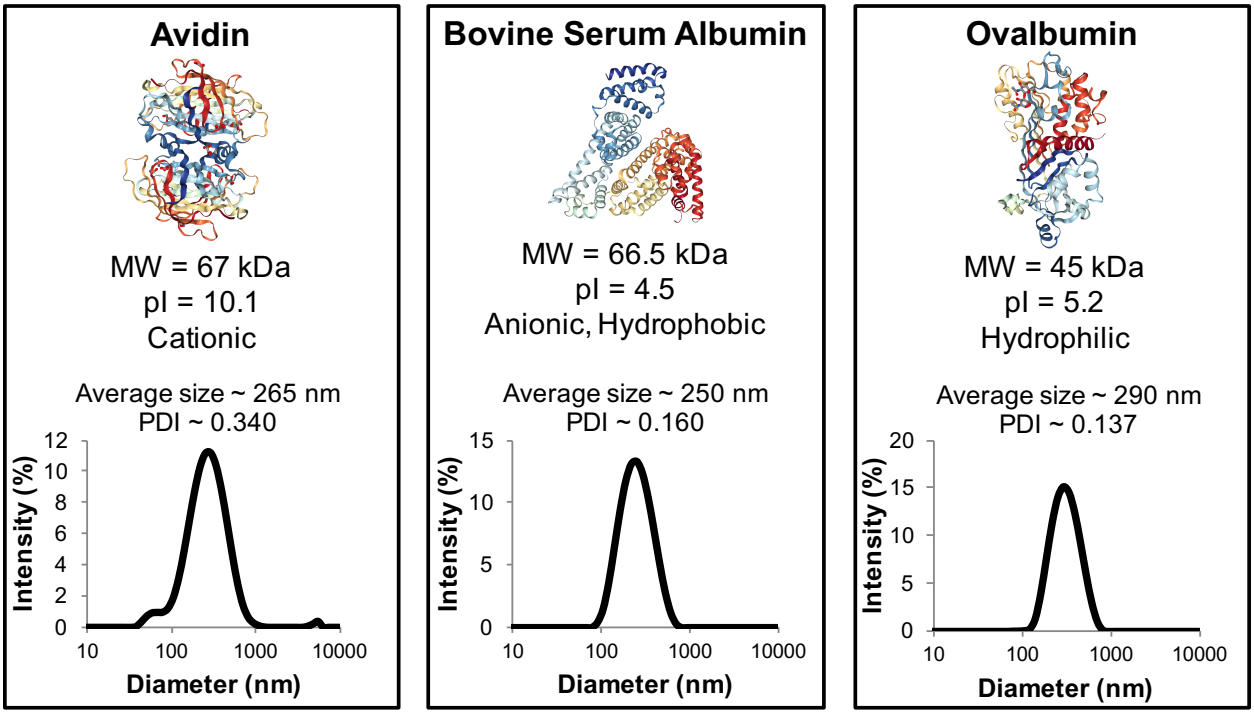

Figure 4.1: Model carrier proteins, their crystal structures obtained from literature, their characteristics, and corresponding DLS plots of NPs made *via* desolvation.

The surface charge of NPs is a commonly studied property that can greatly affect protein corona composition and cellular internalization. Cationic materials have the potential to electrostatically bind negatively charged cellular membranes and have the potential to alter the conformation of corona proteins leading affect what cellular receptors the corona target[293]. The zeta potential of NPs made from avidin, the model cationic protein, and BSA, the model anionic protein were measured and the results are seen below in Figure 4.2.

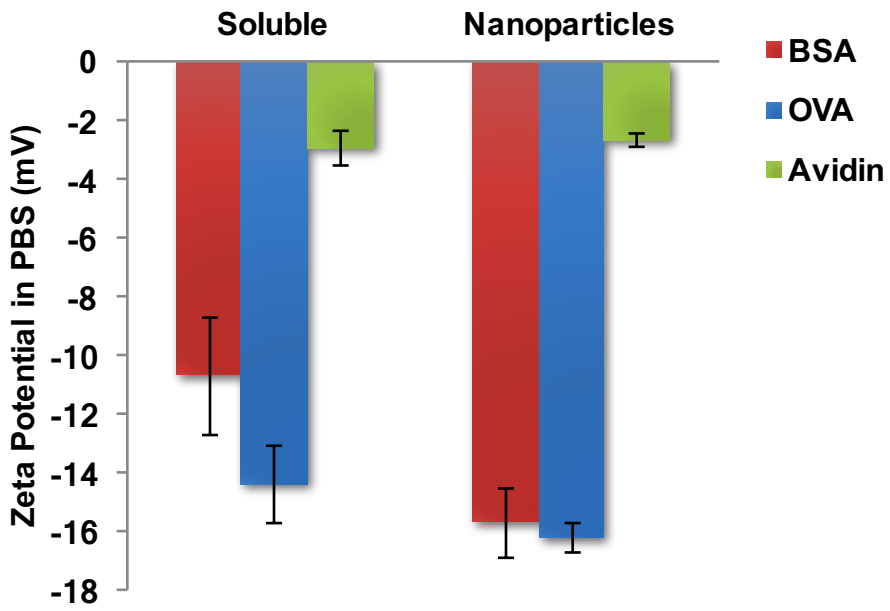

Figure 4.2: The zeta potential of BSA and avidin NPs and soluble proteins.

BSA NPs have a zeta potential of around -15 mV in PBS whereas avidin NPs have a zeta potential of around -2 mV in PBS. Avidin NPs do not appear to be as cationic as expected. It is possibly due to the dispersion media used as when BSA and avidin NPs and soluble proteins were tested in 10 mM HEPES buffer, avidin has a positive zeta potential, whereas BSA retained a negative value (data not shown). The salts in the media form an electric double layer around the NP. The inner layer is comprised of ions with opposite charge called the Stern layer. Beyond this layer, there is a diffuse layer of ions that is dynamic. Zeta potential measures the interface between the diffuse layer with bulk dispersant called the slipping plane during electrophoresis[299]. The reduced ionic strength in 10 mM HEPES means that a smaller electric double layer is present allow a more accurate reading of avidin's surface charge. The zeta potentials in PBS are reported here as it was the more physiological relevant media. Though the zeta potential is not positive for avidin, there is a large difference in zeta potential between BSA and avidin NPs allowing us to elucidate difference in protein corona composition between the two.

Hydrophobicity is another commonly studied property of NPs that is known to contribute to protein corona composition and cellular internalization by affecting the amount of serum proteins that bind the surface[300]. Hydrophilic NPs achieved through PEG conjugation have been used to extend circulation times by blocking adsorption of certain serum proteins to the surface to decrease cellular interactions[183]. To measure NP hydrophobicity, ANS, a hydrophobic fluorescent dye was used[301]. ANS is hardly fluorescent in aqueous environments but becomes highly fluorescent when bound to a solid surface. NPs of BSA, the model hydrophobic protein, and OVA, the model hydrophilic proteins and their soluble forms were incubated with ANS to determine hydrophobicity and the results are seen in Figure 4.3. ANS is only capable of measuring the relative the hydrophobicities between samples. Figure 4.3 shows a large difference in hydrophobicities between BSA and OVA as both NPs and soluble protein in agreement with other reported literature values[298].

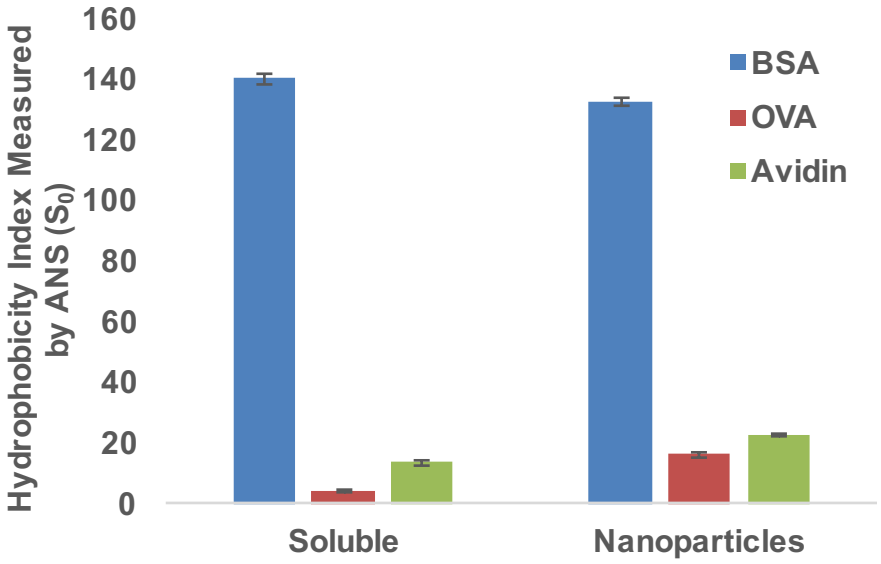

Figure 4.3: The relative hydrophobicity of BSA and OVA NPs and their soluble components.

It appears that OVA and BSA exhibit similar zeta potentials, however, vastly different hydrophilicities, whereas OVA and avidin exhibit similar hydrophobicities and vastly different zeta potentials. Overall, protein NPs made from different carrier proteins were synthesized and the NP properties were characterized. NPs desolvated from model carrier proteins exhibit similar properties to carrier proteins in their soluble form. It is concluded that carrier proteins govern protein NP properties after desolvation. These NPs can be used as tools to study the protein corona that forms when NPs are incubated with serum.

4.3.2 Protein corona formation and analysis on nanoparticles

A common method of qualitatively analyzing the protein corona is using SDS-PAGE[178, 302]. The hard corona on inorganic or polymeric NPs separates from the NP when heated in reducing loading buffer and when the mixture is loaded into a gel, the NPs are unable to enter the gel due to their large size. This separation allows accurate analysis of the hard corona proteins. It should also be noted that the soft outer protein corona is much more difficult to analyze and remains a controversial topic. The reversible binding and dynamic nature of this outer layer makes it challenging to characterize and some literature questions even the existence of a soft corona[302]. Therefore, all future references to the corona refer to the hard corona unless otherwise specified. The difficulty with studying corona formation on protein NPs is that separating the corona from the protein NP results in NP breakup and allows the components of the protein NP to enter the gel as well. Since the amount of proteins that make up the protein NP core is much greater than the corona shell that forms around it, it is hard to distinguish the bands on SDS-PAGE. To overcome this barrier, we conjugated a fluorescent dye to serum proteins to allow

fluorescent detection of the proteins that are specifically associated with the corona[303]. The conjugation of serum can be seen in Figure 4.4 below.

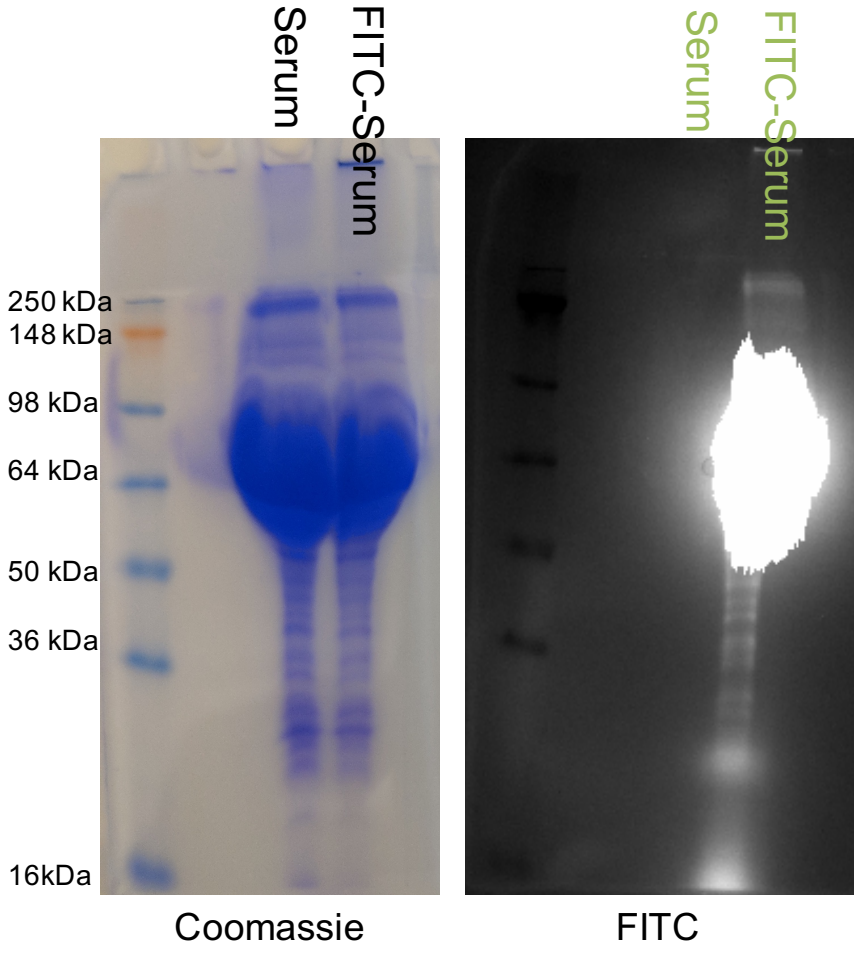

Figure 4.4: Serum and FITC-conjugated serum analyzed using SDS-PAGE. The coomassie signal is seen on the left and the FITC signal is seen on the right.

There is a strong signal resulting from the overloading of serum in the gel, which was done in order to visualize the lower abundancy serum proteins. This is seen in the massive band most likely from BSA as BSA is the majority component (~55%) in fetal bovine serum. It is important to note is that we are able to obtain FITC signal that allows us to distinguish serum proteins from NP proteins. Equal masses of BSA, OVA, avidin, and polystyrene (PS) NPs were

incubated with FITC-conjugated serum and the corona after washing was analyzed using gel electrophoresis. The results are seen below in Figure 4.5.

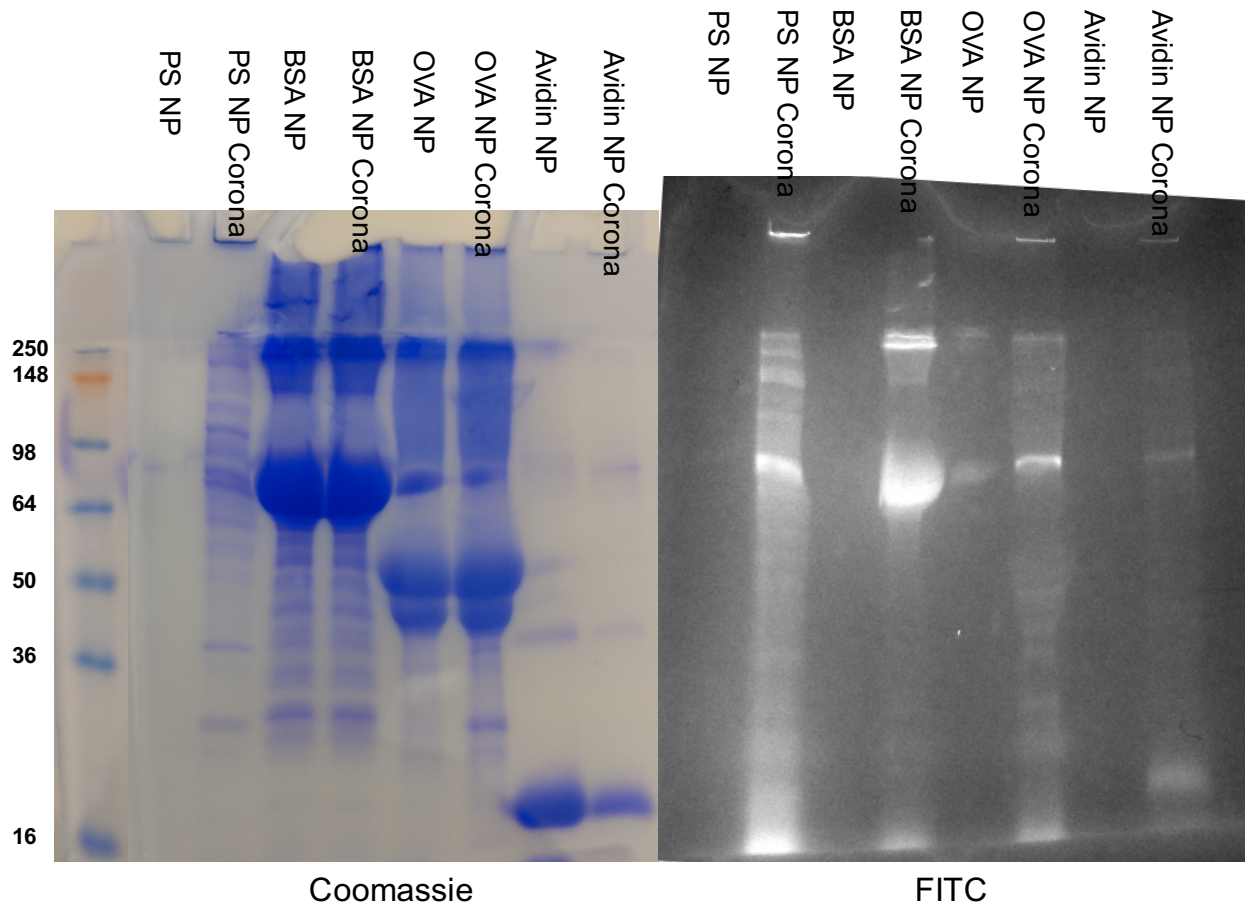

Figure 4.5: PS, BSA, OVA, and avidin NPs and FITC-serum-incubated NPs analyzed in SDS-PAGE imaged with coomassie blue and FITC fluorescence. 1 mg of NPs were used with 1 mL of FITC-serum and approximately 500 μg of NPs were loaded into each lane.

PS NPs are well characterized as well as the corona that forms around them[304]. PS NP therefore can serve as a positive control and a point of comparison to protein NPs. It is difficult to discern between corona and protein NPs in the Coomassie stained gel. The corona is much clearer in the PS lanes. However, when fluorescently imaged, the contributions from serum are much easier to distinguish. In general, it appears that serum proteins adsorb onto PS NP in greater quantities than protein NPs. This could be a due to the protein NPs already possessing a

layer of BSA, OVA, or avidin proteins that could inhibit some binding. The strongest signal is the BSA band and in BSA NPs, there appears to be strong upper globulin bands as well. There is also a difference in FITC intensity and distribution of serum proteins adsorbed between BSA NPs and OVA/avidin NPs. The BSA band is the strongest on all three NPs though in much lower quantities on OVA/avidin NPs. Hydrophilic NPs are known to adsorb less protein than hydrophobic NPs[300]that contribute to reduction in overall intensity. There appears to be presence of lower molecular weight bands present on OVA NPs around 20 kDa – 50 kDa and smearing of upper bands between 65 kDa – 150 kDa that are not seen on BSA NPs. These lower molecular weight bands are possibly apolipoproteins and the upper smear are possibly complement proteins and plasminogen. This difference highlights the how different NP hydrophobicity can contribute to different adsorb serum compositions suggest a greater contribution from hydrophobicity than surface charge. A significantly amount of avidin NPs appear to have been lost during the washing steps making comparisons with avidin NPs difficult. In the future, the amount of NPs loaded into each lane must be normalized following wash steps to allow accurate comparisons between the NPs.

Though we have developed a method to study corona composition on protein NPs, it primarily reveals qualitative differences. Further characterization must be done to determine the exact composition of the corona by mass spectrometry[178]. This will help determine if our protein NPs are being opsonized by immunoglobulins or complement proteins, which increase cellular endocytosis, or if apolipoproteins dominate, and could confer increased blood circulation times[305]. Probing the corona with specific antibodies by western blot can also provide some preliminary indications as to the NP biological identity. Isothermal calorimetry is another useful tool to determine the binding events on different protein NPs to quantify the amount of serum

protein binding. Optimization of the injection and sample concentrations is critical along with the proper controls to distinguish between NP-NP interactions and serum-NP interactions. Ultimately, delivery of an intracellular therapeutic, such as AvrA, is necessary to determine the cytosolic delivery potential of these different protein NPs. Differences in the desolvation conditions will need to be reviewed to ensure equal loading of AvrA into the different protein NPs. Western blot analysis can confirm the loading.

4.3.3 *In vitro* assessment of nanoparticle cellular interactions

We examined whether the qualitative differences between the various NP coronas influenced cellular interactions. BSA, OVA, and avidin NPs were preincubated in media containing 10% fetal bovine serum and then incubated with HeLa cells to image cellular uptake. The images can be seen in Figure 4.6.

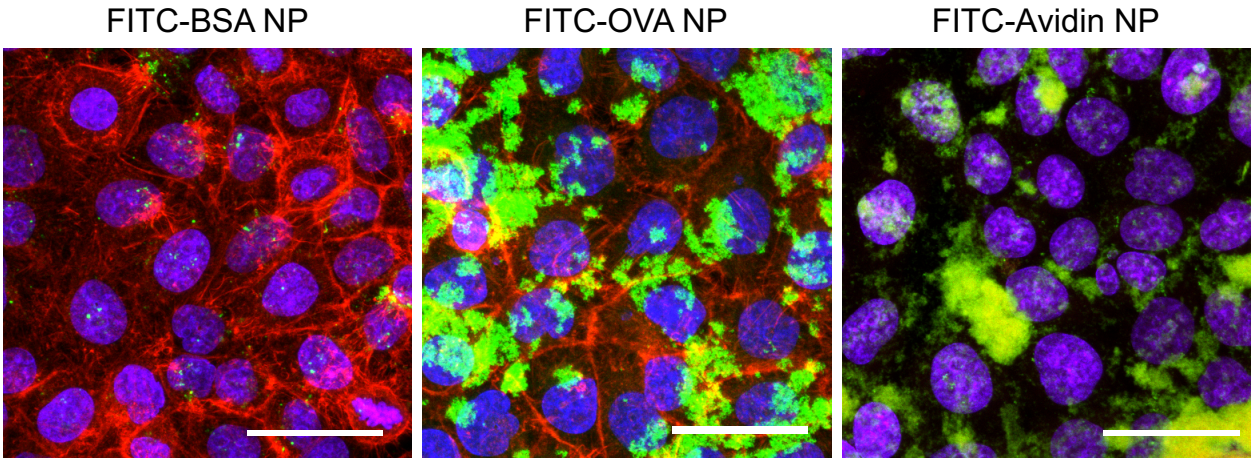

Figure 4.6: Representative images of 500 μg/mL of FITC-BSA, FITC-OVA, and FITC-avidin NPs incubated with HeLa cells for a period of 12 hrs. Images shown are 2D maximum projections of confocal stacks.NPs are seen with the native green FITC signal, actin is stained in red, and the nucleus is stained in blue. Scale bar = 50 μm.

The confocal images seen in Figure 4.6 show the propensity of OVA and avidin NPs to aggregate on the surface of cells, whereas BSA NPs are dispersed and punctate, with less

intensity. These results are interesting because BSA NPs are much more hydrophobic that OVA and avidin NPs, however, don't appear to aggregate. OVA NPs appear to be stuck on top of cells, aggregating into large clusters. Avidin NPs appear to be having a cytotoxic effect on the cells, as seen by the lack of actin staining. To verify whether these protein NPs are cytotoxic, a MTT assay was performed with varying dosages of NPs and the results are seen in Figure 4.8.

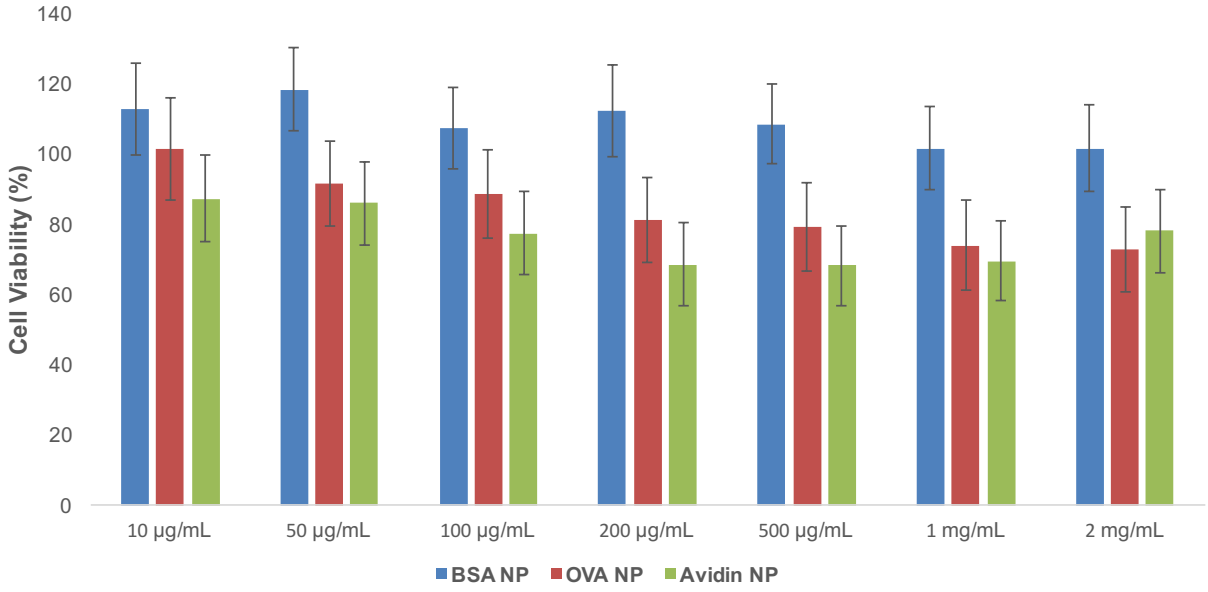

Figure 4.7: Dose-dependent cell viability of BSA, OVA, and avidin NPs preincubated with media determined by MTT assay. Viability was normalized to cells receiving an equal volume of PBS without NPs.

The OVA and avidin NPs concentrations used ranging from 200 µg/mL – 2 mg/mL in Figure 4.7 show a cytotoxic effect (viability < 80%). BSA NPs are extremely well tolerated. OVA and avidin appear to have a dose-dependent increase toxicity when the NP concentration increase above 100 µg/mL. This should inform future experiments with OVA and avidin NPs. We speculate that due to the hydrophilic nature of OVA and avidin NPs, the corona composition is contributing to the cytotoxicity and uptake. Cells appear to be inhibiting the uptake of OVA NPs causing them to cluster on the surface seen in images in Figure 4.6. Avidin NPs exhibit

similar clustering, however, negatively impact the actin structure. More work needs to be done to optimize the proper NP concentration used without compounding cytotoxic effects. Flow cytometry can also quantify the extent of NP uptake and using trypan blue with FITC-conjugated NPs can discern between internalized and attached NPs.

The goal of the work presented in this chapter use carrier proteins to control protein NPs properities and use these NPs to assess corona and cellular interactions. OVA NPs and avidin NPs have cytotoxic effects potentially due to their hydrophilic nature. Comparisons with PEG coated NPs can elucidate the cause of these cytotoxic effects. These NPs can be used in future studies to explore the uptake mechanisms and intracellular trafficking with endocytic pathway knockout experiments and imaging with lysosomal stains. Codesolvate these model carrier proteins with a therapeutic enzyme would provide a functional assay to measure the intracellular delivery and allow direct comparison between the different protein NPs and inform future work with the protein NP delivery system.

4.4 Summary

NPs continue to be developed for their ability to enhance intracellular delivery. The ultimate goal of these NPs is clinical implementation, however, once NPs are administrated *in vivo*, they come in contact the milieu of biological components in the blood that can alter NP properties. The protein corona that forms around NPs *in vivo* confers a biological identity and ultimately influences cellular internalization and trafficking. Studies on NP corona composition are largely biased towards dense inorganic and polymeric NPs. Whether the protein NP delivery

system exhibits different corona behavior and the impact this has on cellular uptake can inform future research with the goal of maximizing cytosolic delivery.

Model cationic, anionic, hydrophobic, and hydrophilic proteins were investigated and shown to govern the NP properties after desolvation. These protein NPs were shown to display different amounts of serum adsorption, cellular uptake and cytotoxicity. Though much work needs to be done to understand how protein NP properties can be utilized to influence and maximize cytosolic delivery, some tools to explore this relationship ave been developed and presented here.

CHAPTER 5 : Conclusions and Future Directions

5.1 Conclusions

The work presented in this thesis focuses on reengineering naturally-derived, evolutionarily optimized molecules as drug delivery vehicles and therapeutics. Pathogenic *Salmonella* has developed tools to promote its survival through the coevolution with the human immune system. We have identified AvrA, used by *Salmonella*, as an effector enzyme with therapeutic potential due to its ability to modulate key intracellular signaling pathways in eukaryotic cells and confer anti-inflammatory and anti-apoptotic effects. This enzyme is unique as its mechanism of action is not currently found in eukaryotic cells, highlighting how pathogenic bacteria can be a source for future therapies. Chronic inflammation in autoimmune diseases, such as inflammatory bowel disease, is a prime target that could benefit from treatment with AvrA. Current therapies rely on small molecule drugs that have poor side effects and emerging therapies focus on using antibodies to target extracellular components. Modulating intracellular components with the use of enzymes presents a new strategy to combat inflammatory bowel disease. *Salmonella* possesses a type three needle-like secretion system used to deliver AvrA which can penetrate the cell membrane, giving direct access to the cytosol. Utilizing AvrA absent of *Salmonella* requires an alternative delivery system.

To address this challenge, we engineered a protein nanoparticle encapsulating AvrA capable of intracellular delivery. AvrA nanoparticles were characterized and evaluated for their potential to treat inflammatory bowel disease and a pH responsive oral delivery vehicle made from naturally derived polysaccharides, alginate and chitosan, was used to encapsulate AvrA nanoparticles to increases it clinical potential. Though we have shown the effectiveness of AvrA

nanoparticles to treat inflammation *in vivo*, nanoparticle delivery vehicles in general suffer from the common problem of endosomal entrapment that limits delivery efficiency. Therefore, we also studied the role of carrier proteins in influencing protein nanoparticle properties. These properties can influence the protein corona that around them when administrated *in vivo* and guide cellular interactions to maximize cytosolic delivery.

The key findings from this thesis are:

1. Protein nanoparticles are suitable alternative intracellular delivery vehicles to *Salmonella* type 3 secretion system. AvrA nanoparticles synthesized using a desolvation method were shown to enhance cellular internalization *in vitro* and maintain AvrA activity. Transrectal delivery of AvrA nanoparticles to two murine colitis models reduced clinical and histological scores of inflammation. AvrA nanoparticles demonstrate the potential of using protein nanoparticles as therapeutic delivery vehicles for the treatment of inflammation bowel disease.
2. Alginate/chitosan microparticles that encapsulate protein nanoparticles can enable oral delivery of AvrA. pH responsive alginate hydrogels provide a gentle means of encapsulating protein nanoparticles for intestinal release. Coating alginate microparticles with chitosan increases protein nanoparticle encapsulation efficiency and improves retention of bioactive nanoparticles after gastric incubation. Oral gavage of AvrA nanoparticles encapsulated in alginate/chitosan microparticles reduced clinical and histological scores of inflammation in a colitis mouse model. Alginate/chitosan

microparticles are effective oral delivery vehicles that provide gastric passage and intestinal release of bioactive protein nanoparticles.

3. Carrier proteins govern protein nanoparticle properties after desolvation. Protein nanoparticles exhibit altered protein corona composition dependent on the carrier protein used. Serum protein adsorb in greater amounts on hydrophobic BSA nanoparticles skewed toward higher molecular weight bands. Hydrophilic OVA nanoparticles have fewer serum proteins adsorbed, however, display a wider range of bands. These differences can be potentially used to influence cellular interactions to increase cytosolic delivery.

The findings of this thesis can inform others in the field of drug development of the remarkable ability of bacterial effector enzymes as therapeutic agents. These effector enzymes are evolutionary-optimized materials with specific immunomodulatory functions. Isolating the enzymatic domains from multiple effector proteins and potentially combining them into a single effector through protein engineering can tailor host stress response. Proteins are also excellent building blocks for drug delivery vehicles with favorable biodegradability profiles and modularity. Carrier proteins designed with specific physiochemical properties and structure through protein engineering can allow complete control of protein nanoparticles properties.

Though we can design and engineer these protein nanoparticle delivery vehicles in lab, the question of what happens to these nanoparticles once administrated to human cannot be overstated. Understanding the biological response to these protein nanoparticles and how these nanoparticles interact with cells can inform future drug delivery vehicle specifications. The adsorption of biological components on protein nanoparticles is relatively unstudied compared to

other nanoparticle carriers. Protein nanoparticles have an inherent pseudo-corona shell that can be altered through the individual protein building blocks it is made from. This system presents biologically recognizable domains on their surface that differs from polymeric and liposomal nanoparticles that can be utilized to control cellular interactions when systemically delivered.

Delivery through the oral route is desirable. Using alginate and chitosan, two naturally-derived polysaccharides, we provide a platform for gastric passage and intestinal release of protein nanoparticle therapeutics. Though our goal was the localized intestinal delivery of protein nanoparticles, systemic delivery of protein nanoparticles is another direction worth exploring. The therapeutics encapsulated within alginate/chitosan microparticles can also be expanded such as vaccines or probiotics. Each therapeutic will have unique oral delivery requirements that potentially necessitate additional coatings onto the alginate/chitosan microparticle.

This work shows the potential for using naturally-derived products as drug delivery vehicles for intracellular protein therapeutics. The modularity and flexibility of these systems described provide potential for optimization and tailoring to toward specific delivery requirements. Future directions improving upon these existing system and other areas of investigation are described below.

5.2 Future Directions

5.2.1 Improving endosomal escape of intracellular proteins

Endosomal escape is a common problem facing all nanoparticle delivery systems. Cell penetrating peptides are a common solution, however, their unclear mechanism and lack of convincing functional evidence suggest that they suffer from the same problems of endosomal

entrapment. It is generally accepted that endocytosis is the major cellular uptake pathway for most cell penetrating peptides[306] as opposed to previously reported direct penetration *via* energy-independent pathways. This suggest that there could be specific cell receptors that recognize these peptides and therefore peptides can be designed to target specific cells and tissues[307]. Cell penetrating peptides were originally derived viral proteins that exhibit nuclear localization also suggesting that subcellular localization is also possible using peptides[105]. Specific amino acids combinations displaying organelle targeting were discussed in Chapter 1.3.2. Peptides can be designed with combinatory cell targeting and subcellular localization domains that would greatly enhance the specificity of protein therapeutics. Utilizing cell penetrating peptides on protein nanoparticle delivery vehicles can be accomplished by two strategies. These peptides can be cloned onto the terminuses of carrier protein and when desolvated will stochastically present onto the surface, though this would most of the peptides would be in the nanoparticle core. Peptides can be covalent conjugated to the surface of nanoparticles or can be adsorbed onto the surface. We observed increase serum adsorption onto the surface of hydrophobic protein nanoparticles in Chapter 4 and can leverage this finding to maximize the adsorption of peptides. Covalent conjugation or adsorption would allow a more complete coating and surface display compared to the cloning strategy.

It has been reported that other bacterial effector enzymes, such as YopM[308], possess membrane translocation properties along with immunomodulatory functions. Harnessing effector proteins with dual penetrating and therapeutic functionality is interesting and contrary to the normal reductionist approach science has taken with penetrating peptides and single chain antibody fragments. Desolvating these dual functioning effectors into protein nanoparticles can stochastically present membrane translocation domains on the outside of the nanoparticle or

YopM can be adsorb onto the surface of nanoparticles. There are many yet-to-be discovered bacteria with useful evolution-optimized functions. CRISPR highlights how studying bacterial defense and survival mechanisms can inspire new tools for engineers to solve societal problems.

5.2.2 Combinatory therapeutics

The protein nanoparticle platform allows for incorporation of multiple therapeutic proteins. The alginate/chitosan microparticle platform also allows for incorporation of multiple therapeutics such as nanoparticles, nucleic acids, small molecules, cells, and probiotics. Being able to treat diseases by multiple modes of action can potentially provide some of the most potent drugs. For example, Lewis and Keselowsky utilize dual microparticles, large microparticles that cannot be internalized that deliver extracellular components to bind cell surface receptors and the small microparticles can be internalized to deliver intracellular components. They have used this strategy to treat diabetes[309] and suppress inflammation[310] and have started multiple companies using this approach to tackle different diseases. Protein nanoparticles and alginate/chitosan microparticles can provide a similar platform for combinatory drug delivery.

Effector enzymes, such as AvrA, can block the signaling pathways leading to cytokine production and siRNAs can prevent mRNA coding inflammatory cytokines from being translated into proteins. This presents a highly potent therapeutic that combats inflammation via two independent mechanisms. Their delivery challenges are similar as they must both access the cytosol while avoiding degradation and clearance. They could potentially be encapsulated in a single protein nanoparticle through siRNA forming electrostatic complexes with soluble protein prior to desolvation or introducing carrier protein with siRNA binding domains. These protein

nanoparticle, if successful, can loaded into alginate/chitosan microparticles with anti-inflammatory small molecule drugs and/or probiotics to restore healthy immunological activity. This is an extreme example, however, highlights the possibility and attractiveness of combinatory therapies.

Another interesting direction for alginate/chitosan microparticle is oral vaccination. Recently, a protein nanoparticle formulations made of conserved influenza viral proteins were shown to be effective in inducing broad protection indicating its potential to be a universal flu vaccine[311]. Encapsulating these nanoparticles in alginate/chitosan microparticles can provide an oral formulation for universal flu vaccine. Peyer's patches function as immune centers in the intestines and the targets of oral vaccination[312]. We speculate in Chapter 3 that alginate/chitosan microparticles release nanoparticles much earlier in the gastrointestinal tract and this feature could be beneficially for oral vaccinations. Peyer's patches are only found in the small intestines and also provides an access point to systemic delivery that bypass the liver, avoiding first pass effect[166]. Preliminary experiments can be done using current eGFP nanoparticles in alginate/chitosan microparticles, gavaging them into mice, harvesting the Peyer's patches and staining for eGFP. This can motivate future studies to test oral vaccination and challenge studies.

5.2.3 Colon-specific delivery

Alginate/chitosan microparticles have an estimated 1% colonic delivery efficiency. This leaves large room for improvement. A common method of achieving colon specificity is utilizing polymethacrylate polymer coating, Eudragit. Other have manufactured similar microparticles on a large scale with Eudragit, through prilling to obtain a colon-targeted delivery system[313]. It is possible to provide an additional Eudragit coating the onto alginate/chitosan microparticles in a

similar 1-step or 2-step method described in Chapter 3. Future work should explore the possibility of an additional alginate/chitosan microparticle coating with Eudragit and possibility switch to naturally-derived coatings such starch that also show similar colon-specific delivery[314] to follow with the themes of this thesis.

5.2.4 Powderized formulations of alginate/chitosan microparticles

Currently, the alginate/chitosan microparticles are stored in water. These microparticles are also stored in the fridge to preserve the activity of the encapsulated protein nanoparticles. Powderized or lyophilized formulations of these microparticles would provide long term storage not reliant on the cold-chain. This feature is highly desirable and would greatly increase the commercial potential of these microparticles. Powderized formulations can be compressed to form tablets or aerosolized to allow delivery into other non-invasive routes. Alginate and chitosan raw materials were purchased as powders that were dissolved in water to form droplets for nanoparticle encapsulation. Therefore, it seems plausible to repowderize these materials following microparticle fabrication.

REFERENCES

1. Bouma, G.; Strober, W., The Immunological and Genetic Basis of Inflammatory Bowel Disease. *Nat. Rev. Immunol.* **2003,** *3*, 521-533.
2. Xavier, R. J.; Podolsky, D. K., Unravelling the Pathogenesis of Inflammatory Bowel Disease. *Nature* **2007,** *448*, 427-434.
3. Levy, M.; Kolodziejczyk, A. A.; Thaiss, C. A.; Elinav, E., Dysbiosis and the Immune System. *Nat. Rev. Immunol.* **2017,** *17*, 219-232.
4. Dahlhamer, J. M., Prevalence of Inflammatory Bowel Disease among Adults Aged≥ 18 Years—United States, 2015. *MMWR. Morbidity and mortality weekly report* **2016,** *65*.
5. Cosnes, J.; Gower-Rousseau, C.; Seksik, P.; Cortot, A., Epidemiology and Natural History of Inflammatory Bowel Diseases. *Gastroenterology* **2011,** *140*, 1785-1794.
6. Molodecky, N. A.; Soon, I. S.; Rabi, D. M.; Ghali, W. A.; Ferris, M.; Chernoff, G.; Benchimol, E. I.; Panaccione, R.; Ghosh, S.; Barkema, H. W.; Kaplan, G. G., Increasing Incidence and Prevalence of the Inflammatory Bowel Diseases with Time, Based on Systematic Review. *Gastroenterology* **2012,** *142*, 46-54 e42; quiz e30.
7. Frank, D. N.; St Amand, A. L.; Feldman, R. A.; Boedeker, E. C.; Harpaz, N.; Pace, N. R., Molecular-Phylogenetic Characterization of Microbial Community Imbalances in Human Inflammatory Bowel Diseases. *Proc. Natl. Acad. Sci. U. S. A.* **2007,** *104*, 13780-13785.
8. Li, J.; Butcher, J.; Mack, D.; Stintzi, A., Functional Impacts of the Intestinal Microbiome in the Pathogenesis of Inflammatory Bowel Disease. *Inflamm Bowel Dis* **2015,** *21*, 139-153.
9. Baumgart, D. C.; Sandborn, W. J., Inflammatory Bowel Disease: Clinical Aspects and Established and Evolving Therapies. *The Lancet* **2007,** *369*, 1641-1657.
10. Burger, D.; Travis, S., Conventional Medical Management of Inflammatory Bowel Disease. *Gastroenterology* **2011,** *140*, 1827-1837 e1822.
11. Plevy, S. E.; Targan, S. R., Future Therapeutic Approaches for Inflammatory Bowel Diseases. *Gastroenterology* **2011,** *140*, 1838-1846.
12. Bilsborough, J.; Targan, S. R.; Snapper, S. B., Therapeutic Targets in Inflammatory Bowel Disease: Current and Future. *The American Journal of Gastroenterology Supplements* **2016,** *3*, 27-37.
13. Wang, D.; DuBois, R. N., The Role of Anti-Inflammatory Drugs in Colorectal Cancer. *Annu Rev Med* **2013,** *64*, 131-144.
14. Dulai, P. S.; Siegel, C. A.; Colombel, J. F.; Sandborn, W. J.; Peyrin-Biroulet, L., Systematic Review: Monotherapy with Antitumour Necrosis Factor Alpha Agents Versus Combination Therapy with an Immunosuppressive for Ibd. *Gut* **2014,** *63*, 1843-1853.
15. Moriasi, C.; Subramaniam, D.; Awasthi, S.; Ramalingam, S.; Anant, S., Prevention of Colitis-Associated Cancer: Natural Compounds That Target the Il-6 Soluble Receptor. *Anti-Cancer Agents in Medicinal Chemistry* **2012,** *12*, 1221-1238.
16. Aberra, F. N.; Lewis, J. D.; Hass, D.; Rombeau, J. L.; Osborne, B.; Lichtenstein, G. R., Corticosteroids and Immunomodulators: Postoperative Infectious Complication Risk in Inflammatory Bowel Disease Patients. *Gastroenterology* **2003,** *125*, 320-327.
17. Ungaro, R.; Mehandru, S.; Allen, P. B.; Peyrin-Biroulet, L.; Colombel, J.-F., Ulcerative Colitis. *The Lancet* **2017,** *389*, 1756-1770.
18. Shah, S. C.; Colombel, J. F.; Sands, B. E.; Narula, N., Systematic Review with Meta-Analysis: Mucosal Healing Is Associated with Improved Long-Term Outcomes in Crohn's Disease. *Alimentary Pharmacology & Therapeutics* **2016,** *43*, 317-333.

19. Bressler, B.; Marshall, J. K.; Bernstein, C. N.; Bitton, A.; Jones, J.; Leontiadis, G. I.; Panaccione, R.; Steinhart, A. H.; Tse, F.; Feagan, B.; Toronto Ulcerative Colitis Consensus, G., Clinical Practice Guidelines for the Medical Management of Nonhospitalized Ulcerative Colitis: The Toronto Consensus. *Gastroenterology* **2015,** *148*, 1035-1058 e1033.
20. Faubion, W. A.; Loftus, E. V.; Harmsen, W. S.; Zinsmeister, A. R.; Sandborn, W. J., The Natural History of Corticosteroid Therapy for Inflammatory Bowel Disease: A Population-Based Study. *Gastroenterology* **2001,** *121*, 255-260.
21. Torres, J.; Mehandru, S.; Colombel, J.-F.; Peyrin-Biroulet, L., Crohn's Disease. *The Lancet* **2017,** *389*, 1741-1755.
22. Ford, A. C.; Peyrin-Biroulet, L., Opportunistic Infections with Anti-Tumor Necrosis Factor-Alpha Therapy in Inflammatory Bowel Disease: Meta-Analysis of Randomized Controlled Trials. *Am J Gastroenterol* **2013,** *108*, 1268-1276.
23. Beaugerie, L.; Itzkowitz, S. H., Cancers Complicating Inflammatory Bowel Disease. *N Engl J Med* **2015,** *372*, 1441-1452.
24. Ben-Horin, S.; Waterman, M.; Kopylov, U.; Yavzori, M.; Picard, O.; Fudim, E.; Awadie, H.; Weiss, B.; Chowers, Y., Addition of an Immunomodulator to Infliximab Therapy Eliminates Antidrug Antibodies in Serum and Restores Clinical Response of Patients with Inflammatory Bowel Disease. *Clin Gastroenterol Hepatol* **2013,** *11*, 444-447.
25. Sandborn, W. J.; Feagan, B. G.; Rutgeerts, P.; Hanauer, S.; Colombel, J. F.; Sands, B. E.; Lukas, M.; Fedorak, R. N.; Lee, S.; Bressler, B.; Fox, I.; Rosario, M.; Sankoh, S.; Xu, J.; Stephens, K.; Milch, C.; Parikh, A.; Group, G. S., Vedolizumab as Induction and Maintenance Therapy for Crohn's Disease. *N Engl J Med* **2013,** *369*, 711-721.
26. Sandborn, W. J.; Gasink, C.; Gao, L. L.; Blank, M. A.; Johanns, J.; Guzzo, C.; Sands, B. E.; Hanauer, S. B.; Targan, S.; Rutgeerts, P.; Ghosh, S.; de Villiers, W. J.; Panaccione, R.; Greenberg, G.; Schreiber, S.; Lichtiger, S.; Feagan, B. G.; Group, C. S., Ustekinumab Induction and Maintenance Therapy in Refractory Crohn's Disease. *N Engl J Med* **2012,** *367*, 1519-1528.
27. Danese, S.; Grisham, M.; Hodge, J.; Telliez, J. B., Jak Inhibition Using Tofacitinib for Inflammatory Bowel Disease Treatment: A Hub for Multiple Inflammatory Cytokines. *Am J Physiol Gastrointest Liver Physiol* **2016,** *310*, G155-162.
28. Monteleone, G.; Neurath, M. F.; Ardizzone, S.; Di Sabatino, A.; Fantini, M. C.; Castiglione, F.; Scribano, M. L.; Armuzzi, A.; Caprioli, F.; Sturniolo, G. C.; Rogai, F.; Vecchi, M.; Atreya, R.; Bossa, F.; Onali, S.; Fichera, M.; Corazza, G. R.; Biancone, L.; Savarino, V.; Pica, R.; Orlando, A.; Pallone, F., Mongersen, an Oral Smad7 Antisense Oligonucleotide, and Crohn's Disease. *N Engl J Med* **2015,** *372*, 1104-1113.
29. Broom, O. J.; Widjaya, B.; Troelsen, J.; Olsen, J.; Nielsen, O. H., Mitogen Activated Protein Kinases: A Role in Inflammatory Bowel Disease? *Clin Exp Immunol* **2009,** *158*, 272-280.
30. Coffey, E. T., Nuclear and Cytosolic Jnk Signalling in Neurons. *Nat Rev Neurosci* **2014,** *15*, 285-299.
31. Kim, E. K.; Choi, E. J., Compromised Mapk Signaling in Human Diseases: An Update. *Arch Toxicol* **2015,** *89*, 867-882.
32. Atreya, I.; Atreya, R.; Neurath, M. F., Nf-Kappab in Inflammatory Bowel Disease. *J Intern Med* **2008,** *263*, 591-596.
33. Mitchell, S.; Vargas, J.; Hoffmann, A., Signaling Via the Nfkappab System. *Wiley Interdiscip Rev Syst Biol Med* **2016,** *8*, 227-241.

34. Zhang, Q.; Lenardo, M. J.; Baltimore, D., 30 Years of Nf-Kappab: A Blossoming of Relevance to Human Pathobiology. *Cell* **2017,** *168*, 37-57.
35. Donnenberg, M. S., Pathogenic Strategies of Enteric Bacteria. *Nature* **2000,** *406*, 768-774.
36. Ruter, C.; Hardwidge, P. R., "Drug from Bugs': Bacterial Effector Protein as Promising Biological (Immune-)Therapeutics. *FEMS Microbiol. Lett.* **2014,** *351*, 126-132.
37. Falnes, P. Ø.; Sandvig, K., Penetration of Protein Toxins into Cells. *Current Opinion in Cell Biology* **2000,** *12*, 407-413.
38. Deng, W.; Marshall, N. C.; Rowland, J. L.; McCoy, J. M.; Worrall, L. J.; Santos, A. S.; Strynadka, N. C. J.; Finlay, B. B., Assembly, Structure, Function and Regulation of Type Iii Secretion Systems. *Nature reviews. Microbiology* **2017,** *15*, 323-337.
39. Jones, R.; Wentworth, C.; Neish, A., Salmonella Avra Modulates Innate Immune Signaling: A Mechanistic Analysis in Drosophila. *Faseb J* **2007,** *21*, A132-A132.
40. Wu, H. X.; Jones, R.; Luo, L. P.; Neish, A. S., Salmonella Evades Host Innate Immunity Via Avra Mediated Inhibition of Cytokine Production and Pro-Apoptotic Pathways. *Faseb J* **2008,** *22*.
41. Collier-Hyams, L. S.; Zeng, H.; Sun, J.; Tomlinson, A. D.; Bao, Z. Q.; Chen, H.; Madara, J. L.; Orth, K.; Neish, A. S., Cutting Edge: Salmonella Avra Effector Inhibits the Key Proinflammatory, Anti-Apoptotic Nf-Kappa B Pathway. *J. Immunol.* **2002,** *169*, 2846-2850.
42. Hao, Y. H.; Wang, Y.; Burdette, D.; Mukherjee, S.; Keitany, G.; Goldsmith, E.; Orth, K., Structural Requirements for Yersinia Yopj Inhibition of Map Kinase Pathways. *PloS one* **2008,** *3*, e1375.
43. Marcus, S. L.; Brumell, J. H.; Pfeifer, C. G.; Finlay, B. B., Salmonella Pathogenicity Islands: Big Virulence in Small Packages. *Microbes and Infection* **2000,** *2*, 145-156.
44. van der Heijden, J.; Finlay, B. B., Type Iii Effector-Mediated Processes in Salmonella Infection. *Future Microbiol* **2012,** *7*, 685-703.
45. Steele-Mortimer, O., The Salmonella-Containing Vacuole: Moving with the Times. *Curr Opin Microbiol* **2008,** *11*, 38-45.
46. Agbor, T. A.; McCormick, B. A., Salmonella Effectors: Important Players Modulating Host Cell Function During Infection. *Cell Microbiol* **2011,** *13*, 1858-1869.
47. Jones, R. M.; Wu, H.; Wentworth, C.; Luo, L.; Collier-Hyams, L.; Neish, A. S., Salmonella Avra Coordinates Suppression of Host Immune and Apoptotic Defenses Via Jnk Pathway Blockade. *Cell Host Microbe* **2008,** *3*, 233-244.
48. Du, F.; Galan, J. E., Selective Inhibition of Type Iii Secretion Activated Signaling by the Salmonella Effector Avra. *PLoS Pathog.* **2009,** *5*, e1000595.
49. Wu, H.; Jones, R. M.; Neish, A. S., The Salmonella Effector Avra Mediates Bacterial Intracellular Survival During Infection in Vivo. *Cell Microbiol* **2012,** *14*, 28-39.
50. Lin, Z.; Zhang, Y. G.; Xia, Y.; Xu, X.; Jiao, X.; Sun, J., Salmonella Enteritidis Effector Avra Stabilizes Intestinal Tight Junctions Via the Jnk Pathway. *J Biol Chem* **2016,** *291*, 26837-26849.
51. Herrera Estrada, L.; Wu, H.; Ling, K.; Zhang, G.; Sumagin, R.; Parkos, C. A.; Jones, R. M.; Champion, J. A.; Neish, A. S., Bioengineering Bacterially Derived Immunomodulants: A Therapeutic Approach to Inflammatory Bowel Disease. *ACS Nano* **2017,** *11*, 9650-9662.
52. Neish, A. S., Prokaryotic Regulation of Epithelial Responses by Inhibition of Ikappa B-Alpha Ubiquitination. *Science* **2000,** *289*, 1560-1563.

53. Zhou, Y.; Dong, N.; Hu, L.; Shao, F., The Shigella Type Three Secretion System Effector Ospg Directly and Specifically Binds to Host Ubiquitin for Activation. *PloS one* **2013,** *8*, e57558.
54. Schroeder, G. N.; Hilbi, H., Molecular Pathogenesis of Shigella Spp.: Controlling Host Cell Signaling, Invasion, and Death by Type Iii Secretion. *Clinical microbiology reviews* **2008,** *21*, 134-156.
55. Arbibe, L.; Kim, D. W.; Batsche, E.; Pedron, T.; Mateescu, B.; Muchardt, C.; Parsot, C.; Sansonetti, P. J., An Injected Bacterial Effector Targets Chromatin Access for Transcription Factor Nf-Kappab to Alter Transcription of Host Genes Involved in Immune Responses. *Nat Immunol* **2007,** *8*, 47-56.
56. Kim, D. W.; Lenzen, G.; Page, A. L.; Legrain, P.; Sansonetti, P. J.; Parsot, C., The Shigella Flexneri Effector Ospg Interferes with Innate Immune Responses by Targeting Ubiquitin-Conjugating Enzymes. *Proc. Natl. Acad. Sci. U. S. A.* **2005,** *102*, 14046-14051.
57. Trosky, J. E.; Li, Y.; Mukherjee, S.; Keitany, G.; Ball, H.; Orth, K., Vopa Inhibits Atp Binding by Acetylating the Catalytic Loop of Mapk Kinases. *J. Biol. Chem.* **2007,** *282*, 34299-34305.
58. Trosky, J. E.; Mukherjee, S.; Burdette, D. L.; Roberts, M.; McCarter, L.; Siegel, R. M.; Orth, K., Inhibition of Mapk Signaling Pathways by Vopa from Vibrio Parahaemolyticus. *J Biol Chem* **2004,** *279*, 51953-51957.
59. Jones, R. M.; Luo, L.; Moberg, K. H., Aeromonas Salmonicida-Secreted Protein Aopp Is a Potent Inducer of Apoptosis in a Mammalian and a Drosophila Model. *Cell Microbiol* **2012,** *14*, 274-285.
60. Buttner, D.; He, S. Y., Type Iii Protein Secretion in Plant Pathogenic Bacteria. *Plant Physiol* **2009,** *150*, 1656-1664.
61. Orth, K., Function of the Yersinia Effector Yopj. *Current Opinion in Microbiology* **2002,** *5*, 38-43.
62. Mukherjee, S.; Keitany, G.; Li, Y.; Wang, Y.; Ball, H. L.; Goldsmith, E. J.; Orth, K., Yersinia Yopj Acetylates and Inhibits Kinase Activation by Blocking Phosphorylation. *Science* **2006,** *312*, 1211-1214.
63. Mittal, R.; Peak-Chew, S. Y.; McMahon, H. T., Acetylation of Mek2 and I Kappa B Kinase (Ikk) Activation Loop Residues by Yopj Inhibits Signaling. *Proc. Natl. Acad. Sci. U. S. A.* **2006,** *103*, 18574-18579.
64. Palmer, L. E.; Hobbie, S.; Galan, J. E.; Bliska, J. B., Yopj of Yersinia Pseudotuberculosis Is Required for the Inhibition of Macrophage Tnf-Alpha Production and Downregulation of the Map Kinases P38 and Jnk. *Mol. Microbiol.* **1998,** *27*, 953-965.
65. Spinner, J. L.; Seo, K. S.; O'Loughlin, J. L.; Cundiff, J. A.; Minnich, S. A.; Bohach, G. A.; Kobayashi, S. D., Neutrophils Are Resistant to Yersinia Yopj/P-Induced Apoptosis and Are Protected from Ros-Mediated Cell Death by the Type Iii Secretion System. *PloS one* **2010,** *5*, e9279.
66. Giacomodonato, M. N.; Noto Llana, M.; Aya Castaneda Mdel, R.; Buzzola, F. R.; Sarnacki, S. H.; Cerquetti, M. C., Avra Effector Protein of Salmonella Enterica Serovar Enteritidis Is Expressed and Translocated in Mesenteric Lymph Nodes at Late Stages of Infection in Mice. *Microbiology* **2014,** *160*, 1191-1199.
67. Zhang, Z. M.; Ma, K. W.; Yuan, S.; Luo, Y.; Jiang, S.; Hawara, E.; Pan, S.; Ma, W.; Song, J., Structure of a Pathogen Effector Reveals the Enzymatic Mechanism of a Novel Acetyltransferase Family. *Nat Struct Mol Biol* **2016,** *23*, 847-852.

68. Mittal, R.; Peak-Chew, S. Y.; Sade, R. S.; Vallis, Y.; McMahon, H. T., The Acetyltransferase Activity of the Bacterial Toxin Yopj of Yersinia Is Activated by Eukaryotic Host Cell Inositol Hexakisphosphate. *J Biol Chem* **2010,** *285*, 19927-19934.
69. Zhang, Z. M.; Ma, K. W.; Gao, L.; Hu, Z.; Schwizer, S.; Ma, W.; Song, J., Mechanism of Host Substrate Acetylation by a Yopj Family Effector. *Nat Plants* **2017,** *3*, 17115.
70. Kaur, J.; Jain, S. K., Role of Antigens and Virulence Factors of Salmonella Enterica Serovar Typhi in Its Pathogenesis. *Microbiol. Res.* **2012,** *167*, 199-210.
71. Lu, R.; Wu, S.; Zhang, Y. g.; Xia, Y.; Liu, X.; Zheng, Y.; Chen, H.; Schaefer, K. L.; Zhou, Z.; Bissonnette, M.; Li, L.; Sun, J., Enteric Bacterial Protein Avra Promotes Colonic Tumorigenesis and Activates Colonic Beta-Catenin Signaling Pathway. *Oncogenesis* **2014,** *3*, e105.
72. Lu, R.; Wu, S.; Zhang, Y. G.; Xia, Y.; Zhou, Z.; Kato, I.; Dong, H.; Bissonnette, M.; Sun, J., Salmonella Protein Avra Activates the Stat3 Signaling Pathway in Colon Cancer. *Neoplasia* **2016,** *18*, 307-316.
73. Marschall, A. L.; Zhang, C.; Frenzel, A.; Schirrmann, T.; Hust, M.; Perez, F.; Dubel, S., Delivery of Antibodies to the Cytosol: Debunking the Myths. *MAbs* **2014,** *6*, 943-956.
74. Finan, C.; Gaulton, A.; Kruger, F. A.; Lumbers, R. T.; Shah, T.; Engmann, J.; Galver, L.; Kelley, R.; Karlsson, A.; Santos, R.; Overington, J. P.; Hingorani, A. D.; Casas, J. P., The Druggable Genome and Support for Target Identification and Validation in Drug Development. *Science translational medicine* **2017,** *9*.
75. Hopkins, A. L.; Groom, C. R., The Druggable Genome. *Nature reviews. Drug discovery* **2002,** *1*, 727-730.
76. Mitragotri, S.; Burke, P. A.; Langer, R., Overcoming the Challenges in Administering Biopharmaceuticals: Formulation and Delivery Strategies. *Nature reviews. Drug discovery* **2014,** *13*, 655-672.
77. Yu, M.; Wu, J.; Shi, J.; Farokhzad, O. C., Nanotechnology for Protein Delivery: Overview and Perspectives. *J. Controlled Release* **2016,** *240*, 24-37.
78. Leader, B.; Baca, Q. J.; Golan, D. E., Protein Therapeutics: A Summary and Pharmacological Classification. *Nature reviews. Drug discovery* **2008,** *7*, 21-39.
79. Walsh, G., Biopharmaceutical Benchmarks 2014. *Nature biotechnology* **2014,** *32*, 992-1000.
80. Ray, M.; Lee, Y. W.; Scaletti, F.; Yu, R.; Rotello, V. M., Intracellular Delivery of Proteins by Nanocarriers. *Nanomedicine (Lond)* **2017,** *12*, 941-952.
81. Sharei, A.; Mao, S.; Langer, R.; Jensen, K. F., Intracellular Delivery of Biomolecules by Mechanical Deformation. **2016**, 143-176.
82. Meacham, J. M.; Durvasula, K.; Degertekin, F. L.; Fedorov, A. G., Physical Methods for Intracellular Delivery: Practical Aspects from Laboratory Use to Industrial-Scale Processing. *J Lab Autom* **2014,** *19*, 1-18.
83. Dinca, A.; Chien, W. M.; Chin, M. T., Intracellular Delivery of Proteins with Cell-Penetrating Peptides for Therapeutic Uses in Human Disease. *Int J Mol Sci* **2016,** *17*, 263.
84. Lohcharoenkal, W.; Wang, L.; Chen, Y. C.; Rojanasakul, Y., Protein Nanoparticles as Drug Delivery Carriers for Cancer Therapy. *Biomed Res Int* **2014,** *2014*, 180549.
85. Gordon, J. W.; Scangos, G. A.; Plotkin, D. J.; Barbosa, J. A.; Ruddle, F. H., Genetric Transformation of Mouse Embryos by Microinjection of Purified DNA. *Proc. Natl. Acad. Sci. U. S. A.* **1980,** *77*, 7380-7384.

86. Adamo, A.; Roushdy, O.; Dokov, R.; Sharei, A.; Jensen, K. F., Microfluidic Jet Injection for Delivering Macromolecules into Cells. *J Micromech Microeng* **2013,** *23*.
87. Sharei, A.; Zoldan, J.; Adamo, A.; Sim, W. Y.; Cho, N.; Jackson, E.; Mao, S.; Schneider, S.; Han, M. J.; Lytton-Jean, A.; Basto, P. A.; Jhunjhunwala, S.; Lee, J.; Heller, D. A.; Kang, J. W.; Hartoularos, G. C.; Kim, K. S.; Anderson, D. G.; Langer, R.; Jensen, K. F., A Vector-Free Microfluidic Platform for Intracellular Delivery. *Proc. Natl. Acad. Sci. U. S. A.* **2013,** *110*, 2082-2087.
88. Stewart, M. P.; Sharei, A.; Ding, X.; Sahay, G.; Langer, R.; Jensen, K. F., In Vitro and Ex Vivo Strategies for Intracellular Delivery. *Nature* **2016,** *538*, 183-192.
89. Venslauskas, M. S.; Satkauskas, S., Mechanisms of Transfer of Bioactive Molecules through the Cell Membrane by Electroporation. *Eur Biophys J* **2015,** *44*, 277-289.
90. Sarisozen, C.; Torchilin, V. P., Intracellular Delivery of Proteins and Peptides. **2016**, 576-622.
91. Boukany, P. E.; Morss, A.; Liao, W. C.; Henslee, B.; Jung, H.; Zhang, X.; Yu, B.; Wang, X.; Wu, Y.; Li, L.; Gao, K.; Hu, X.; Zhao, X.; Hemminger, O.; Lu, W.; Lafyatis, G. P.; Lee, L. J., Nanochannel Electroporation Delivers Precise Amounts of Biomolecules into Living Cells. *Nature nanotechnology* **2011,** *6*, 747-754.
92. Fu, A.; Tang, R.; Hardie, J.; Farkas, M. E.; Rotello, V. M., Promises and Pitfalls of Intracellular Delivery of Proteins. *Bioconjugate chemistry* **2014,** *25*, 1602-1608.
93. Bischof, J. C.; Padanilam, J.; Holmes, W. H.; Ezzell, R. M.; Lee, R. C.; Tompkins, R. G.; Yarmush, M. L.; Toner, M., Dynamics of Cell Membrane Permeability Changes at Supraphysiological Temperatures. *Biophysical Journal* **1995,** *68*, 2608-2614.
94. Stevenson, D. J.; Gunn-Moore, F. J.; Campbell, P.; Dholakia, K., Single Cell Optical Transfection. *J R Soc Interface* **2010,** *7*, 863-871.
95. Walev, I.; Bhakdi, S. C.; Hofmann, F.; Djonder, N.; Valeva, A.; Aktories, K.; Bhakdi, S., Delivery of Proteins into Living Cells by Reversible Membrane Permeabilization with Streptolysin-O. *Proc. Natl. Acad. Sci. U. S. A.* **2001,** *98*, 3185-3190.
96. Frenkel, N.; Makky, A.; Sudji, I. R.; Wink, M.; Tanaka, M., Mechanistic Investigation of Interactions between Steroidal Saponin Digitonin and Cell Membrane Models. *The journal of physical chemistry. B* **2014,** *118*, 14632-14639.
97. Mellott, A. J.; Forrest, M. L.; Detamore, M. S., Physical Non-Viral Gene Delivery Methods for Tissue Engineering. *Ann Biomed Eng* **2013,** *41*, 446-468.
98. Bloomfield, G.; Kay, R. R., Uses and Abuses of Macropinocytosis. *J Cell Sci* **2016,** *129*, 2697-2705.
99. Zhang, D.; Wang, J.; Xu, D., Cell-Penetrating Peptides as Noninvasive Transmembrane Vectors for the Development of Novel Multifunctional Drug-Delivery Systems. *J. Controlled Release* **2016,** *229*, 130-139.
100. Schwarze, S. R., In Vivo Protein Transduction: Delivery of a Biologically Active Protein into the Mouse. *Science* **1999,** *285*, 1569-1572.
101. Agrawal, P.; Bhalla, S.; Usmani, S. S.; Singh, S.; Chaudhary, K.; Raghava, G. P.; Gautam, A., Cppsite 2.0: A Repository of Experimentally Validated Cell-Penetrating Peptides. *Nucleic Acids Res* **2016,** *44*, D1098-1103.
102. Patel, L. N.; Zaro, J. L.; Shen, W. C., Cell Penetrating Peptides: Intracellular Pathways and Pharmaceutical Perspectives. *Pharm. Res.* **2007,** *24*, 1977-1992.

103. Green, I.; Christison, R.; Voyce, C. J.; Bundell, K. R.; Lindsay, M. A., Protein Transduction Domains: Are They Delivering? *Trends in pharmacological sciences* **2003,** *24*, 213-215.
104. Guidotti, G.; Brambilla, L.; Rossi, D., Cell-Penetrating Peptides: From Basic Research to Clinics. *Trends in pharmacological sciences* **2017,** *38*, 406-424.
105. Cerrato, C. P.; Kunnapuu, K.; Langel, U., Cell-Penetrating Peptides with Intracellular Organelle Targeting. *Expert Opin Drug Deliv* **2017,** *14*, 245-255.
106. Milletti, F., Cell-Penetrating Peptides: Classes, Origin, and Current Landscape. *Drug Discov Today* **2012,** *17*, 850-860.
107. Tunnemann, G.; Ter-Avetisyan, G.; Martin, R. M.; Stockl, M.; Herrmann, A.; Cardoso, M. C., Live-Cell Analysis of Cell Penetration Ability and Toxicity of Oligo-Arginines. *J Pept Sci* **2008,** *14*, 469-476.
108. Benjaminsen, R. V.; Mattebjerg, M. A.; Henriksen, J. R.; Moghimi, S. M.; Andresen, T. L., The Possible "Proton Sponge " Effect of Polyethylenimine (Pei) Does Not Include Change in Lysosomal Ph. *Molecular therapy : the journal of the American Society of Gene Therapy* **2013,** *21*, 149-157.
109. Munyendo, W. L.; Lv, H.; Benza-Ingoula, H.; Baraza, L. D.; Zhou, J., Cell Penetrating Peptides in the Delivery of Biopharmaceuticals. *Biomolecules* **2012,** *2*, 187-202.
110. Cronican, J. J.; Beier, K. T.; Davis, T. N.; Tseng, J. C.; Li, W.; Thompson, D. B.; Shih, A. F.; May, E. M.; Cepko, C. L.; Kung, A. L.; Zhou, Q.; Liu, D. R., A Class of Human Proteins That Deliver Functional Proteins into Mammalian Cells in Vitro and in Vivo. *Chemistry & biology* **2011,** *18*, 833-838.
111. Cronican, J. J.; Thompson, D. B.; Beier, K. T.; McNaughton, B. R.; Cepko, C. L.; Liu, D. R., Potent Delivery of Functional Proteins into Mammalian Cells in Vitro and in Vivo Using a Supercharged Protein. *ACS Chem Biol* **2010,** *5*, 747-752.
112. Martin, I.; Teixido, M.; Giralt, E., Design, Synthesis and Characterization of a New Anionic Cell-Penetrating Peptide: Sap(E). *Chembiochem : a European journal of chemical biology* **2011,** *12*, 896-903.
113. Marks, J. R.; Placone, J.; Hristova, K.; Wimley, W. C., Spontaneous Membrane-Translocating Peptides by Orthogonal High-Throughput Screening. *J Am Chem Soc* **2011,** *133*, 8995-9004.
114. Ross, M. F.; Filipovska, A.; Smith, R. A.; Gait, M. J.; Murphy, M. P., Cell-Penetrating Peptides Do Not Cross Mitochondrial Membranes Even When Conjugated to a Lipophilic Cation: Evidence against Direct Passage through Phospholipid Bilayers. *The Biochemical journal* **2004,** *383*, 457-468.
115. Bolhassani, A., Potential Efficacy of Cell-Penetrating Peptides for Nucleic Acid and Drug Delivery in Cancer. *Biochim Biophys Acta* **2011,** *1816*, 232-246.
116. Bonifacino, J. S.; Dell'Angelica, E. C., Molecular Bases for the Recognition of Tyrosine-Based Sorting Signals: Figure 1. *The Journal of cell biology* **1999,** *145*, 923-926.
117. Dekiwadia, C. D.; Lawrie, A. C.; Fecondo, J. V., Peptide-Mediated Cell Penetration and Targeted Delivery of Gold Nanoparticles into Lysosomes. *J Pept Sci* **2012,** *18*, 527-534.
118. Szeto, H. H., Cell-Permeable, Mitochondrial-Targeted, Peptide Antioxidants. *The AAPS journal* **2006,** *8*, E277-E283.
119. Zhang, J.; Sun, A.; Xu, R.; Tao, X.; Dong, Y.; Lv, X.; Wei, D., Cell-Penetrating and Endoplasmic Reticulum-Locating Tat-Il-24-Kdel Fusion Protein Induces Tumor Apoptosis. *J Cell Physiol* **2016,** *231*, 84-93.

120. Roy, R. N.; Lomakin, I. B.; Gagnon, M. G.; Steitz, T. A., The Mechanism of Inhibition of Protein Synthesis by the Proline-Rich Peptide Oncocin. *Nat Struct Mol Biol* **2015,** *22*, 466-469.
121. Gaj, T.; Liu, J.; Anderson, K. E.; Sirk, S. J.; Barbas, C. F., 3rd, Protein Delivery Using Cys2-His2 Zinc-Finger Domains. *ACS Chem Biol* **2014,** *9*, 1662-1667.
122. Kratz, F., Albumin as a Drug Carrier: Design of Prodrugs, Drug Conjugates and Nanoparticles. *J. Controlled Release* **2008,** *132*, 171-183.
123. Larsen, M. T.; Kuhlmann, M.; Hvam, M. L.; Howard, K. A., Albumin-Based Drug Delivery: Harnessing Nature to Cure Disease. *Mol Cell Ther* **2016,** *4*, 3.
124. Turecek, P. L.; Bossard, M. J.; Schoetens, F.; Ivens, I. A., Pegylation of Biopharmaceuticals: A Review of Chemistry and Nonclinical Safety Information of Approved Drugs. *Journal of pharmaceutical sciences* **2016,** *105*, 460-475.
125. Pisal, D. S.; Kosloski, M. P.; Balu-Iyer, S. V., Delivery of Therapeutic Proteins. *Journal of pharmaceutical sciences* **2010,** *99*, 2557-2575.
126. Kay, M. A., State-of-the-Art Gene-Based Therapies: The Road Ahead. *Nat Rev Genet* **2011,** *12*, 316-328.
127. Gilleron, J.; Querbes, W.; Zeigerer, A.; Borodovsky, A.; Marsico, G.; Schubert, U.; Manygoats, K.; Seifert, S.; Andree, C.; Stoter, M.; Epstein-Barash, H.; Zhang, L.; Koteliansky, V.; Fitzgerald, K.; Fava, E.; Bickle, M.; Kalaidzidis, Y.; Akinc, A.; Maier, M.; Zerial, M., Image-Based Analysis of Lipid Nanoparticle-Mediated Sirna Delivery, Intracellular Trafficking and Endosomal Escape. *Nature biotechnology* **2013,** *31*, 638-646.
128. Sahay, G.; Querbes, W.; Alabi, C.; Eltoukhy, A.; Sarkar, S.; Zurenko, C.; Karagiannis, E.; Love, K.; Chen, D.; Zoncu, R.; Buganim, Y.; Schroeder, A.; Langer, R.; Anderson, D. G., Efficiency of Sirna Delivery by Lipid Nanoparticles Is Limited by Endocytic Recycling. *Nature biotechnology* **2013,** *31*, 653-658.
129. Sperling, R. A.; Parak, W. J., Surface Modification, Functionalization and Bioconjugation of Colloidal Inorganic Nanoparticles. *Philos Trans A Math Phys Eng Sci* **2010,** *368*, 1333-1383.
130. Xu, D.; Hu, Z.; Su, J.; Wu, F.; Yuan, W., Micro and Nanotechnology for Intracellular Delivery Therapy Protein. *Nano-Micro Letters* **2012,** *4*, 118-123.
131. Kam, N. W.; Liu, Z.; Dai, H., Carbon Nanotubes as Intracellular Transporters for Proteins and DNA: An Investigation of the Uptake Mechanism and Pathway. *Angewandte Chemie* **2006,** *45*, 577-581.
132. Kam, N. W.; Dai, H., Carbon Nanotubes as Intracellular Protein Transporters: Generality and Biological Functionality. *J Am Chem Soc* **2005,** *127*, 6021-6026.
133. Gu, Z.; Biswas, A.; Zhao, M.; Tang, Y., Tailoring Nanocarriers for Intracellular Protein Delivery. *Chem Soc Rev* **2011,** *40*, 3638-3655.
134. Chorny, M.; Hood, E.; Levy, R. J.; Muzykantov, V. R., Endothelial Delivery of Antioxidant Enzymes Loaded into Non-Polymeric Magnetic Nanoparticles. *J. Controlled Release* **2010,** *146*, 144-151.
135. Boisselier, E.; Astruc, D., Gold Nanoparticles in Nanomedicine: Preparations, Imaging, Diagnostics, Therapies and Toxicity. *Chem Soc Rev* **2009,** *38*, 1759-1782.
136. Tang, R.; Kim, C. S.; Solfiell, D. J.; Rana, S.; Mout, R.; Velazquez-Delgado, E. M.; Chompoosor, A.; Jeong, Y.; Yan, B.; Zhu, Z. J.; Kim, C.; Hardy, J. A.; Rotello, V. M., Direct Delivery of Functional Proteins and Enzymes to the Cytosol Using Nanoparticle-Stabilized Nanocapsules. *ACS Nano* **2013,** *7*, 6667-6673.

137. Mout, R.; Ray, M.; Tay, T.; Sasaki, K.; Yesilbag Tonga, G.; Rotello, V. M., General Strategy for Direct Cytosolic Protein Delivery Via Protein-Nanoparticle Co-Engineering. *ACS Nano* **2017,** *11*, 6416-6421.
138. Kim, T.; Hyeon, T., Applications of Inorganic Nanoparticles as Therapeutic Agents. *Nanotechnology* **2014,** *25*, 012001.
139. Lee, K.; Conboy, M.; Park, H. M.; Jiang, F.; Kim, H. J.; Dewitt, M. A.; Mackley, V. A.; Chang, K.; Rao, A.; Skinner, C.; Shobha, T.; Mehdipour, M.; Liu, H.; Huang, W.-c.; Lan, F.; Bray, N. L.; Li, S.; Corn, J. E.; Kataoka, K.; Doudna, J. A.; Conboy, I.; Murthy, N., Nanoparticle Delivery of Cas9 Ribonucleoprotein and Donor DNA in Vivo Induces Homology-Directed DNA Repair. *Nature Biomedical Engineering* **2017,** *1*, 889-901.
140. Chen, Y.; Chen, H.; Shi, J., In Vivo Bio-Safety Evaluations and Diagnostic/Therapeutic Applications of Chemically Designed Mesoporous Silica Nanoparticles. *Adv Mater* **2013,** *25*, 3144-3176.
141. Peer, D.; Karp, J. M.; Hong, S.; Farokhzad, O. C.; Margalit, R.; Langer, R., Nanocarriers as an Emerging Platform for Cancer Therapy. *Nature nanotechnology* **2007,** *2*, 751-760.
142. Kube, S.; Hersch, N.; Naumovska, E.; Gensch, T.; Hendriks, J.; Franzen, A.; Landvogt, L.; Siebrasse, J. P.; Kubitscheck, U.; Hoffmann, B.; Merkel, R.; Csiszar, A., Fusogenic Liposomes as Nanocarriers for the Delivery of Intracellular Proteins. *Langmuir : the ACS journal of surfaces and colloids* **2017,** *33*, 1051-1059.
143. Torchilin, V. P., Recent Approaches to Intracellular Delivery of Drugs and DNA and Organelle Targeting. *Annu Rev Biomed Eng* **2006,** *8*, 343-375.
144. Vermonden, T.; Censi, R.; Hennink, W. E., Hydrogels for Protein Delivery. *Chem Rev* **2012,** *112*, 2853-2888.
145. Ha, D.; Yang, N.; Nadithe, V., Exosomes as Therapeutic Drug Carriers and Delivery Vehicles across Biological Membranes: Current Perspectives and Future Challenges. *Acta Pharm Sin B* **2016,** *6*, 287-296.
146. El-Sherbiny, I.; Khalil, I.; Ali, I.; Yacoub, M., Updates on Smart Polymeric Carrier Systems for Protein Delivery. *Drug development and industrial pharmacy* **2017,** *43*, 1567-1583.
147. Li, D.; van Nostrum, C. F.; Mastrobattista, E.; Vermonden, T.; Hennink, W. E., Nanogels for Intracellular Delivery of Biotherapeutics. *J. Controlled Release* **2017,** *259*, 16-28.
148. Palivan, C. G.; Goers, R.; Najer, A.; Zhang, X.; Car, A.; Meier, W., Bioinspired Polymer Vesicles and Membranes for Biological and Medical Applications. *Chem Soc Rev* **2016,** *45*, 377-411.
149. Williams, R. J.; Dove, A. P.; O'Reilly, R. K., Self-Assembly of Cyclic Polymers. *Polymer Chemistry* **2015,** *6*, 2998-3008.
150. Kaczmarczyk, S. J.; Sitaraman, K.; Young, H. A.; Hughes, S. H.; Chatterjee, D. K., Protein Delivery Using Engineered Virus-Like Particles. *Proc. Natl. Acad. Sci. U. S. A.* **2011,** *108*, 16998-17003.
151. Herrera Estrada, L. P.; Champion, J. A., Protein Nanoparticles for Therapeutic Protein Delivery. *Biomaterials science* **2015,** *3*, 787-799.
152. Zeltins, A., Construction and Characterization of Virus-Like Particles: A Review. *Mol Biotechnol* **2013,** *53*, 92-107.
153. Lopez-Sagaseta, J.; Malito, E.; Rappuoli, R.; Bottomley, M. J., Self-Assembling Protein Nanoparticles in the Design of Vaccines. *Comput Struct Biotechnol J* **2016,** *14*, 58-68.
154. Bhaskar, S.; Lim, S., Engineering Protein Nanocages as Carriers for Biomedical Applications. *NPG Asia Materials* **2017,** *9*, e371-e371.

155. Kedersha, N. L., Isolation and Characterization of a Novel Ribonucleoprotein Particle: Large Structures Contain a Single Species of Small Rna. *The Journal of cell biology* **1986,** *103*, 699-709.
156. DiMarco, R. L.; Heilshorn, S. C., Multifunctional Materials through Modular Protein Engineering. *Adv Mater* **2012,** *24*, 3923-3940.
157. MacEwan, S. R.; Chilkoti, A., Applications of Elastin-Like Polypeptides in Drug Delivery. *J. Controlled Release* **2014,** *190*, 314-330.
158. Lee, S. C.; Park, K.; Han, J.; Lee, J. J.; Kim, H. J.; Hong, S.; Heu, W.; Kim, Y. J.; Ha, J. S.; Lee, S. G.; Cheong, H. K.; Jeon, Y. H.; Kim, D.; Kim, H. S., Design of a Binding Scaffold Based on Variable Lymphocyte Receptors of Jawless Vertebrates by Module Engineering. *Proc. Natl. Acad. Sci. U. S. A.* **2012,** *109*, 3299-3304.
159. Lee, J. J.; Kang, J. A.; Ryu, Y.; Han, S. S.; Nam, Y. R.; Rho, J. K.; Choi, D. S.; Kang, S. W.; Lee, D. E.; Kim, H. S., Genetically Engineered and Self-Assembled Oncolytic Protein Nanoparticles for Targeted Cancer Therapy. *Biomaterials* **2017,** *120*, 22-31.
160. Collins, L.; Parker, A. L.; Gehman, J. D.; Eckley, L.; Perugini, M. A.; Separovic, F.; Fabre, J. W., Self-Assembly of Peptides into Spherical Nanoparticles for Delivery of Hydrophilic Moieties to the Cytosol. *ACS Nano* **2010,** *4*, 2856-2864.
161. Elzoghby, A. O.; Samy, W. M.; Elgindy, N. A., Protein-Based Nanocarriers as Promising Drug and Gene Delivery Systems. *J. Controlled Release* **2012,** *161*, 38-49.
162. Weber, C.; Coester, C.; Kreuter, J.; Langer, K., Desolvation Process and Surface Characterisation of Protein Nanoparticles. *Int J Pharm* **2000,** *194*, 91-102.
163. Qian, L.; Fu, J.; Yuan, P.; Du, S.; Huang, W.; Li, L.; Yao, S. Q., Intracellular Delivery of Native Proteins Facilitated by Cell-Penetrating Poly(Disulfide)S. *Angewandte Chemie* **2018,** *57*, 1532-1536.
164. Jahanshahi, M.; Babaei, Z., Protein Nanoparticle - a Unique System as Drug Delivery Vehicles. *African Journal of Biotechnology* **2008,** *7*, 4926-4934.
165. Akinc, A.; Battaglia, G., Exploiting Endocytosis for Nanomedicines. *Cold Spring Harb Perspect Biol* **2013,** *5*, a016980.
166. Kou, L.; Sun, J.; Zhai, Y.; He, Z., The Endocytosis and Intracellular Fate of Nanomedicines: Implication for Rational Design. *Asian Journal of Pharmaceutical Sciences* **2013,** *8*, 1-10.
167. Sahay, G.; Alakhova, D. Y.; Kabanov, A. V., Endocytosis of Nanomedicines. *J. Controlled Release* **2010,** *145*, 182-195.
168. Hillaireau, H.; Couvreur, P., Nanocarriers' Entry into the Cell: Relevance to Drug Delivery. *Cellular and molecular life sciences : CMLS* **2009,** *66*, 2873-2896.
169. Aderem, A.; Underhill, D. M., Mechanisms of Phagocytosis in Macrophages. *Annu Rev Immunol* **1999,** *17*, 593-623.
170. Kaksonen, M.; Roux, A., Mechanisms of Clathrin-Mediated Endocytosis. *Nature reviews. Molecular cell biology* **2018**.
171. Conner, S. D.; Schmid, S. L., Regulated Portals of Entry into the Cell. *Nature* **2003,** *422*, 37-44.
172. Parton, R. G.; Richards, A. A., Lipid Rafts and Caveolae as Portals for Endocytosis: New Insights and Common Mechanisms. *Traffic* **2003,** *4*, 724-738.
173. Pelkmans, L.; Puntener, D.; Helenius, A., Local Actin Polymerization and Dynamin Recruitment in Sv40-Induced Internalization of Caveolae. *Science* **2002,** *296*, 535-539.

174. Iversen, T.-G.; Skotland, T.; Sandvig, K., Endocytosis and Intracellular Transport of Nanoparticles: Present Knowledge and Need for Future Studies. *Nano Today* **2011,** *6*, 176-185.
175. Yeung, T.; Gilbert, G. E.; Shi, J.; Silvius, J.; Kapus, A.; Grinstein, S., Membrane Phosphatidylserine Regulates Surface Charge and Protein Localization. *Science* **2008,** *319*, 210-213.
176. Vandamme, T. F.; Brobeck, L., Poly(Amidoamine) Dendrimers as Ophthalmic Vehicles for Ocular Delivery of Pilocarpine Nitrate and Tropicamide. *J. Controlled Release* **2005,** *102*, 23-38.
177. Voigt, J.; Christensen, J.; Shastri, V. P., Differential Uptake of Nanoparticles by Endothelial Cells through Polyelectrolytes with Affinity for Caveolae. *Proc. Natl. Acad. Sci. U. S. A.* **2014,** *111*, 2942-2947.
178. Cedervall, T.; Lynch, I.; Lindman, S.; Berggard, T.; Thulin, E.; Nilsson, H.; Dawson, K. A.; Linse, S., Understanding the Nanoparticle-Protein Corona Using Methods to Quantify Exchange Rates and Affinities of Proteins for Nanoparticles. *Proc. Natl. Acad. Sci. U. S. A.* **2007,** *104*, 2050-2055.
179. Nguyen, V. H.; Lee, B. J., Protein Corona: A New Approach for Nanomedicine Design. *Int. J. Nanomed.* **2017,** *12*, 3137-3151.
180. Kokkinopoulou, M.; Simon, J.; Landfester, K.; Mailander, V.; Lieberwirth, I., Visualization of the Protein Corona: Towards a Biomolecular Understanding of Nanoparticle-Cell-Interactions. *Nanoscale* **2017,** *9*, 8858-8870.
181. Fleischer, C. C.; Payne, C. K., Nanoparticle-Cell Interactions: Molecular Structure of the Protein Corona and Cellular Outcomes. *Acc Chem Res* **2014,** *47*, 2651-2659.
182. Bertrand, N.; Grenier, P.; Mahmoudi, M.; Lima, E. M.; Appel, E. A.; Dormont, F.; Lim, J. M.; Karnik, R.; Langer, R.; Farokhzad, O. C., Mechanistic Understanding of in Vivo Protein Corona Formation on Polymeric Nanoparticles and Impact on Pharmacokinetics. *Nat Commun* **2017,** *8*, 777.
183. Gref, R.; Lück, M.; Quellec, P.; Marchand, M.; Dellacherie, E.; Harnisch, S.; Blunk, T.; Müller, R. H., 'Stealth' Corona-Core Nanoparticles Surface Modified by Polyethylene Glycol (Peg): Influences of the Corona (Peg Chain Length and Surface Density) and of the Core Composition on Phagocytic Uptake and Plasma Protein Adsorption. *Colloids and Surfaces B: Biointerfaces* **2000,** *18*, 301-313.
184. O'Brien, J.; Shea, K. J., Tuning the Protein Corona of Hydrogel Nanoparticles: The Synthesis of Abiotic Protein and Peptide Affinity Reagents. *Acc Chem Res* **2016,** *49*, 1200-1210.
185. Harrison, R. E.; Bucci, C.; Vieira, O. V.; Schroer, T. A.; Grinstein, S., Phagosomes Fuse with Late Endosomes and/or Lysosomes by Extension of Membrane Protrusions Along Microtubules: Role of Rab7 and Rilp. *Molecular and Cellular Biology* **2003,** *23*, 6494-6506.
186. Medina-Kauwe, L. K., "Alternative" Endocytic Mechanisms Exploited by Pathogens: New Avenues for Therapeutic Delivery? *Adv. Drug Delivery Rev.* **2007,** *59*, 798-809.
187. Parton, R. G.; Simons, K., The Multiple Faces of Caveolae. *Nature reviews. Molecular cell biology* **2007,** *8*, 185-194.
188. Hayer, A.; Stoeber, M.; Ritz, D.; Engel, S.; Meyer, H. H.; Helenius, A., Caveolin-1 Is Ubiquitinated and Targeted to Intralumenal Vesicles in Endolysosomes for Degradation. *The Journal of cell biology* **2010,** *191*, 615-629.
189. Rewatkar, P. V.; Parton, R. G.; Parekh, H. S.; Parat, M. O., Are Caveolae a Cellular Entry Route for Non-Viral Therapeutic Delivery Systems? *Adv. Drug Delivery Rev.* **2015,** *91*, 92-108.

190. Mayor, S.; Pagano, R. E., Pathways of Clathrin-Independent Endocytosis. *Nature reviews. Molecular cell biology* **2007,** *8*, 603-612.
191. Commisso, C.; Davidson, S. M.; Soydaner-Azeloglu, R. G.; Parker, S. J.; Kamphorst, J. J.; Hackett, S.; Grabocka, E.; Nofal, M.; Drebin, J. A.; Thompson, C. B.; Rabinowitz, J. D.; Metallo, C. M.; Vander Heiden, M. G.; Bar-Sagi, D., Macropinocytosis of Protein Is an Amino Acid Supply Route in Ras-Transformed Cells. *Nature* **2013,** *497*, 633-637.
192. Elkin, S. R.; Lakoduk, A. M.; Schmid, S. L., Endocytic Pathways and Endosomal Trafficking: A Primer. *Wien Med Wochenschr* **2016,** *166*, 196-204.
193. Varkouhi, A. K.; Scholte, M.; Storm, G.; Haisma, H. J., Endosomal Escape Pathways for Delivery of Biologicals. *J. Controlled Release* **2011,** *151*, 220-228.
194. Zelikin, A. N.; Ehrhardt, C.; Healy, A. M., Materials and Methods for Delivery of Biological Drugs. *Nat Chem* **2016,** *8*, 997-1007.
195. Moroz, E.; Matoori, S.; Leroux, J. C., Oral Delivery of Macromolecular Drugs: Where We Are after Almost 100years of Attempts. *Adv. Drug Delivery Rev.* **2016,** *101*, 108-121.
196. Muheem, A.; Shakeel, F.; Jahangir, M. A.; Anwar, M.; Mallick, N.; Jain, G. K.; Warsi, M. H.; Ahmad, F. J., A Review on the Strategies for Oral Delivery of Proteins and Peptides and Their Clinical Perspectives. *Saudi Pharm J* **2016,** *24*, 413-428.
197. Lundquist, P.; Artursson, P., Oral Absorption of Peptides and Nanoparticles across the Human Intestine: Opportunities, Limitations and Studies in Human Tissues. *Adv. Drug Delivery Rev.* **2016,** *106*, 256-276.
198. Park, K.; Kwon, I. C.; Park, K., Oral Protein Delivery: Current Status and Future Prospect. *Reactive and Functional Polymers* **2011,** *71*, 280-287.
199. Collnot, E. M.; Ali, H.; Lehr, C. M., Nano- and Microparticulate Drug Carriers for Targeting of the Inflamed Intestinal Mucosa. *J. Controlled Release* **2012,** *161*, 235-246.
200. Lamprecht, A.; Schafer, U.; Lehr, C. M., Size-Dependent Bioadhesion of Micro- and Nanoparticulate Carriers to the Inflamed Colonic Mucosa. *Pharm. Res.* **2001,** *18*, 788-793.
201. Jubeh, T. T.; Barenholz, Y.; Rubinstein, A., Differential Adhesion of Normal and Inflamed Rat Colonic Mucosa by Charged Liposomes. *Pharm. Res.* **2004,** *21*, 447-453.
202. Hua, S.; Marks, E.; Schneider, J. J.; Keely, S., Advances in Oral Nano-Delivery Systems for Colon Targeted Drug Delivery in Inflammatory Bowel Disease: Selective Targeting to Diseased Versus Healthy Tissue. *Nanomedicine* **2015,** *11*, 1117-1132.
203. Bakhru, S. H.; Furtado, S.; Morello, A. P.; Mathiowitz, E., Oral Delivery of Proteins by Biodegradable Nanoparticles. *Adv. Drug Delivery Rev.* **2013,** *65*, 811-821.
204. Kumar, A.; Montemagno, C.; Choi, H. J., Smart Microparticles with a Ph-Responsive Macropore for Targeted Oral Drug Delivery. *Scientific reports* **2017,** *7*, 3059.
205. Bhavsar, M. D.; Amiji, M. M., Gastrointestinal Distribution and in Vivo Gene Transfection Studies with Nanoparticles-in-Microsphere Oral System (Nimos). *J. Controlled Release* **2007,** *119*, 339-348.
206. Kriegel, C.; Amiji, M., Oral Tnf-Alpha Gene Silencing Using a Polymeric Microsphere-Based Delivery System for the Treatment of Inflammatory Bowel Disease. *J. Controlled Release* **2011,** *150*, 77-86.
207. Kriegel, C.; Attarwala, H.; Amiji, M., Multi-Compartmental Oral Delivery Systems for Nucleic Acid Therapy in the Gastrointestinal Tract. *Adv. Drug Delivery Rev.* **2013,** *65*, 891-901.
208. Zhang, Y.; Wei, W.; Lv, P.; Wang, L.; Ma, G., Preparation and Evaluation of Alginate-Chitosan Microspheres for Oral Delivery of Insulin. *Eur J Pharm Biopharm* **2011,** *77*, 11-19.

209. Sarmento, B.; Ribeiro, A.; Veiga, F.; Sampaio, P.; Neufeld, R.; Ferreira, D., Alginate/Chitosan Nanoparticles Are Effective for Oral Insulin Delivery. *Pharm. Res.* **2007,** *24*, 2198-2206.
210. Mukhopadhyay, P.; Chakraborty, S.; Bhattacharya, S.; Mishra, R.; Kundu, P. P., Ph-Sensitive Chitosan/Alginate Core-Shell Nanoparticles for Efficient and Safe Oral Insulin Delivery. *Int J Biol Macromol* **2015,** *72*, 640-648.
211. Anal, A. K.; Bhopatkar, D.; Tokura, S.; Tamura, H.; Stevens, W. F., Chitosan-Alginate Multilayer Beads for Gastric Passage and Controlled Intestinal Release of Protein. *Drug development and industrial pharmacy* **2003,** *29*, 713-724.
212. Coppi, G.; Iannuccelli, V.; Leo, E.; Bernabei, M. T.; Cameroni, R., Chitosan-Alginate Microparticles as a Protein Carrier. *Drug development and industrial pharmacy* **2001,** *27*, 393-400.
213. Ribeiro, A. J.; Silva, C.; Ferreira, D.; Veiga, F., Chitosan-Reinforced Alginate Microspheres Obtained through the Emulsification/Internal Gelation Technique. *European journal of pharmaceutical sciences : official journal of the European Federation for Pharmaceutical Sciences* **2005,** *25*, 31-40.
214. Chavarri, M.; Maranon, I.; Ares, R.; Ibanez, F. C.; Marzo, F.; Villaran Mdel, C., Microencapsulation of a Probiotic and Prebiotic in Alginate-Chitosan Capsules Improves Survival in Simulated Gastro-Intestinal Conditions. *Int J Food Microbiol* **2010,** *142*, 185-189.
215. Cook, M. T.; Tzortzis, G.; Charalampopoulos, D.; Khutoryanskiy, V. V., Production and Evaluation of Dry Alginate-Chitosan Microcapsules as an Enteric Delivery Vehicle for Probiotic Bacteria. *Biomacromolecules* **2011,** *12*, 2834-2840.
216. Tan, W. H.; Takeuchi, S., Monodisperse Alginate Hydrogel Microbeads for Cell Encapsulation. *Advanced Materials* **2007,** *19*, 2696-2701.
217. Smidsrod, O.; Skjakbrk, G., Alginate as Immobilization Matrix for Cells. *Trends in Biotechnology* **1990,** *8*, 71-78.
218. Gombotz, W. R.; Wee, S. F., Protein Release from Alginate Matrices. *Adv. Drug Delivery Rev.* **2012,** *64*, 194-205.
219. George, M.; Abraham, T. E., Polyionic Hydrocolloids for the Intestinal Delivery of Protein Drugs: Alginate and Chitosan--a Review. *J. Controlled Release* **2006,** *114*, 1-14.
220. Nugent, S. G., Intestinal Luminal Ph in Inflammatory Bowel Disease: Possible Determinants and Implications for Therapy with Aminosalicylates and Other Drugs. *Gut* **2001,** *48*, 571-577.
221. Lee, K. Y.; Mooney, D. J., Alginate: Properties and Biomedical Applications. *Prog Polym Sci* **2012,** *37*, 106-126.
222. Hamid, R.; Khan, M. A.; Ahmad, M.; Ahmad, M. M.; Abdin, M. Z.; Musarrat, J.; Javed, S., Chitinases: An Update. *J Pharm Bioallied Sci* **2013,** *5*, 21-29.
223. Thakral, S.; Thakral, N. K.; Majumdar, D. K., Eudragit: A Technology Evaluation. *Expert Opin Drug Deliv* **2013,** *10*, 131-149.
224. Wilson, D. S.; Dalmasso, G.; Wang, L. X.; Sitaraman, S. V.; Merlin, D.; Murthy, N., Orally Delivered Thioketal Nanoparticles Loaded with Tnf-Alpha-Sirna Target Inflammation and Inhibit Gene Expression in the Intestines. *Nat. Mater.* **2010,** *9*, 923-928.
225. Mane, V.; Muro, S., Biodistribution and Endocytosis of Icam-1-Targeting Antibodies Versus Nanocarriers in the Gastrointestinal Tract in Mice. *Int. J. Nanomed.* **2012,** *7*, 4223-4237.
226. Floch, M. H.; Walker, W. A., Advances in Clinical Use of Probiotics. *J. Clin. Gastroenterol.* **2008,** *42 Suppl 2*, S45.

227. Galan, J. E., Common Themes in the Design and Function of Bacterial Effectors. *Cell Host Microbe* **2009,** *5*, 571-579.
228. Lai, S. K.; Wang, Y. Y.; Hanes, J., Mucus-Penetrating Nanoparticles for Drug and Gene Delivery to Mucosal Tissues. *Adv. Drug Delivery Rev.* **2009,** *61*, 158-171.
229. Li, M. G.; Lu, W. L.; Wang, H. C.; Zhang, X.; Wang, X. Q.; Zheng, A. P.; Zhang, Q., Distribution, Transition, Adhesion and Release of Insulin Loaded Nanoparticles in the Gut of Rats. *Int. J. Pharm.* **2007,** *329*, 182-191.
230. Lamprecht, A.; Ubrich, N.; Yamamoto, H.; Schafer, U.; Takeuchi, H.; Maincent, P.; Kawashima, Y.; Lehr, C. M., Biodegradable Nanoparticles for Targeted Drug Delivery in Treatment of Inflammatory Bowel Disease. *J. Pharmacol. Exp. Ther.* **2001,** *299*, 775-781.
231. Makhof, A.; Tozuka, Y.; Takeuchi, H., Ph-Sensitive Nanospheres for Colon-Specific Drug Delivery in Experimentally Induced Colitis Rat Model. *Eur. J. Pharm. Biopharm.* **2009,** *72*, 1-8.
232. Meissner, Y.; Lamprecht, A., Alternative Drug Delivery Approaches for the Therapy of Inflammatory Bowel Disease. *J. Pharm. Sci.* **2008,** *97*, 2878-2891.
233. Moulari, B.; Pertuit, D.; Pellequer, Y.; Lamprecht, A., The Targeting of Surface Modified Silica Nanoparticles to Inflamed Tissue in Experimental Colitis. *Biomaterials* **2008,** *29*, 4554-4560.
234. Pertuit, D.; Moulari, B.; Betz, T.; Nadaradjane, A.; Neumann, D.; Ismaili, L.; Refouvelet, B.; Pellequer, Y.; Lamprecht, A., 5-Amino Salicylic Acid Bound Nanoparticles for the Therapy of Inflammatory Bowel Disease. *J. Controlled Release* **2007,** *123*, 211-218.
235. Theiss, A. L.; Laroui, H.; Obertone, T. S.; Chowdhury, I.; Thompson, W. E.; Merlin, D.; Sitaraman, S. V., Nanoparticle-Based Therapeutic Delivery of Prohibitin to the Colonic Epithelial Cells Ameliorates Acute Murine Colitis. *Inflammatory Bowel Dis.* **2011,** *17*, 1163-1176.
236. Swidsinski, A.; Loening-Baucke, V.; Theissig, F.; Engelhardt, H.; Bengmark, S.; Koch, S.; Lochs, H.; Dorffel, Y., Comparative Study of the Intestinal Mucus Barrier in Normal and Inflamed Colon. *Gut* **2007,** *56*, 343-350.
237. Cheng, X.; Liu, R.; He, Y., A Simple Method for the Preparation of Monodisperse Protein-Loaded Microspheres with High Encapsulation Efficiencies. *Eur. J. Pharm. Biopharm.* **2010,** *76*, 336-341.
238. Jin, T.; Zhu, J.; Wu, F.; Yuan, W.; Geng, L. L.; Zhu, H., Preparing Polymer-Based Sustained-Release Systems without Exposing Proteins to Water-Oil or Water-Air Interfaces and Cross-Linking Reagents. *J. Controlled Release* **2008,** *128*, 50-59.
239. Park, T. G.; Lu, W.; Crotts, G., Importance of in Vitro Experimental Conditions on Protein Release Kinetics, Stability and Polymer Degradation in Protein Encapsulated Poly (-Lactic Acid-Co-Glycolic Acid) Microspheres. *J. Controlled Release* **1995,** *33*, 211-222.
240. Vila, A.; Sánchez, A.; TobIo, M.; Calvo, P.; Alonso, M. J., Design of Biodegradable Particles for Protein Delivery. *J. Controlled Release* **2002,** *78*, 15-24.
241. Langer, K.; Anhorn, M. G.; Steinhauser, I.; Dreis, S.; Celebi, D.; Schrickel, N.; Faust, S.; Vogel, V., Human Serum Albumin (Hsa) Nanoparticles: Reproducibility of Preparation Process and Kinetics of Enzymatic Degradation. *Int. J. Pharm.* **2008,** *347*, 109-117.
242. Herrera Estrada, L.; Chu, S.; Champion, J. A., Protein Nanoparticles for Intracellular Delivery of Therapeutic Enzymes. *J. Pharm. Sci.* **2014,** *103*, 1863-1871.
243. Estrada, L. H.; Chu, S.; Champion, J. A., Protein Nanoparticles for Intracellular Delivery of Therapeutic Enzymes. *Journal of pharmaceutical sciences* **2014**.

244. Cheng, R.; Feng, F.; Meng, F.; Deng, C.; Feijen, J.; Zhong, Z., Glutathione-Responsive Nano-Vehicles as a Promising Platform for Targeted Intracellular Drug and Gene Delivery. *J. Controlled Release* **2011,** *152*, 2-12.
245. Schlumberger, M. C.; Muller, A. J.; Ehrbar, K.; Winnen, B.; Duss, I.; Stecher, B.; Hardt, W. D., Real-Time Imaging of Type Iii Secretion: Salmonella Sipa Injection into Host Cells. *Proc. Natl. Acad. Sci. U. S. A.* **2005,** *102*, 12548-12553.
246. Madara, J. L.; Stafford, J.; Dharmsathaphorn, K.; Carlson, S., Structural Analysisof a Human Intestinal Epithelial Cell Line. *Gastroenterology* **1987,** *92*, 1133-1145.
247. Yen, H. J.; Hsu, S. H.; Tsai, C. L., Cytotoxicity and Immunological Response of Gold and Silver Nanoparticles of Different Sizes. *Small* **2009,** *5*, 1553-1561.
248. Prabhu, A.; Shelburne, C. E.; Gibbons, D. F., Cellular Proliferation and Cytokine Responses of Murine Macrophage Cell Line J774a.1to Polymethylmethacrylate and Cobalt-Chrome Alloy Particles. *J. Biomed. Res.* **1998,** *42*, 655-663.
249. Hardt, W. D.; Galan, J. E., A Secreted Salmonella Protein with Homology to an Avirulence Determinant of Plant Pathogenic Bacteria. *Proc. Natl. Acad. Sci. U. S. A.* **1997,** *94*, 9887-9892.
250. Monack, D. M.; Mecsas, J.; Ghori, N.; Falkow, S., Yersinia Signals Macrophages to Undergo Apoptosis and Yopj Is Necessary for This Cell Death. *Proc. Natl. Acad. Sci. U. S. A.* **1997,** *94*, 10385-10390.
251. Yao, C.; Tai, Z.; Wang, X.; Liu, J.; Zhu, Q.; Wu, X.; Zhang, L.; Zhang, W.; Tian, J.; Gao, Y., Reduction-Responsive Cross-Linked Stearyl Peptide for Effective Delivery of Plasmid DNA. *Int. J. Nanomed.* **2015,** *10*, 3403.
252. Martens, T. F.; Remaut, K.; Demeester, J.; De Smedt, S. C.; Braeckmans, K., Intracellular Delivery of Nanomaterials: How to Catch Endosomal Escape in the Act. *Nano Today* **2014,** *9*, 344-364.
253. Ye, Z.; Petrof, E. O.; Boone, D.; Claud, E. C.; Sun, J., Salmonella Effector Avra Regulation of Colonic Epithelial Cell Inflammation by Deubiquitination. *Am. J. Pathol.* **2007,** *171*, 882-892.
254. Schesser, K.; Spiik, A. K.; Dukuzumuremyi, J. M.; Neurath, M. F.; Pettersson, S.; Wolf-Watz, H., The Yopj Locus Is Required for Yersinia-Mediated Inhibition of Nf-Kb Activation and Cytokine Expression: Yopj Contains a Eukaryotic Sh2-Like Domain That Is Essential for Its Repressive Activity. *Mol. Microbiol.* **1998,** *28*, 1067-1079.
255. Srikanth, C.; Wall, D. M.; Maldonado-Contreras, A.; Shi, H. N.; Zhou, D.; Demma, Z.; Mumy, K. L.; McCormick, B. A., Salmonella Pathogenesis and Processing of Secreted Effectors by Caspase-3. *Science* **2010,** *330*, 390-393.
256. Herrera Estrada, L.; Padmore, T. J.; Champion, J. A., Bacterial Effector Nanoparticles as Breast Cancer Therapeutics. *Mol. Pharmaceutics* **2016,** *13*, 710-719.
257. Wei, P.; Wong, W. W.; Park, J. S.; Corcoran, E. E.; Peisajovich, S. G.; Onuffer, J. J.; Weiss, A.; Lim, W. A., Bacterial Virulence Proteins as Tools to Rewire Kinase Pathways in Yeast and Immune Cells. *Nature* **2012,** *488*, 384-388.
258. Roda, G.; Sartini, A.; Zambon, E.; Calaflore, A.; Marocchi, M.; Caponi, A.; Belluzi, A.; Roda, E., Intestinal Epithelial Cells in Inflammatory Bowel Disease. *World J. Gastroenterol.* **2010,** *16*, 4264-4271.
259. Mizoguchi, A., Animal Models of Inflammatory Bowel Disease. *Prog. Mol. Biol. Transl. Sci.* **2012,** *105*, 263-320.

260. Garrett, W. S.; Lord, G. M.; Punit, S.; Lugo-Villarino, G.; Mazmanian, S. K.; Ito, S.; Glickman, J. N.; Glimcher, L. H., Communicable Ulcerative Colitis Induced by T-Bet Deficiency in the Innate Immune System. *Cell* **2007,** *131*, 33-45.
261. Belkaid, Y.; Hand, T. W., Role of the Microbiota in Immunity and Inflammation. *Cell* **2014,** *157*, 121-141.
262. Guarner, F.; Malagelada, J.-R., Gut Flora in Health and Disease. *The Lancet* **2003,** *361*, 512-519.
263. Bhavsar, A. P.; Guttman, J. A.; Finlay, B. B., Manipulation of Host-Cell Pathways by Bacterial Pathogens. *Nature* **2007,** *449*, 827-834.
264. Fyderek, K., Mucosal Bacterial Microflora and Mucus Layer Thickness in Adolescents with Inflammatory Bowel Disease. *World Journal of Gastroenterology* **2009,** *15*, 5287.
265. Cormack, B. P.; Valdivia, R. H.; Falkow, S., Facs-Optimized Mutants of the Green Fluorescent Protein (Gfp). *Gene* **1996,** *173*, 33-38.
266. Jantratid, E.; Janssen, N.; Reppas, C.; Dressman, J. B., Dissolution Media Simulating Conditions in the Proximal Human Gastrointestinal Tract: An Update. *Pharm. Res.* **2008,** *25*, 1663-1676.
267. Vranic, S.; Boggetto, N.; Contremoulins, V.; Mornet, S.; Reinhardt, N.; Marano, F.; Baeza-Squiban, A.; Boland, S., Deciphering the Mechanisms of Cellular Uptake of Engineered Nanoparticles by Accurate Evaluation of Internalization Using Imaging Flow Cytometry. *Part Fibre Toxicol* **2013,** *10*, 2.
268. Alam, M. A.; Al-Jenoobi, F. I.; Al-Mohizea, A. M., Everted Gut Sac Model as a Tool in Pharmaceutical Research: Limitations and Applications. *J Pharm Pharmacol* **2012,** *64*, 326-336.
269. Nava, P.; Koch, S.; Laukoetter, M. G.; Lee, W. Y.; Kolegraff, K.; Capaldo, C. T.; Beeman, N.; Addis, C.; Gerner-Smidt, K.; Neumaier, I.; Skerra, A.; Li, L.; Parkos, C. A.; Nusrat, A., Interferon-Gamma Regulates Intestinal Epithelial Homeostasis through Converging Beta-Catenin Signaling Pathways. *Immunity* **2010,** *32*, 392-402.
270. Smith, D. B.; Johnson, K. S., Single-Step Purification of Polypeptides Expressed in Escherichia Coli as Fusions with Glutathione S-Transferase. *Gene* **1988,** *67*, 31-40.
271. Lopez-Mirabal, H. R.; Winther, J. R., Redox Characteristics of the Eukaryotic Cytosol. *Biochim Biophys Acta* **2008,** *1783*, 629-640.
272. Erickson, H. P., Size and Shape of Protein Molecules at the Nanometer Level Determined by Sedimentation, Gel Filtration, and Electron Microscopy. *Biol Proced Online* **2009,** *11*, 32-51.
273. Malik, A.; Rudolph, R.; Sohling, B., Use of Enhanced Green Fluorescent Protein to Determine Pepsin at High Sensitivity. *Analytical biochemistry* **2005,** *340*, 252-258.
274. Haupts, U.; Maiti, S.; Schwille, P.; Webb, W. W., Dynamics of Fluorescence Fluctuations in Green Fluorescent Protein Observed by Fluorescence Correlation Spectroscopy. *Proceedings of the National Academy of Sciences* **1998,** *95*, 13573-13578.
275. Dang, T. D.; Joo, S. W., Preparation of Tadpole-Shaped Calcium Alginate Microparticles with Sphericity Control. *Colloids Surf B Biointerfaces* **2013,** *102*, 766-771.
276. Huguet, M. L.; Neufeld, R. J.; Dellacherie, E., Calcium-Alginate Beads Coated with Polycationic Polymers: Comparison of Chitosan and Deae-Dextran. *Process Biochemistry* **1996,** *31*, 347-353.
277. Murata, Y.; Maeda, T.; Miyamoto, E.; Kawashima, S., Preparation of Chitosan-Reinforced Alginate Gel Beads — Effects of Chitosan on Gel Matrix Erosion. *International Journal of Pharmaceutics* **1993,** *96*, 139-145.

278. Richard, I.; Thibault, M.; De Crescenzo, G.; Buschmann, M. D.; Lavertu, M., Ionization Behavior of Chitosan and Chitosan-DNA Polyplexes Indicate That Chitosan Has a Similar Capability to Induce a Proton-Sponge Effect as Pei. *Biomacromolecules* **2013,** *14*, 1732-1740.
279. Mao, H.-Q.; Roy, K.; Troung-Le, V. L.; Janes, K. A.; Lin, K. Y.; Wang, Y.; August, J. T.; Leong, K. W., Chitosan-DNA Nanoparticles as Gene Carriers: Synthesis, Characterization and Transfection Efficiency. *J. Controlled Release* **2001,** *70*, 399-421.
280. Peterson, L. W.; Artis, D., Intestinal Epithelial Cells: Regulators of Barrier Function and Immune Homeostasis. *Nat. Rev. Immunol.* **2014,** *14*, 141-153.
281. McConnell, E. L.; Basit, A. W.; Murdan, S., Measurements of Rat and Mouse Gastrointestinal Ph, Fluid and Lymphoid Tissue, and Implications for in-Vivo Experiments. *J Pharm Pharmacol* **2008,** *60*, 63-70.
282. Evans, D. F.; Pye, G.; Bramley, R.; Clark, A. G.; Dyson, T. J.; Hardcastle, J. D., Measurement of Gastrointestinal Ph Profiles in Normal Ambulant Human Subjects. *Gut* **1988,** *29*, 1035-1041.
283. Wirtz, S.; Popp, V.; Kindermann, M.; Gerlach, K.; Weigmann, B.; Fichtner-Feigl, S.; Neurath, M. F., Chemically Induced Mouse Models of Acute and Chronic Intestinal Inflammation. *Nat. Protoc.* **2017,** *12*, 1295-1309.
284. Wirtz, S.; Neufert, C.; Weigmann, B.; Neurath, M. F., Chemically Induced Mouse Models of Intestinal Inflammation. *Nat. Protoc.* **2007,** *2*, 541-546.
285. Laroui, H.; Geem, D.; Xiao, B.; Viennois, E.; Rakhya, P.; Denning, T.; Merlin, D., Targeting Intestinal Inflammation with Cd98 Sirna/Pei-Loaded Nanoparticles. *Molecular therapy : the journal of the American Society of Gene Therapy* **2014,** *22*, 69-80.
286. Krawisz, J. E.; Sharon, P.; Stenson, W. F., Quantitative Assay for Acute Intestinal Inflammation Based on Myeloperoxidase Activity. *Gastroenterology* **1984,** *87*, 1344 - 1350.
287. Blanco, E.; Shen, H.; Ferrari, M., Principles of Nanoparticle Design for Overcoming Biological Barriers to Drug Delivery. *Nature biotechnology* **2015,** *33*, 941-951.
288. Stewart, M. P.; Lorenz, A.; Dahlman, J.; Sahay, G., Challenges in Carrier-Mediated Intracellular Delivery: Moving Beyond Endosomal Barriers. *Wiley Interdiscip Rev Nanomed Nanobiotechnol* **2016,** *8*, 465-478.
289. Schafer, V.; von Briesen, H.; Andreesen, R.; Steffan, A. M.; Royer, C.; Troster, S.; Kreuter, J.; Rubsamen-Waigmann, H., Phagocytosis of Nanoparticles by Human Immunodeficiency Virus (Hiv)-Infected Macrophages: A Possibility for Antiviral Drug Targeting. *Pharmaceutical research* **1992,** *9*, 541-546.
290. Kreuter, J., Evaluation of Nanoparticles as Drug-Delivery Systems. Ii: Comparison of the Body Distribution of Nanoparticles with the Body Distribution of Microspheres (Diameter Greater Than 1 Micron), Liposomes, and Emulsions. *Pharmaceutica acta Helvetiae* **1983,** *58*, 217-226.
291. Zhu, M.; Nie, G.; Meng, H.; Xia, T.; Nel, A.; Zhao, Y., Physicochemical Properties Determine Nanomaterial Cellular Uptake, Transport, and Fate. *Acc Chem Res* **2013,** *46*, 622-631.
292. Jiang, W.; Kim, B. Y.; Rutka, J. T.; Chan, W. C., Nanoparticle-Mediated Cellular Response Is Size-Dependent. *Nature nanotechnology* **2008,** *3*, 145-150.
293. Fleischer, C. C.; Payne, C. K., Nanoparticle Surface Charge Mediates the Cellular Receptors Used by Protein-Nanoparticle Complexes. *The journal of physical chemistry. B* **2012,** *116*, 8901-8907.

294. Fleischer, C. C.; Kumar, U.; Payne, C. K., Cellular Binding of Anionic Nanoparticles Is Inhibited by Serum Proteins Independent of Nanoparticle Composition. *Biomaterials science* **2013,** *1*, 975-982.
295. Georgieva, J. V.; Kalicharan, D.; Couraud, P. O.; Romero, I. A.; Weksler, B.; Hoekstra, D.; Zuhorn, I. S., Surface Characteristics of Nanoparticles Determine Their Intracellular Fate in and Processing by Human Blood-Brain Barrier Endothelial Cells in Vitro. *Molecular therapy : the journal of the American Society of Gene Therapy* **2011,** *19*, 318-325.
296. Harush-Frenkel, O.; Debotton, N.; Benita, S.; Altschuler, Y., Targeting of Nanoparticles to the Clathrin-Mediated Endocytic Pathway. *Biochemical and biophysical research communications* **2007,** *353*, 26-32.
297. Nakai, S., Measurement of Protein Hydrophobicity. **2004**.
298. Haskard, C. A.; Li-Chan, E. C. Y., Hydrophobicity of Bovine Serum Albumin and Ovalbumin Determined Using Uncharged (Prodan) and Anionic (Ans-) Fluorescent Probes. *Journal of Agricultural and Food Chemistry* **1998,** *46*, 2671-2677.
299. Bhattacharjee, S., Dls and Zeta Potential - What They Are and What They Are Not? *J. Controlled Release* **2016,** *235*, 337-351.
300. Gessner, A.; Waicz, R.; Lieske, A.; Paulke, B. R.; Mäder, K.; Müller, R. H., Nanoparticles with Decreasing Surface Hydrophobicities: Influence on Plasma Protein Adsorption. *International Journal of Pharmaceutics* **2000,** *196*, 245-249.
301. Hawe, A.; Sutter, M.; Jiskoot, W., Extrinsic Fluorescent Dyes as Tools for Protein Characterization. *Pharm. Res.* **2008,** *25*, 1487-1499.
302. Docter, D.; Distler, U.; Storck, W.; Kuharev, J.; Wunsch, D.; Hahlbrock, A.; Knauer, S. K.; Tenzer, S.; Stauber, R. H., Quantitative Profiling of the Protein Coronas That Form around Nanoparticles. *Nat. Protoc.* **2014,** *9*, 2030-2044.
303. Bertoli, F.; Garry, D.; Monopoli, M. P.; Salvati, A.; Dawson, K. A., The Intracellular Destiny of the Protein Corona: A Study on Its Cellular Internalization and Evolution. *ACS Nano* **2016,** *10*, 10471-10479.
304. Lundqvist, M.; Stigler, J.; Elia, G.; Lynch, I.; Cedervall, T.; Dawson, K. A., Nanoparticle Size and Surface Properties Determine the Protein Corona with Possible Implications for Biological Impacts. *Proc. Natl. Acad. Sci. U. S. A.* **2008,** *105*, 14265-14270.
305. Furumoto, K.; Ogawara, K.-i.; Nagayama, S.; Takakura, Y.; Hashida, M.; Higaki, K.; Kimura, T., Important Role of Serum Proteins Associated on the Surface of Particles in Their Hepatic Disposition. *J. Controlled Release* **2002,** *83*, 89-96.
306. Madani, F.; Lindberg, S.; Langel, U.; Futaki, S.; Graslund, A., Mechanisms of Cellular Uptake of Cell-Penetrating Peptides. *Journal of biophysics* **2011,** *2011*, 414729.
307. LeCher, J. C.; Nowak, S. J.; McMurry, J. L., Breaking in and Busting Out: Cell-Penetrating Peptides and the Endosomal Escape Problem. *Biomol Concepts* **2017,** *8*, 131-141.
308. Scharnert, J.; Greune, L.; Zeuschner, D.; Lubos, M. L.; Alexander Schmidt, M.; Ruter, C., Autonomous Translocation and Intracellular Trafficking of the Cell-Penetrating and Immune-Suppressive Effector Protein Yopm. *Cellular and molecular life sciences : CMLS* **2013,** *70*, 4809-4823.
309. Yoon, Y. M.; Lewis, J. S.; Carstens, M. R.; Campbell-Thompson, M.; Wasserfall, C. H.; Atkinson, M. A.; Keselowsky, B. G., A Combination Hydrogel Microparticle-Based Vaccine Prevents Type 1 Diabetes in Non-Obese Diabetic Mice. *Scientific reports* **2015,** *5*, 13155.

310. Lewis, J. S.; Roche, C.; Zhang, Y.; Brusko, T. M.; Wasserfall, C. H.; Atkinson, M.; Clare-Salzler, M. J.; Keselowsky, B. G., Combinatorial Delivery of Immunosuppressive Factors to Dendritic Cells Using Dual-Sized Microspheres. *J Mater Chem B* **2014,** *2*, 2562-2574.
311. Deng, L.; Mohan, T.; Chang, T. Z.; Gonzalez, G. X.; Wang, Y.; Kwon, Y. M.; Kang, S. M.; Compans, R. W.; Champion, J. A.; Wang, B. Z., Double-Layered Protein Nanoparticles Induce Broad Protection against Divergent Influenza a Viruses. *Nat Commun* **2018,** *9*, 359.
312. Neutra, M. R.; Kozlowski, P. A., Mucosal Vaccines: The Promise and the Challenge. *Nat. Rev. Immunol.* **2006,** *6*, 148-158.
313. Auriemma, G.; Mencherini, T.; Russo, P.; Stigliani, M.; Aquino, R. P.; Del Gaudio, P., Prilling for the Development of Multi-Particulate Colon Drug Delivery Systems: Pectin Vs. Pectin-Alginate Beads. *Carbohydr Polym* **2013,** *92*, 367-373.
314. Sivapragasam, N.; Thavarajah, P.; Ohm, J. B.; Ohm, J. B.; Margaret, K.; Thavarajah, D., Novel Starch Based Nano Scale Enteric Coatings from Soybean Meal for Colon-Specific Delivery. *Carbohydr Polym* **2014,** *111*, 273-279.